ON THE ASYMPTOTIC BOUNDARY CONDITION AT THE FREE-FLUID/ POROUS-MEDIUM INTERFACE IN PCL DUE TO THE CILIARY MOVEMENT

SUDAPORN POOPRA

A THESIS SUBMITTED IN PARTIAL FULFILLMENT OF THE REQUIREMENT FOR THE DEGREE OF DOCTOR OF PHILOSOPHY IN APPLIED MATHEMATICS

DEPARTMENT OF MATHEMATICS SCHOOL OF SCIENCE
KING MONGKUT'S INSTITUTE OF TECHNOLOGY LADKRABANG

2022
KMITL-2022-SC-D-001-086

Thesis Title	On the asymptotic boundary at the free-fluid/ porous-medium interface in PCL due to the ciliary movement
Student Name	Miss Sudaporn Poopra
Student ID	57605022
Degree	Doctor of Philosophy (Applied Mathematics)
Department	Mathematics
Year	2022
Thesis Advisor	Assoc. Prof. Dr.Kanognudge Wuttanachamsri

Abstract

Humans breathe air into the respiratory system through the trachea, but with all the pollutants around them, the air they breathe may not be clean. When this is happened, the respiratory system secretes mucus to trap the debris that is inhaled through the nostrils. The respiratory tract contains hair-like structures on the epithelial tissue, called cilia. They wave back and forth to expel particles of dust, mucus, and contaminants from the body. The layer containing cilia is called Periciliary Layer (PCL). The fluid in this layer is named PCL fluid. Usually, fluids move due to pressure changes, but in this study, the velocity of solids or cilia moves the PCL fluid. The moving of cilia results in two different domains in the PCL: porous-medium and free-fluid regions. When cilia are perpendicular to the horizontal plane ($\theta = 90^\circ$), the PCL, containing only cilia, is considered a porous-medium domain. When cilia make an angle θ ($\theta < 90^\circ$) with the horizontal plane the PCL consists of two different domains: the porous medium and a free-fluid domain overlying the cilia. The objective of this work is to study the consistency of the Beaver-Joseph boundary condition with this problem and to determine the appropriate boundary conditions between those two regions. The asymptotic expansion method is applied to the Stokes–Brinkman equations in a macroscopic scale to determine the velocity of the PCL fluid with the Beaver-Joseph boundary condition. Moreover, a matching condition is employed to find the applicable boundary condition at the free-fluid/porous-medium interface. Two boundary conditions of the PCL velocity are obtained, which are the relationship between the two solutions and the derivative of those in the two domains.

Keywords: Periciliary Layer, Moving Solid phases, Asymptotic expansion method, Stokes-Brinkman equations

Acknowledgments

First, I would like to big thank my advisor, Associate Professor Dr. Kanognudge Wuttanachamsri, for her suggestions, and encouragement throughout this research.

I am grateful to all of the committee members Assistant Professor Dr.Sukrawan Mavecha, Dr.Wannaporn Sanprasert, and Assistant Professor Dr.Puttha Sakkaplangkul for many useful recommendations and suggestions. Next, I also give thanks to the external committee member, Associate Professor Dr.Montri Maleewong, from Kasetsart University, for his valuable advice and comments.

I am also thankful to the Department of Mathematics, King Mongkut's Institute of Technology Ladkrabang for providing me with the necessary facilities.

Furthermore, I would like to thank my sister and brother, Assistant Professor Dr.Rachada Pongprairat, Dr.Nontarat Bumrungkiat, Dr.Krongkaew Migkhanetara, Dr.Pravitra Oyjinda, Miss Wunwisa Punkhoom, Dr.Piyada Phosri, Dr.Sarawut Nabnean, and Dr.Apirat Siraworakul for their attentiveness, encouragement and for providing suggestions regarding the mathematical computations featured and help to improve English in this research.

Last, I also thank my parents, my husband, and my sister for their love and patience, which made my study successful.

Sudaporn Poopra

Table of Contents

List of Tables

Table **Page**

List of Figures

Figure **Page**

Chapter 1
Introduction

1.1 The Velocity of PCL Fluids in Human Lungs

Breathing is one of the most important bodily functions that keep us alive. When we breathe air in through the nose it is not just oxygen but also small substances containing particles and pathogens that pass through lungs. However, the respiratory system has filters to trap and remove the strange pathogens, thus allowing us to breathe without irritation. The filters lining the bronchus within the respiratory system are called cilia, hair-like structure, scattered throughout the ciliated cells, which are vital components of the immune system. Beside cilia, there are goblet cells scattering among the ciliated cells in the respiratory system. One of the primary functions of the goblet cells is to secrete mucus to trap the particles or microorganisms that pass through our respiratory system. Then mucus forms a layer at the tips of cilia. The cilia aid in transporting these foreign particles out of the body by sweeping the mucus upwards towards the throat. The tips of the cilia make contact with the mucus layer on the forward stroke and bend sideways and backwards on the reverse stroke. Essentially, this causes the mucus to be propelled only in the forward direction on the forward stroke [1]. The excreted mucus is ejected through the vocal cords and into the pharynx. The primary innate defense mechanism is called mucociliary clearance [2]. Under optimal lung conditions, cilia beat at 12 to 15 Hz in coordinated waves propelling mucus at 4 to 20 mm/min [1].

The left of Figure 1.1 shows the respiratory system. In the middle of the picture shows the cross section of the trachea and the right of the picture shows the inside of the cross section: there exists three main layers, air, mucus and the periciliary layers (PCL). The PCL is a moist layer composed of cilia covering the ciliated cells. The fluid in this layer is called PCL fluid. Below the PCL is epithelial cells.

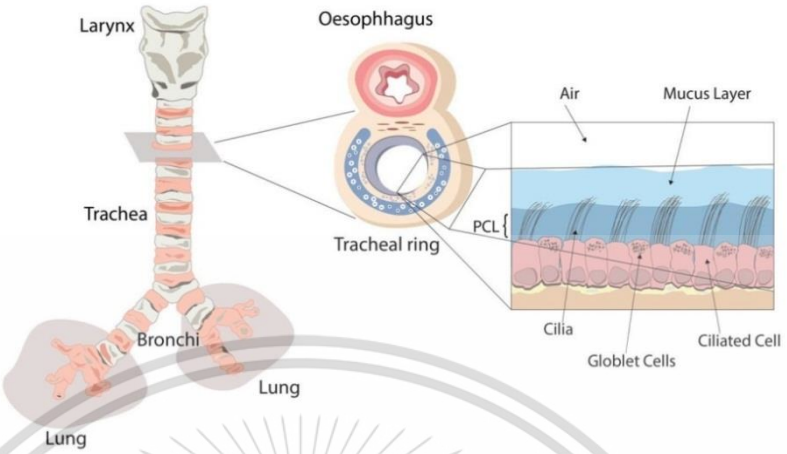

Figure 1.1 The respiratory system and the layers in the respiratory tracts

Cilia are found in the PCL layer. The function of the cilia is to filter out dust and other inhaled foreign particles. Cilia work as a part of the immune system protecting the body against pathogens in the air. Goblet cells among the ciliated cells (vital component cells of the immune system) secrete mucus to trap the inhaled particles and cilia help to transport these particles out of the body by cilia-generated flow.

We consider that the movement of cilia results in two different patterns in the PCL as shown in Figure 1.2. The left of Figure 1.2 shows the cilia perpendicular to the horizontal plane. In this case, the PCL has only one domain, which contains only cilia. When the cilia move forward and form an angle $\theta, \theta < 90^{\circ}$ with the horizontal plane, the PCL can be divided into two domains, the layer containing cilia and the layer above the cilia as shown on the right of Figure 1.2. Since the PCL layer consists of the PCL fluid, assisting to treat the cilia to operate normally, and the solid phases, cilia, this part in PCL is considered as a porous medium. The layer above the cilia in the PCL is called free-fluid domain, as shown on the right of Figure 1.2. The PCL domain is denoted by $\Omega = \Omega_1 \cup \Omega_2$ where Ω_1 is the free-fluid region above the porous layer Ω_2 when the cilia form an angle $\theta, \theta < 90^{\circ}$ with the horizontal plane. With the perpendicular case, we have only Ω_2. The variable y_{Stoke} is the height of the domain Ω_2. It changes according to the angle θ. In this thesis, we study the fluid flow in the periciliary layer (PCL) of the respiratory tract. For the equation applied in the free-fluid region was described by the Stokes equation or Navier–Stokes equations, while flow in the porous-medium region was usually modelled by using Darcy's Law or Brinkman equations [3-9]. In general, the Brinkman model is used for the porous media with high

porosity [10]. In this study, the Stokes equation is employed in the free-fluid domain and the Brinkman equation is applied in the porous medium. The Beavers-Joseph (BJ) boundary condition is employed at the interface between the porous medium and the free-fluid region. The asymptotic expansion method is used to determine the velocity of PCL fluid in order to let us know the velocity of the fluid in the PCL layer to drive mucus out to the patient. For the second goal, we develope the boundary condition at the porous medium/ free-fluid interface that is proper to the problem by using the method of matched asymptotic expansion related to the velocity of the cilia in the model.

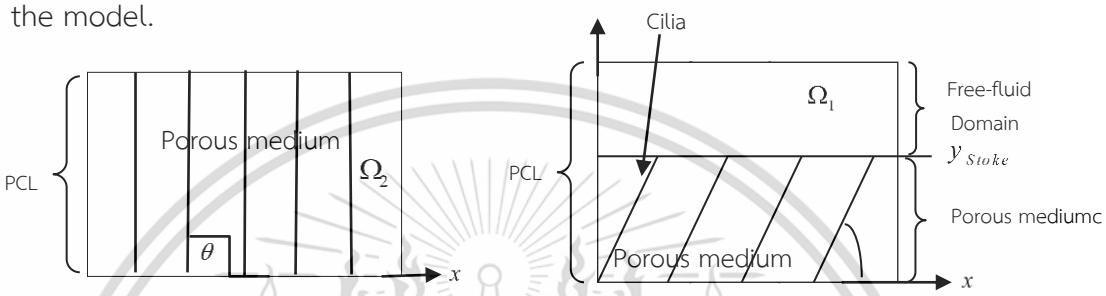

Figure 1.2 From left to right, the cilia are perpendicular and from an angle $\theta, \theta < 90^{\circ}$ with the horizontal plane, respectively

1.2 Literature review

A considerable amount of literature has been published on the PCL and mucus layers both numerical and experimental studies [11-20]. In terms of numerical methods, Jayathilake et al. [21] developed a three-dimensional numerical model to simulate human pulmonary cilia motion in the PCL using the immersed boundary method combined with the projection method. The numerical results indicated that the phase differences of cilia in both stream wise and span wise directions resulted in the maximum PCL velocity in the stream wise direction. In terms of experimental studies, Matsui et al. [22] studied the movements of mucus and PCL liquid in airway surfaces, using conventional and confocal microscopy of fluorescent microspheres photoactivated fluorescent dyes and well-differentiated human tracheobronchial epithelial cell cultures that exhibitited spontaneous, radial mucociliary transport. The findings showed that the entire PCL liquid was transported at approximately the same rate as mucus, 39.2 ± 4.7 and 39.8 ± 4.2 micrometer/sec.

For the mathematical model used in a porous medium and a free-fluid region, for example, Valdes-Parada and Lasseux [23] provided a new approach for modeling flow in porous and free-fluid domains that based on Beaver and Joseph configuration by using Darcy's Law and Navier-Stokes equation. Carraro et al [24] figured out a high-precision simulation of the slow viscous flow over a porous bed by applying a finite element method to Stokes equation in flow domain and Darcy's Law in porous bed.

Naqvi and Bottaro [25] studied boundary conditions between an isotropic porous medium and a free fluid region by using the Stokes-like equation and homogenization theory. Du and Zu [26] proposed a local and parallel finite element method to the mixed Navier-Stokes/Darcy model with the Beaver-Joseph interface condition for an incompressible fluid flow. Wuttanachamsri [6] used one-dimensional Stokes-Brinkman equations to find the shape of free interface between a porous medium and a free-fluid region. In this thesis, we use the Stokes equation in the free-fluid region and the Brinkman equation in the porous medium in order to analytical study the Stokes-Brinkman equations.

The two-layer configuration that use different equations in different domains requires proper boundary conditions at the interface between the free-fluid and porous-medium regions. The difficulty in determining boundary conditions results from the fact that the orders of the corresponding differential operators are often different [10]. The boundary conditions at the interface between the porous-medium and the free-fluid regions had been studied by several authors [27-30, 31, 23]. For example, Beavers and Joseph [30] proposed a slip boundary condition based on repeated experiments with a Poiseuille flow over a permeable porous block. Sahraoui and Kaviany [31] determined an appropriate hydrodynamic boundary condition at the interface between a porous medium and a plain domain using the pressure correction method. Valdes-Parada and Lasseux [23] studied three different boundary conditions; creeping flow under no-slip conditions, inertial flow no-slip conditions and creeping flow with slip conditions with Navier-Stokes-Darcy equations. The solutions were calculated by using Direct Numerical Simulation (DNS).

The asymptotic expansion method has been widely used to solve a system of equations in a number of studies [23, 32, 3]. Chandesris and Jamet [3] find the boundary condition at the interface between the porous medium and the free fluid based on the Poiseuille flow over a permeable block the used matched asymptotic expansion method. The domains were described using volume averaged transport equation. With the assumption this equation still held in the heterogeneous transition zone by considering variable porosity and permeability. It should be noted that, in this study, the solid phases in the porous domain are self-propelled motion and we provide proper boundary conditions for the problem. On the contrary, in previous studies, solid phases are stationary. Although, they are moved but available literatures have not provided appropriate boundary conditions for the fluid flow in PCL.

1.3 Objectives of the thesis

1). To determine the velocity of PCL fluid due to the movement of cilia where the Beaver-Joseph boundary condition is employed at the free-fluid/porous medium interface by using the asymptotic expansion method.

2). To determine the boundary conditions at the porous medium/ free-fluid interface due to the movement of the cilia by using asymptotic expansion method.

1.4 Scopes of the thesis

1). Consider the problem in a one-dimensional domain.

2). The velocity of the PCL fluid can be expanded in the form of asymptotic expansion.

3). The maximum velocity of motile cilia value is assumed to occure at the tips of cilia and cilia stop beating when the angle between cilia and horizontal plane is 40° [36].

4). The velocity of the solid phase is a linear function.

5). The maximum velocity of motile is assumed to occure at the angle 90°.

6). The velocity v of PCL fluid must be continuous enough so that $\lim_{y^+ \to y^+_{Stoke}} \frac{df\left(y^+,\varepsilon\right)}{dy^+} = \frac{d}{dy^+} \lim_{y^+ \to y^+_{Stoke}} \left(f\left(y^+,\varepsilon\right)\right)$.

7). The considered fluid is a Newtonian fluid.

1.5 Plan of the thesis

Plan of the thesis	Aug. 2016	Aug. 2017	Aug. 2018	Aug. 2019	Aug. 2020	Aug. 2021	Aug. 2022
1. Study the basic knowledge about the governing equations: the n-dimensional Stokes–Brinkman equations and the boundary conditions at the porous/ free-fluid interface.	←	—	→				
2. Study and review the literatures and related researches.		←	—	—	→		
3. Normalize the Stokes–Brinkman equations and the boundary conditions at the free-fluid/ porous medium interface used in our domain.			←	—	→		
4. Determine the velocity of PCL fluid due to the movement of cilia where the Beaver-Joseph boundary condition is employed at the free-fluid/porous medium interface.				←	→		
5. Publish the first research paper.					← →		
6. Study the method of matched asymptotic expansion.			←	—	—	→	
7. Find the boundary conditions at the porous medium/ free-fluid interface that proper to our problem				←	—	→	
8. Publish the second research paper.					←	— →	
9. Write a complete research report.					←	—	→

1.6 Expected results

1). Obtain the velocity of PCL fluid due to the movement of cilia.

2). Obtain the proper boundary conditions at the interface between the free-fluid and the porous medium with the moving solid phases.

3). Comparison the velocity of PCL fluid in the free-fluid region with our boundary condition at the interface with an experimental study data to confirm that the solution we get tends to be consistent with the experimental results, when the velocity of the solid phases are set to be zero.

4). Comparison the velocity of PCL fluid with our boundary condition at the free-fluid/ porous-medium interface with the velocity of the PCL fluid using the Beaver-Joseph boundary condition at the free-fluid/ porous-medium interface, in order to study the results obtained our boundary condition at the free-fluid/ porous-medium interface and the result using the Beaver-Joseph boundary condition at the free-fluid/ porous-medium interface that are similar or different, when the velocity of the solid phases are moving.

.

Chapter 2
Asymptotic Expansion Method

Differential equations have been widely used in mathematical models for finding problem solutions. However, some solutions of partial differential equations such as diffusion equations, mass/heat transfer equations, cannot be solved for exact solutions. These problems, then, need approximation methods for finding approximate solution such as finite difference, finite element, and asymptotic expansion approaches. In this thesis we use asymptotic expansion method to determine the velocity of PCL fluid and match asymptotic expansion method to define the boundary at the interface between the porous medium and free fluid region by using Stokes-Brinkman equation.

2.1 Asymptotic expansion method

The asymptotic expansion method is the tool for finding analytical approximate solutions to complicated practical problem, for example, the problem in ordinary differential equations in term of regular perturbation and singular perturbation. We construct different asymptotic solutions inside and outside the region of rapid change and match term together to determine a global solution. Other methods used for finding exact and approximate solutions for linear and nonlinear partial differential equations is the homotopy perturbation method which is only a special case of the homotopy analysis method. The basic ideas of the homotopy perturbation method is a coupling of the traditional perturbation method and homotopy in topology deforming continuously the problem to a simple one which can be easily solved. The advantage of this method is that it can be applied to various nonlinear problems, and the disadvantage is that we should suitably choose an initial guess, or infinite iterations are required. The asymptotic expansion method and the homotopy perturbation method are principally based on a Taylor series with respect to an embedding parameter. While the asymptotic expansion method can be used to study the interface between the porous media region and the free fluid region, the homotopy perturbation method and the fractal derivative model are only adopted for the porous media domain. These three approaches are the tools for finding analytical approximate solutions to the problem in ordinary differential equations or partial differential equations. Another difference is that the asymptotic expansion method can be applied to solve linear ordinary differential equations and perturbation equations. On the other hand, the homotopy perturbation method and the fractal derivative model are used to derive the solutions to nonlinear ordinary differential equations or partial differential

equations. Asymptotic analysis is a powerful tool for deriving approximate solutions to problems, allowing us to determine concise and precise estimates of quantities of interest when analyzing problems. Its rigorous foundation was established by Poincare and Stieltjes in 1886 [37]. In their work, the motion of a fluid or gas with small viscosity along a body was examined. In the case of an airfoil moving through air, such problem is described by the Navier – Stokes equations with large Reynolds number. The method of singular perturbation was proposed.

Definition of Big-O and little-o

Big-O and little-o notations have very similar definitions, and their difference lies in how strict they are regarding the upper bound they represent [41].

2.1.1 Big-o

For a given function $g(n)$, $O(g(n))$ is defined as: $O(g(n)) = \{ f(n) :$ there exist positive constants c and n_0 such that $0 \le f(n) \le cg(n)$ for all $n \ge n_0 \}$. So $O(g(n))$ is a set of functions that are, after n_0, smaller than or equal to $g(n)$. The function's behavior before n_0, is unimportant since big-O notation (also little-o notation) analyzes the function for huge numbers. As an example, let's have a look at the following figure [42]:

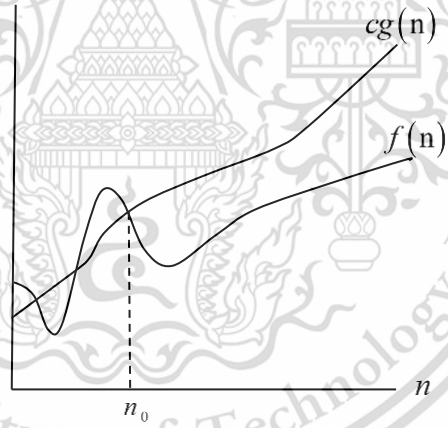

$f(n) = O(g(n))$

Here, $f(n)$ is only one of the possible functions that belong to $O(g(n))$. Before $f(n)$ is not always smaller than or equal to $g(n)$, but after n_0, it never goes above $g(n)$.

The equal sign in the definition represents the concept of asymptotical tightness, meaning that when n gets very large, $f(n)$ and $g(n)$ grow at the same rate. For instance, $3n^3 = O(n^3)$ satisfies the equal sign, hence it is asymptotically tight, while $3n = O(n^3)$ is not.

2.1.2 Little-o

Little-o notation is used to denote an upper-bound that is not asymptotically tight. It is formally defined as: $o(g(n)) = \{ f(n) :$ for any positive constant c, there exists positive constant n_0 such that $0 \le f(n) < cg(n)$ for all $n \ge n_0 \}$. Note that in this definition, the set of functions $f(n)$ are strictly smaller than $cg(n)$, meaning that little-o notation is a stronger upper bound than big-O notation. In other words, the little-o notation does not allow the function $f(n)$ to have the same growth rate as $g(n)$. Intuitively, this means that as the n approaches infinity, $f(n)$ becomes insignificant compared to $g(n)$. In mathematical terms:

$$\lim_{n\to\infty} \frac{f(n)}{g(n)} = 0.$$

In addition, the inequality in the definition of little-o should hold for any constant c, whereas for big-O, it is enough to find some c that satisfies the inequality.
If we drew an analogy between asymptotic comparison of $f(n)$ and $g(n)$ and the comparison of real numbers a and b, we would have $f(n) = O(g(n)) \approx a \le b$ while $f(n) = o(g(n)) \approx a < b$. For example, let $d(n) = 3n^3 + 2n + 10$. Suppose we need to prove that $d(n) = O(n^3)$. This means we need to find two positive integers, c and n_1 such that $0 \le d(n) \le cn^3$ for all $n \ge n_1$. We know that
$d(n) = 3n^3 + 2n + 10 \le 3n^3 + 2n^3 + 10x^3 = 15n^3$ for $n \ge 1$. So $d(n) \le 15n^3$.
If we set $n_1 = 1$ and $c = 15$, then we have that for any $n \ge n_1, 0 \le d(n) \le cn^3$. So $d(n) = O(n^3)$. We can have other values for n_1 and c which satisfy the above condition. Therefore, there exist x_1 and c which satisfy the condition [41].

2.2 Basic Definition of Asymptotic Expansion Method

In this section, the basic definitions of the asymptotic expansion method are presented as well as some notations for this study. Define $D \subset R^d$ with $d \in \mathbb{N}$ be an open subset in R^d. Let f, g and $h : D \to R$ are real continuous functions. We denote a small quantity by ε [40].

Definition 2.2.1 Asymptotic Sequence

A sequence $\{\varphi_n(x)\}$ of gauge functions, a device used to make measurements or in order to display certain dimensional information. when $n = 0,1,2,...$ is said to be an asymptotic sequence as $x \to x_0$, if

$$\varphi_{n+1}(x) = O(\varphi_n(x))$$

Definition 2.2.2 Asymptotic Expansion

If $\varphi_n(x)$ is an asymptotic sequence of gauge functions as $x \to x_0$, we say that

$$f(x) = \sum_{n=1}^{N} a_n \varphi_n(x) + O(\varphi_N(x)),$$

is an asymptotic expansion and a_n is a constant [40].

2.3 Solution of asymptotic expansion

With the ordinary differential equation

$$L_0[u] + \varepsilon L_1[u] = f_0 + \varepsilon f_1, \text{ in } D, \tag{2.3.1}$$

when L_0 and L_1 are known as the operators, f_0 and f_1 are the body forces in the case that $\varepsilon \to 0$, we have

$$L_0[u] = f. \text{ in } D. \tag{2.3.2}$$

The coefficient of ε, $L_1[u]$ and f_1, are called perturbations.

Let E_ε denotes the problem (2.3.1), and E_0 denotes the problem (2.3.2). The solution of problems (2.3.1) and (2.3.2) are denoted by u^ε and u^0, respectively [40].

2.4 Perturbation Method

A perturbation method is a method that has a dimensionless small parameter ε in the problem. This method is used to find an approximate solution of a problem.The perturbation methods are divided into regular perturbation and singularperturbation. Mathematical equations arising from physical sciences contain parameters. Perturbation theory examines parameter dependence of solutions locally. To present basic ideas simply, consider a one-parameter family of functions: For each in a set and real parameter in a punctured neighborhood of the values of the functions are in a metric space. The range is a metric space so that convergence of as can be discussed. Is to be regarded as a solution of some set of equations containing as a paremeter. The equations are called a regular perturbed problem if all solutions converge uniformly on as If there is a solution which does not converge uniformly, the problem is called singular perturbed. Notice that the category, regular or singular, is formulated in terms of the solutions, and not the equations [38]. To construct an asymptotic expansion, we define the following formula:

$$x^\varepsilon = \varepsilon^{\alpha_0}\left(x_0 + \varepsilon^{\alpha_1} x_1 + \varepsilon^{\alpha_2} x_2 + \ldots\right), \tag{2.4.1}$$

where $\alpha_i (i = 0,1,2,\ldots)$ are constant to be determined, and it is assumed without the loss of generality that

$$x_0 \text{ and } x_1 \neq 0, \text{ and } 0 < \alpha_1 < \alpha_2 < \ldots \text{ and} \tag{2.4.2}$$

α_0 is needed to be determined, and there are three cases that should be taken into account. That is

Case I) $\alpha_0 > 0$

Case II) $\alpha_0 < 0$

Case III) $\alpha_0 = 0$

Next, we show that only the case III) is possible to get an asymptotic expansion. Substituting (2.4.1) into (2.4.8), we have

$$\varepsilon^{2\alpha_0} x_0^2 + 2\varepsilon^{2\alpha_0+\alpha_1} x_0 x_1 + \varepsilon^{2(\alpha_0+\alpha_1)} x_1^2 - \varepsilon^{\alpha_0} x_0 - \varepsilon^{\alpha_0+\alpha_1} x_1 - 1 + \ldots = 0. \tag{2.4.3}$$

For the case I), $\alpha_0 > 0$, it becomes that the coefficient of ε^{α_0} is zero. Then $x_0 = 0.$ This is in the contradiction to the assumption that $x_0 \neq 0$. For case II), $\alpha_0 < 0$, from (2.4.4), we have $2\alpha_0 < \alpha_0 < \alpha_0 + \alpha_1.$ Then the coefficient of $\varepsilon^{2\alpha_0}$ is equal to zero from (2.4.5). Thus $x_0^2 = 0.$ Therefore $x_0 = 0.$ This is also in contradiction to the assumption that $x_0 \neq 0$. Therefore, it is asserted that only the case III), $\alpha_0 = 0,$ is possible, so (2.4.6) becomes

$$x^{\varepsilon} = x_0 + \varepsilon^{\alpha_1} x_1 + \varepsilon^{\alpha_2} x_2 + \ldots. \tag{2.4.7}$$

2.4.1 Regular Perturbation

A regular perturbation is one of the perturbed problems depending on a small, nonzero parameter $\varepsilon.$ The solution of the regular perturbation problem is the same as the unperturbed problem for $\varepsilon \to 0$ [40].

An example of regular perturbation is as follows. Let

$$x^2 - \varepsilon x - 1 = 0. \tag{2.4.8}$$

Then (2.3.1) becomes

$$x^2 - 1 = 0. \tag{2.4.9}$$

From (2.4.8), the solutions are

$$x_1^{\varepsilon} = \frac{\varepsilon + \sqrt{\varepsilon^2 + 4}}{2} \quad \text{and} \quad x_2^{\varepsilon} = \frac{\varepsilon - \sqrt{\varepsilon^2 + 4}}{2} \tag{2.4.10}$$

From (2.4.9), the solutions are

$$x_1^0 = 1 \quad \text{and} \quad x_2^0 = -1. \tag{2.4.11}$$

Then, it is seen that x_i^{ε} converge to x_i^0 when $\varepsilon \to 0$, $i = 1, 2.$ Then

$$x_1^{\varepsilon} \to x_1^0 \quad \text{and} \quad x_2^{\varepsilon} \to x_2^0. \tag{2.4.12}$$

Therefore, (2.4.8) is called a regular perturbation of (2.4.9). It should be taken some note that x^{ε} depends on ε. Next, we find the solution of (2.4.8) using the asymptotic expansion method.

$$x^{\varepsilon} = x_0 + \varepsilon^1 x_1 + \varepsilon^2 x_2 + \ldots. \tag{2.4.13}$$

Substituting (2.4.13) into (2.4.8), we have

$$\left(x_0 + \varepsilon x_1 + \varepsilon^2 x_2 + \ldots\right)^2 - \varepsilon\left(x_0 + \varepsilon x_1 + \ldots\right) - 1 = 0.$$

Collecting the same orders of ε, we obtain

$$\varepsilon^0 : x_0^2 - 1 = 0 \tag{2.4.14}$$

$$\varepsilon^1 : 2x_0x_1 - x_0 = 0 \tag{2.4.15}$$

$$\varepsilon^2 : 2x_0x_2 + x_1^2 - x_1 = 0. \tag{2.4.16}$$

The solutions of (2.4.14) are $x_0 = 1$ or $x_0 = -1$. In case of $x_0 = 1$, we have $x_1 = \frac{1}{2}$ and $x_2 = \frac{1}{8}$ respectively. The solution up to the second order of ε is

$$x^\varepsilon = 1 + \frac{\varepsilon}{2} + \frac{\varepsilon^2}{8}. \tag{2.4.17}$$

In case of $x_0 = 1$, we have $x_1 = \frac{1}{2}$ and $x_2 = -\frac{1}{8}$ Therefore, we expand x^ε as follows.

$$x^\varepsilon = 1 + \frac{\varepsilon}{2} - \frac{\varepsilon^2}{8}. \tag{2.4.18}$$

An example ordinary differential equation with regular perturbation is

$$\frac{du^\varepsilon}{dx} + u^\varepsilon = \varepsilon x, \tag{2.4.19}$$

$$u^\varepsilon(0) = 1. \tag{2.4.20}$$

If $\varepsilon \to 0$, Eqs. (2.4.19) – (2.4.20) become

$$\frac{du}{dx} + u = 0, \tag{2.4.21}$$

$$u(0) = 1. \tag{2.4.22}$$

Then the solutions of (2.4.19) – (2.4.20) and (2.4.21)– (2.4.22) are

$$u^\varepsilon(x) = (1+\varepsilon)e^{-x} + \varepsilon(x-1), \tag{2.4.23}$$

and

$$u^0(x) = e^{-x}, \tag{2.4.24}$$

respectively. The asymptotic expansion of u^ε is defined in the form

$$u^\varepsilon(x) = u_0(x) + \varepsilon u_1(x) + \varepsilon^2 u_2(x) + \ldots \tag{2.4.25}$$

Substituting (2.4.25) into (2.4.19) and collecting the same orders of ε, we obtain

$$\varepsilon^0 : u_0' + u_0 = 0 \tag{2.4.26}$$

$$\varepsilon^1 : u_1' + u_1 = x \tag{2.4.27}$$

$$\varepsilon^2 : u_2' + u_2 = 0. \tag{2.4.28}$$

From (2.4.20) and (2.4.25), we have

$$1 = u^\varepsilon(0) = u_0(0) + \varepsilon u_1(0) + \varepsilon^2 u_2(0) + \ldots \tag{2.4.29}$$

Then, $u_0(0) = 1$ and

$$0 = \varepsilon u_1(0) + \varepsilon^2 u_2(0) + \ldots \tag{2.4.30}$$

Therefore

$$0 = u_1(0) + \varepsilon u_2(0) + \ldots \tag{2.4.31}$$

If $\varepsilon \to 0$, then $u_1(0) = 0.$ According to the same condition, we obtain

$$u_0(0) = 1, \tag{2.4.32}$$

$$u_1(0) = 0, \tag{2.4.33}$$

$$u_2(0) = 0. \tag{2.4.34}$$

Finding the solutions of (2.4.26) - (2.4.28) with the boundary conditions (2.4.32) - (2.4.34), we have

$$u_0(x) = e^{-x} \tag{2.4.35}$$

$$u_1(x) = x - 1 + e^{-x} \tag{2.4.36}$$

$$u_2(x) = 0. \tag{2.4.37}$$

Therefore, from (2.4.25), The solution up to the second order of ε is the approximate solution of (2.4.19) is

$$u^{\varepsilon}(x) \approx (1+\varepsilon)e^{-x} + \varepsilon(x-1). \tag{2.4.38}$$

2.4.2 Singular Perturbation

A singular perturbation is one of the perturbed problem, where the solution of the singular problem is different from the unperturbed problem when $\varepsilon \to 0$. An example of ordinary differential equation with singular perturbation is as follows [40]. Let

$$\varepsilon \frac{du^{\varepsilon}}{dx} + u^{\varepsilon} = x \tag{2.4.39}$$

$$u^{\varepsilon}(0) = 1. \tag{2.4.40}$$

The solution of the associated one $\varepsilon \to 0$ is

$$u(x) = x \tag{2.4.41}$$

Therefore

$$u(0) = D. \tag{2.4.42}$$

Note that (2.4.42) and (2.4.40) are different. Then (2.4.39) and (2.4.40) are singular perturbation.

2.5 The Method of Matched Asymptotic Expansion

Since some problems have transition zones between two adjacent and

different regions, the transition zone is called inner region and the others are named outer region. From Figure 2.1, the outer regions of the problem are the free-fluid domain and the porous medium. The inner zone of the problem is the area at the interface between the free fluid/porous-medium domain. Then the solutions obtained from these different regions are matched by a condition, which is enable us to establish a solution which is valid uniformly in the whole domain. Next, we show how to find the outer and inner solutions and provide a matching condition used in this work [40].

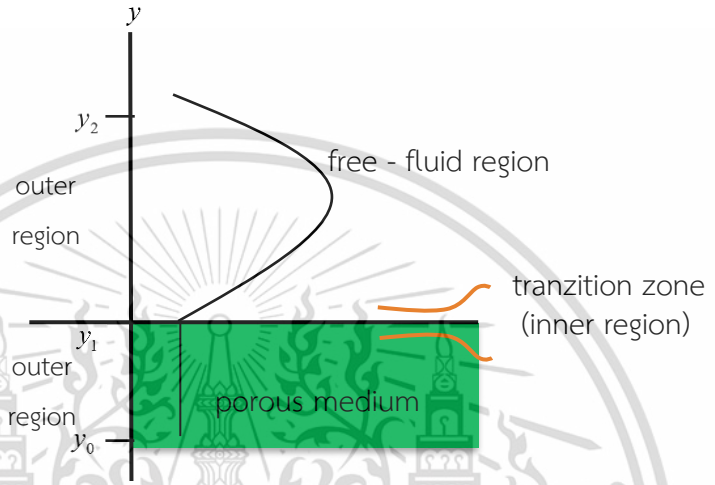

Figure 2.1 Shows the outer and inner regions [3]

Figure 2.1 shows the outer regions: the free-fluid region (y_1 - y_2) and the porous medium domain (y_0 - y_1), and the inner region which is the domain between the free-fluid region and the porous medium domain called transition zone.

2.5.1 Outer Expansion

We expand the outer solution in the asymptotic form. That is

$$u^{\varepsilon}(x,\varepsilon) = u_0(x) + \varepsilon u_1(x) + \varepsilon^2 u_2(x) + ..., \tag{2.5.1}$$

Substituting (2.5.1) into (2.4.39) and collecting the same orders of ε, we have

$$\varepsilon^0 : u_0(x) = x, \tag{2.5.2}$$

$$\varepsilon^1 : u_1(x) + u_0'(x) = 0, \tag{2.5.3}$$

$$\varepsilon^2 : u_2(x) + u_1'(x) = 0. \tag{2.5.4}$$

Solving the problems (2.5.2) - (2.5.4), the outcomes yield

$$u_0(x) = x, \tag{2.5.5}$$

$$u_1(x) = -1, \tag{2.5.6}$$

$$u_2(x) = 0, \tag{2.5.7}$$

Substituting (2.5.5) - (2.5.7) into (2.5.1), The solution up to the second order of ε is we obtain the outer solution

$$u(x) = x - \varepsilon. \tag{2.5.8}$$

Note that from (2.5.5), then we have which is different from the given condition (2.4.40). Then $u_0(0) \neq \varepsilon u_1(0) + \varepsilon^2 u_2(0) + \ldots = 1.$

2.5.2 Inner Expansion

To construct the inner expansions, we introduce the variable.

$$\xi = \frac{x}{\varepsilon}. \tag{2.5.9}$$

For a beginner, it may not be easy to understand why ξ is defined in this form, and the power of ε which is shown above. From the previous section, one may assume a more general form of $\xi = \frac{x}{\varepsilon^{\alpha}}$ with $\alpha \in \mathbb{R}$. Then, repeating all the above procedure again, it is proved that α must be equaled to 1 in order to get an asymptotic expansion. Moreover, it already has that a boundary layer occurs at $x = 0.$ Therefore, if the assumption is incorrect, the procedure will break down when the inner and outer expansions are being matched in the intermediate region. At this point, it can be assumed that there exists a boundary layer near a point $x = x_0$ [40].

If an inner expansion is an expansion in terms of ξ, it can be assumed that:

$$U^{\varepsilon}(\xi, \varepsilon) = U_o(\xi) + \varepsilon U_1(\xi) + \varepsilon^2 U_2(\xi) + \ldots \tag{2.5.10}$$

From (2.5.10), we obtain

$$\frac{dU_i(\xi)}{dx} = \frac{1}{\varepsilon}\frac{dU_i(\xi)}{d\xi}, i = 0,1,2,\ldots \tag{2.5.11}$$

Substituting (2.5.11) into (2.4.39), and collecting the coefficient of $\varepsilon^i, i = -1,0,1,2,\ldots$, then we have

$$\varepsilon^{-1} : U_0' + U_0 = 0, \tag{2.5.12}$$

$$\varepsilon^{0} : U_1' + U_1 = \xi, \tag{2.5.13}$$

$$\varepsilon^{1} : U_2' + U_2 = 0. \tag{2.5.14}$$

Therefore

$$U_0(\xi) = C_0 e^{-\xi}, \tag{2.5.15}$$

$$U_1(\xi) = C_1 e^{-\xi} + \xi - 1, \tag{2.5.16}$$

$$U_2(\xi) = C_2 e^{-\xi}. \tag{2.5.17}$$

From $x = \xi\varepsilon,$ and $U_0(0) = 1,$ then we obtain

$$U_0(0) + \varepsilon U_1(0) + \ldots = 1. \tag{2.5.18}$$

Therefore $U_0(0) = 1, U_1(0) = 0, U_2(0) = 0.$ Then $C_0 = 1, C_1 = 1,$ and $C_2 = 0.$

Therefore, The solution up to the second order of ε is we obtain an inner expansion as follows.

$$U(\xi)=(1+\varepsilon)e^{-\xi}+\varepsilon(\xi-1). \tag{2.5.19}$$

2.5.3 Matched Asymptotic Expansion of Solutions

In this section, we discuss an approach used to combine the inner and outer solutions. The matching condition is Van Dyke's rule [40], then

$$\lim_{\xi\to\infty}U^{\varepsilon}(\xi,\varepsilon)=\lim_{x\to 0}u^{\varepsilon}(x,\varepsilon). \tag{2.5.20}$$

With the outer and inner varaibles,

$$u^{\varepsilon}(x,\varepsilon)=u_0(x)+\varepsilon u_1(x)+\varepsilon^2u_2(x)+O(\varepsilon^3) \tag{2.5.21}$$

$$U^{\varepsilon}(\xi,\varepsilon)=U_o(\xi)+\varepsilon U_1(\xi)+\varepsilon^2U_2(\xi)+O(\varepsilon^3), \tag{2.5.22}$$

we find the matching condition of u_0 by substituting (2.5.21) and (2.5.22) into (2.5.20), we obtain

$$\lim_{\xi\to\infty}\left[U_o(\xi)+\varepsilon U_1(\xi)+\varepsilon^2U_2(\xi)+O(\varepsilon^3)\right]=\lim_{x\to 0}\left[u_0(x)+\varepsilon u_1(x)+\varepsilon^2u_2(x)+O(\varepsilon^3)\right]. \tag{2.5.23}$$

Suppose that $\lim_{x\to 0}u_i(x)$ and $\lim_{\xi\to\infty}U_i(\xi)$ exist, $i=0,1,2,\ldots$ Then, considering the zeroth order term of ε, we have

$$\lim_{\xi\to\infty}U_i(\xi)=\lim_{x\to 0}u_i(x), \tag{2.5.24}$$

for all $i=0,1,2,\ldots$ Next, we find another matching condition by applying the Tayloy's series expansion to each u_i in (2.5.21) around the point 0, and we assume that $u_i(x), i=0,1,2,3,\ldots$ are continuous so that

$$u_i(0)=\lim_{x\to 0}u_i(x),\ i=1,2,3,\ldots \tag{2.5.25}$$

Therefore,

$$u^{\varepsilon}(x,\varepsilon)=\lim_{x\to 0}\left[u_0(x)+\varepsilon u_1(x)+\varepsilon^2u_2(x)+O(\varepsilon^3)\right] \tag{2.5.26}$$

$$u^{\varepsilon}(x,\varepsilon)=\lim_{x\to 0}\left[\begin{array}{l}u_0(x)+\dfrac{(x-0)}{1!}\dfrac{du_0(x)}{dx}+\dfrac{(x-0)^2}{2!}\dfrac{d^2u_0(x)}{dx}+O(x-0)^3\\ +\varepsilon\left(u_1(x)+\dfrac{(x-0)}{1!}\dfrac{du_1(x)}{dx}+O(x-0)^2\right)+O(\varepsilon^2)\end{array}\right] \tag{2.5.27}$$

$$\begin{aligned}u^{\varepsilon}(x,\varepsilon)=&\left[\lim_{x\to 0}u_0(x)+\lim_{x\to 0}\frac{(x-0)}{1!}\frac{du_0(x)}{dx}+\lim_{x\to 0}\frac{(x-0)^2}{2!}\frac{d^2u_0(x)}{dx}+\lim_{x\to 0}O(x-0)^3\right]\\&+\varepsilon\left[\lim_{x\to 0}u_1(x)+\lim_{x\to 0}\frac{(x-0)}{1!}\frac{du_1(x)}{dx}+\lim_{x\to 0}O(x-0)^2\right]+O(\varepsilon^2).\end{aligned} \tag{2.5.28}$$

From $x=\varepsilon\xi,$ then we have

$$u^{\varepsilon}(x,\varepsilon)=\left[\lim_{x\to 0}u_0(x)+\varepsilon\xi\lim_{x\to 0}\frac{du_0(x)}{dx}+\frac{(\varepsilon\xi)^2}{2!}\lim_{x\to 0}\frac{d^2u_0(x)}{dx}+O(\varepsilon\xi)^3\right]$$
$$+\varepsilon\left[\lim_{x\to 0}u_1(x)+(\varepsilon\xi)\lim_{x\to 0}\frac{du_1(x)}{dx}+O(\varepsilon\xi)^2\right]+O(\varepsilon^2).$$

(2.5.29)

Diferrentiating (2.5.29) with respect to $\xi,$ taking $x\to 0$ on both sides and ommiting the big O, then we obtain

$$\lim_{x\to 0}\frac{du^{\varepsilon}(x,\varepsilon)}{d\xi}=\varepsilon\lim_{x\to 0}\frac{du_0(x)}{dx}+\varepsilon^2\xi\lim_{x\to 0}\frac{d^2u_0(x)}{dx}+\varepsilon^2\lim_{x\to 0}\frac{du_1(x)}{dx}. \qquad (2.5.30)$$

To find the matching condition for the first derivative of $U^{\varepsilon}(\xi,\varepsilon),$ we differentiating (2.5.22) with respect to ξ and taking limit $\xi\to\infty$ on both sides, we obtain

$$\lim_{\xi\to\infty}\frac{dU^{\varepsilon}(\xi,\varepsilon)}{d\xi}=\lim_{\xi\to\infty}\left[\frac{dU_o(\xi)}{d\xi}+\varepsilon\frac{dU_1(\xi)}{d\xi}+\varepsilon^2\frac{d^2U_2(\xi)}{d\xi}\right]. \qquad (2.5.31)$$

Since we assume that the velocity of PCL fluid is continuous enough to the differentiation can be switched with the limit, from (2.5.20), we have

$$\lim_{x\to 0}\frac{du^{\varepsilon}(x,\varepsilon)}{d\xi}=\lim_{\xi\to\infty}\frac{dU^{\varepsilon}(\xi,\varepsilon)}{d\xi}. \qquad (2.5.32)$$

Note that (2.5.30) and (2.5.31) are equal. Then we get

$$\varepsilon\lim_{x\to 0}\frac{du_0(x)}{dx}+\varepsilon^2\xi\lim_{x\to 0}\frac{d^2u_0(x)}{dx}+\varepsilon^2\lim_{x\to 0}\frac{du_1(x)}{dx}=\lim_{\xi\to\infty}\left[\frac{dU_o(\xi)}{d\xi}+\varepsilon\frac{dU_1(\xi)}{d\xi}+\varepsilon^2\frac{d^2U_2(\xi)}{d\xi}\right]. \qquad (2.5.33)$$

Collecting the same order of ε in (2.5.33), we obtain

$$\varepsilon^0:\lim_{\xi\to\infty}\frac{dU_o(\xi)}{d\xi}=0, \qquad (2.5.34)$$

$$\varepsilon^1:\lim_{\xi\to\infty}\frac{dU_1(\xi)}{d\xi}=\lim_{x\to 0}\frac{du_0(x)}{dx}, \qquad (2.5.35)$$

$$\varepsilon^2:\lim_{\xi\to\infty}\frac{d^2U_2(\xi)}{d\xi}=\xi\lim_{x\to 0}\frac{d^2u_0(x)}{dx}+\lim_{x\to 0}\frac{du_1(x)}{dx}. \qquad (2.5.36)$$

The solution up to the second order of ε is next, we will work on the matching condition (2.5.34) - (2.5.36) to match the solution of both the outer zone and inner zone in Chapter 3.

Chapter 3

One dimensional problem of Stokes – Brinkman equations

In this chapter, we provide the Stokes-Brinkman equations and boundary conditions used in this study including their dimensionless forms. The governing equations and boundary conditions are provided in Sections 3.1 and 3.2, respectively. The dimensionalization of the governing equation and boundary conditions are presented in Section 3.3.

3.1 Stokes – Brinkman equations

In this section, we introduce our governing equations, the Stokes–Brinkman equations, for n dimension derived by using an upscaling method of changing a microscale equation to be a macroscale equation where the variables are arranged quantities. The Stokes–Brinkman equations in the macroscopic scale are [33]

$$\mu k^{-1}\cdot\left(\varepsilon^{l}v^{l}\right)+\nabla p-\frac{\mu}{\varepsilon^{l}}\Delta\left(\varepsilon^{l}v^{l}\right)=\rho g+\mu k^{-1}\cdot\varepsilon^{l}v^{s}+\frac{\mu}{\varepsilon^{l}}\nabla f, \tag{3.1}$$

$$\nabla\cdot\left(\varepsilon^{l}\mathbf{v}^{l}\right)=f, \tag{3.2}$$

where the function $f=\frac{-\varepsilon^{\cdot l}}{\left(1-\varepsilon^{l}\right)}+\nabla\cdot\varepsilon^{l}\mathbf{v}^{s}$; μ is a dynamic viscosity; k^{-1} is the inverse of the permeability tensor; ε^{l} is the porosity; v^{l} and v^{S} are the velocities of the liquid and solid phases, respectively; p is the pressure; ρ is the fluid density; g is gravity; and $\varepsilon^{\cdot l}$ is the material time derivative of the porosity with respect to the solid phase, $\varepsilon^{\cdot l}=\frac{\partial\varepsilon^{l}}{\partial t}+\mathbf{v}^{s}\cdot\nabla\varepsilon^{l}$. The equation (3.1) is derived from the conservation of momentum, while the equation (3.2) derived from the continuty equation [39]. The equation (3.1) is the Brinkman equation. Without the first and fifth terms in the equation, it is the Stokes equation. Thus, in general, the equation (3.1) is called Stokes-Brinkman equations.

The left of Figure 3.1 shows the cilia in PCL layer in 3-dimensianal domain. The right of the picture shows the cilia move forward and form an angle $\theta,\theta<90^{\circ}$ with the horizontal plane. The blue arrow shows the direction of fluid flow.

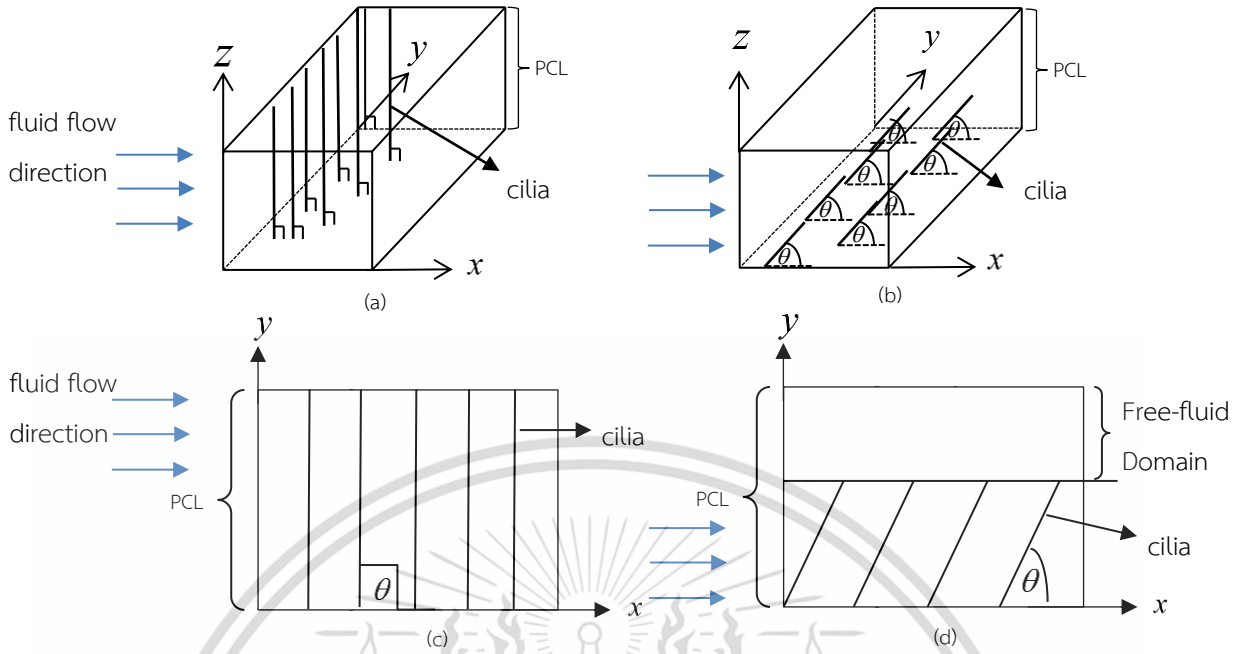

Figure 3.1 illustrates the direction of fluid flow over the porous medium

In this study, we assume that the solid velocity depends on only the y direction; the fluid flows along the x-axis; and the pressure depends on the x direction as shown in Figure 3.1. We assume that the pressure gradient is a constant along x direction. The velocity of the PCL fluid depends on the movement of cilia, where the velocity of cilia depends only on y direction. From Figure 3.1(a), when simplify into one-dimension, it is shown in Figure 3.1(c) and from Figure 3.1(b), when simplify into one-dimension, it is shown in Figure 3.1(d). As in Figure 3.1, (3.1) becomes

$$\frac{2\mu}{\varepsilon^l}\frac{d^2\left(\varepsilon^l v^l\right)}{dy^2}-\mu k_{11}^{-1}\left(\varepsilon^l v^l\right)+\rho g=\frac{dp}{dx}-\mu k_{11}^{-1}\left(\varepsilon^l v^s\right). \tag{3.3}$$

The Stokes equation is the equation (3.3) without the terms consisting of the permeability k_{11} and $\varepsilon^l=1$. That is

$$2\mu\frac{d^2\left(\varepsilon^l v^l\right)}{dy^2}+\rho g=\frac{dp}{dx}. \tag{3.4}$$

The continuity equation applied in the free-fluid region is

$$\frac{\partial\left(\varepsilon^l v^l\right)}{\partial y}=0. \tag{3.5}$$

Let $u = \varepsilon^l v^l$.

Therefore (3.1) and (3.2) becomes

$$\frac{2\mu}{\varepsilon^l}\frac{d^2u}{dy^2} - \mu k_{11}^{-1}u + \rho g = \frac{dp}{dx} - \mu k_{11}^{-1}\left(\varepsilon^l v^s\right), \tag{3.6}$$

$$\frac{du}{dy} = f. \tag{3.7}$$

In this thesis, we use (3.6) and (3.7) in the asymptotic solution with the velocity to be a function of G and (3.4) and (3.5) becomes

$$2\mu\frac{d^2u}{dy^2} + \rho g = \frac{dp}{dx}, \tag{3.8}$$

$$\frac{du}{dy} = 0. \tag{3.9}$$

In this thesis, we use (3.8) and (3.9) in the asymptotic solution with the other velocity.

Notice that we have two different and adjacent domains. Therefore, boundary used at the interface is special. In this work we first applied the Beavers-Joseph boundary condition at the interface between the free-fluid region and the porous medium domain in the next section

3.2 Boundary conditions

No free-fluid region exists in the PCL when the cilia is perpendicular to the horizontal plane. Figure 3.1(a) shows that the PCL has only domain Ω_2. Figure 3.1(b) shows both domains Ω_1 and Ω_2 ; the boundary condition between Ω_1 and Ω_2 is at y_{Stoke}, the tips of the cilia. Note that y_{Stoke} depends on the angle θ

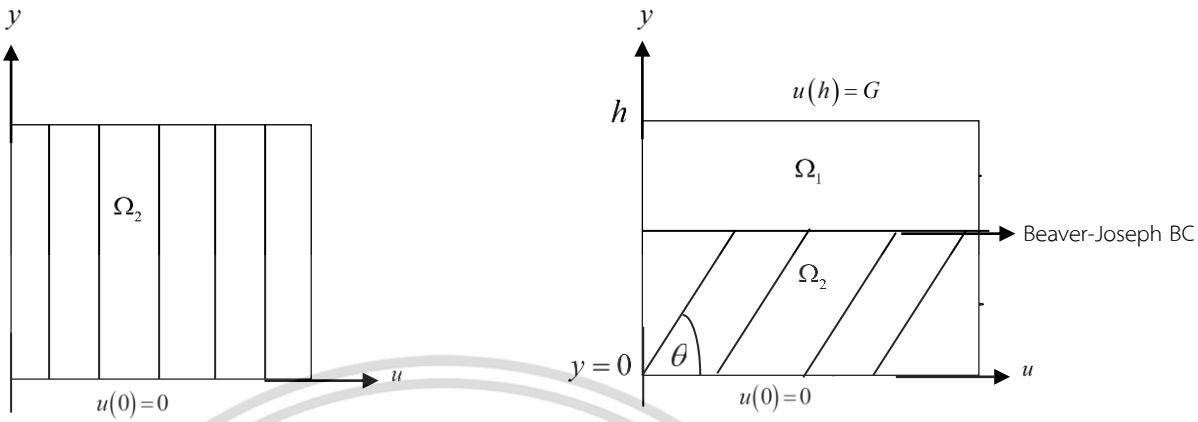

Figure 3.2 Cartoon picture of cilia; (a) cilia are perpendicular to the horizontal plane; (b) cilia making angle θ, $40^\circ \le \theta \le 90^\circ$, with the horizontal plane

Because the cilia are immobilized at the bottom of the domain, we assume that the PCL fluid has a no-slip condition at $y = 0$, that is

$$u = 0 \quad \text{at} \quad y = 0 \tag{3.10}$$

At the top boundary condition of the domain, we assume that the velocity is bounded by a constant and we use Beaver-Joseph boundary condition [30] at the free-fluid/ porous medium interface,

$$u = G \quad \text{at} \quad y = h \tag{3.11}$$

$$\left.\frac{du}{dy}\right|_{y=y^{+}_{stoke}} - \frac{1}{\varepsilon^{l}}\left.\frac{du}{dy}\right|_{y=y^{-}_{stoke}} = \frac{\beta}{\sqrt{k_{11}}}\left.u\right|_{y=y_{stoke}} \quad \text{at} \quad y = y_{Stoke}, \tag{3.12}$$

where β is a dimensionless parameter of the order of one, ε^{l} is porosity of the homogeneous porous medium, k_{11} is a permeability tensor, and G is a function depending on the angle θ.

3.3 Dimensionless Stokes–Brinkman Equations

In this section, we normalize the Stokes–Brinkman equations by introducing the following new variables,

$$y^{+} = \frac{y}{h}\ y^{+} = \frac{y}{h},\ U^{+} = \frac{\varepsilon^{l} v^{l}}{U_0}, v^{+} = \frac{v^{s}}{U_0},\ x^{+} = \frac{x}{h},\ K^{+} = \frac{k_{11}}{K_0},\ p^{+} = p\frac{h}{U_0 \mu} \ \text{and}\ g^{+} = \frac{g}{g_0}. \tag{3.13}$$

where h is the characteristic length; U_0 is volumetric average velocity in the porous medium; K_0 is characteristic permeability; and g_0 is characteristic gravity.

3.3.1 Dimensionless of Brinkman equation

We normalize the Brinkman equation by substituting (3.13) into (3.6). We then have

$$\frac{2\mu}{\varepsilon^l}\frac{d^2U^+U_0}{d\left(y^+h\right)^2}-\frac{\mu U^+U_0}{K^+K_0}+\rho g^+g_0=\frac{d\left(\frac{p^+U_0\mu}{h}\right)}{d\left(x^+h\right)}-\frac{\mu\left(\varepsilon^l v^+U_0\right)}{K^+K_0}. \tag{3.14}$$

Dividing μ both sides, we have

$$\frac{2}{\varepsilon^l}\frac{d^2U^+U_0}{d\left(y^+h\right)^2}-\frac{U^+U_0}{K^+K_0}\frac{\rho g^+g_0}{\mu}=\frac{d\left(\frac{p^+U_0}{h}\right)}{d\left(x^+h\right)}-\frac{\left(\varepsilon^l v^+U_0\right)}{K^+K_0} \tag{3.15}$$

Dividing U_0 both sides, we have

$$\frac{2}{\varepsilon^l}\frac{d^2U^+}{d\left(y^+h\right)^2}-\frac{U^+}{K^+K_0}+\frac{\rho g^+g_0}{\mu U_0}=\frac{d\left(\frac{p^+}{h}\right)}{d\left(x^+h\right)}-\frac{\left(\varepsilon^l v^+\right)}{K^+K_0}. \tag{3.16}$$

Multiplying h^2 both sides, we have

$$\frac{2}{\varepsilon^l}\frac{d^2U^+}{dy^{+2}}-\frac{h^2}{K_0K^+}U^++\frac{h^2\rho g^+g_0}{\mu U_0}=\frac{dp^+}{dx^+}-\frac{h^2\varepsilon^l v^+}{K_0K^+}. \tag{3.17}$$

Let $M_1=\frac{1}{\varepsilon^l},M_2=\frac{h^2}{K_0K^+},M_3=\frac{h^2\rho g^+g_0}{\mu U_0}$ are constants and $H\left(y^+\right)=\frac{h^2\varepsilon^l v^+}{K_0K^+}$ (3.18)

is a function of y^+. Then (3.17) can be rewritten as

$$2M_1\frac{d^2U^+}{dy^{+2}}-M_2U^++M_3=\frac{dp^+}{dx^+}-H\left(y^+\right). \tag{3.19}$$

3.3.2 Dimensionless Stokes equation

We normalize the Stokes equation (3.8) by substituting (3.13) into (3.8). We then obtain

$$2\mu\frac{d^2\left(U^+U_0\right)}{d\left(y^+h\right)^2}+\rho g^+g_0=\frac{d\left(\frac{p^+U_0\mu}{h}\right)}{d\left(x^+h\right)}. \tag{3.20}$$

Dividing μ both sides, we have

$$2\frac{d^2\left(U^+U_0\right)}{d\left(y^+h\right)^2}+\frac{\rho g^+ g_0}{\mu}=\frac{d\left(\frac{p^+U_0}{h}\right)}{d\left(x^+h\right)}. \tag{3.21}$$

Dividing U_0 both sides, we have

$$2\frac{d^2\left(U^+\right)}{d\left(y^+h\right)^2}+\frac{\rho g^+ g_0}{\mu U_0}=\frac{d\left(\frac{p^+}{h}\right)}{d\left(x^+h\right)}. \tag{3.22}$$

Multiplying h^2 both sides, we have

$$2\frac{d^2\left(U^+\right)}{dy^{+2}}+\frac{h^2\rho g^+ g_0}{\mu U_0}=\frac{d\,p^+}{dx^+}. \tag{3.23}$$

Then we have

$$2\frac{d^2U^+}{d\left(y^+\right)^2}=\frac{dp^+}{dx^+}-\frac{h^2\rho g^+ g_0}{\mu U_0}. \tag{3.24}$$

Then (3.24) can be rewritten as

$$2\frac{d^2U^+}{dy^{+2}}=\frac{dp^+}{dx^+}-M_3 \tag{3.25}$$

where M_3 are constants defined in (3.18).

3.3.3 Dimensionless boundary conditions by using Beaver-Joseph boundary condition at the free-fluid/ porous medium interface

In this section we normalize the Beaver-Joseph boundary conditions at the free-fluid/ porous medium interface used in our domain.

Substituting (3.13) into (3.12), we have

$$\left.\frac{d\left(U^+U_0\right)}{d\left(y^+h\right)}\right|_{y^+=\frac{y^+_{stoke}}{h}}-\frac{1}{\varepsilon^l}\left.\frac{d\left(U^+U_0\right)}{d\left(y^+h\right)}\right|_{y^+=\frac{y^-_{stoke}}{h}}=\frac{\beta}{\sqrt{K^+K_0}}\left(U^+U_0\right)\Big|_{y^+=\frac{y_{stoke}}{h}}. \tag{3.26}$$

Dividing U_0 both sides, we have

$$\left.\frac{d\left(U^+\right)}{d\left(y^+h\right)}\right|_{y^+=\frac{y^+_{stoke}}{h}}-\frac{1}{\varepsilon^l}\left.\frac{d\left(U^+\right)}{d\left(y^+h\right)}\right|_{y^+=\frac{y^-_{stoke}}{h}}=\frac{\beta}{\sqrt{K^+K_0}}\left(U^+\right)\Big|_{y^+=\frac{y_{stoke}}{h}}. \tag{3.27}$$

Multiplying h both sides, we have

$$\left.\frac{dU^+}{dy^+}\right|_{y^+=\frac{y^+_{stoke}}{h}}-\frac{1}{\varepsilon^l}\left.\frac{dU^+}{dy^+}\right|_{y^+=\frac{y^-_{stoke}}{h}}=\frac{h\beta}{\sqrt{K^+K_0}}U^+\Big|_{y^+=\frac{y_{stoke}}{h}}. \tag{3.28}$$

Next, we normalize the bottom and top boundary conditions by substituting (3.13) into (3.10), Therefore

$$U^+U_0=0 \qquad \text{at} \quad y^+h=0. \tag{3.29}$$

Then, we have

$$U^+=0 \qquad \text{at} \quad y^+=0 \tag{3.30}$$

Substituting (3.13) into (3.11), we obtain

$$U^+ = \frac{G}{U_0} \qquad \text{at} \quad y^+ = 1. \tag{3.31}$$

3.3.4 Dimensionless other boundary conditions

For the case of finding the proper boundary condition at the free-fluid/porous medium interface, we have the bottom boundary condition is $U^+ = 0$ at $y^+ = 0$ and the top boundary condition is

$$\lim_{y^+ \to 1} U^+\left(y^+\right) = \frac{C_0}{U_0} = D_0, \tag{3.32}$$

where D_0 is a constant as illustrated in Figure 3.2.

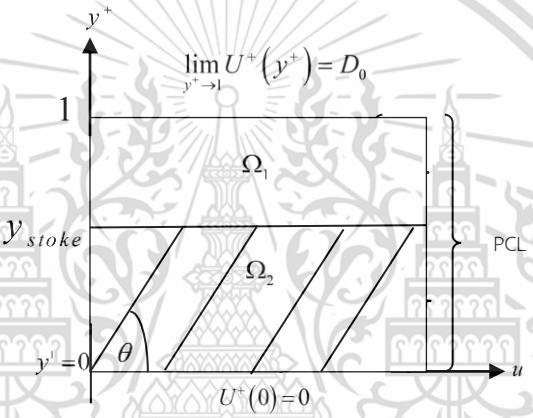

Figure 3.3 The cilia forming angle θ with the horizontal plane and boundary conditions

Chapter 4
The Zero-Order Solution of the Stokes-Brinkman Equations

In this chapter, we employ the method of asymptotic expansion to find the solutions in both domains Ω_1 and Ω_2. Because there exists a transition layer at the free-fluid/porous-medium interface, the approximation of this part of the domain is called inner solution. The approximation of other parts of the domain $\Omega_1 \cup \Omega_2$ is named outer solution. Then the solutions are combined through matching conditions provided in Section 4.3. The outer and inner solutions are provided in Sections 4.1 and 4.2, respectively. The zeroth-order results after applying the matching conditions are provided in Section 4.4. We compare our solution with an experimental data where the velocity of the solid phases in our solution is set to be zero in Section 4.5.

4.1 Outer Solution

As mentioned in Section 3.2, we have two different domains where the domain Ω_1 is the region that $y > y_{Stoke}$ and the region Ω_2 is the layer that $y < y_{Stoke}$. In this section, we find the analytical solution of the governing equations with the asymptotic expansion method. Section 4.1.1 shows the result of the Brinkman equation and Section 4.1.2 and 4.1.3 shows the result of the Stokes equation.

4.1.1 Asymptotic expansion method of the Brinkman equation

Using the method of asymptotic expansion, we assume that

$$U^{+} = U^{+(0)} + \varepsilon U^{+(1)} + \varepsilon^2 U^{+(2)} + O\left(\varepsilon^3\right). \tag{4.1}$$

Therefor. $$U^{+}\left(y^{+}\right) = U^{+(0)}\left(y^{+}\right) + \varepsilon U^{+(1)}\left(y^{+}\right) + \varepsilon^2 U^{+(2)}\left(y^{+}\right) + O\left(\varepsilon^3\right). \tag{4.2}$$

Substituting (3.30) into (4.2), we have

$$U^{+}\left(0\right) = U^{+(0)}\left(0\right) + \varepsilon U^{+(1)}\left(0\right) + \varepsilon^2 U^{+(2)}\left(0\right) + O\left(\varepsilon^3\right). \tag{4.3}$$

$$0 = U^{+(0)}\left(0\right) + \varepsilon U^{+(1)}\left(0\right) + \varepsilon^2 U^{+(2)}\left(0\right) + O\left(\varepsilon^3\right). \tag{4.4}$$

Then we have $U^{+(0)}\left(0\right) = 0, U^{+(1)}\left(0\right) = 0$ and $U^{+(2)}\left(0\right) = 0$. (4.5)

Therefore, the bottom boundary condition (3.30) becomes

$$U^{+(0)} = 0 \qquad \text{at } y^{+} = 0 \tag{4.6}$$

$$U^{+(1)} = 0 \qquad \text{at } y^{+} = 0 \tag{4.7}$$

In the case $y^{+} < \frac{y_{Stoke}}{h}$, substituting (4.2) into (3.19) we have

$$2M_1\frac{d^2(U^{+(0)}+\varepsilon U^{+(1)}+o(\varepsilon^2)}{dy^{+2}}-M_2\left(U^{+(0)}+\varepsilon U^{+(1)}+o(\varepsilon^2)\right)+M_3=\frac{dp^+}{dx^+}-H\left(y^+\right). \tag{4.8}$$

Considering the zeroth order of ε^0, we obtain

$$2M_1\frac{d^2U^{+(0)}}{dy^{+2}}-M_2U^{+(0)}+M_3=\frac{dp^+}{dx^+}-H\left(y^+\right). \tag{4.9}$$

Since $H\left(y^+\right)$ is a known source term, in this work we assume that it is a linear function. That is

$$H\left(y^+\right)=\frac{h^2\varepsilon^l}{k_{11}}\left(c_1y^++c_0\right), \tag{4.10}$$

where c_0 and c_1 are constants. Thus, the equation (4.9) becomes

$$2M_1\frac{d^2U^{+(0)}}{dy^{+2}}-M_2U^{+(0)}=-M_3+\frac{dp^+}{dx^+}-\frac{h^2\varepsilon^l}{k_{11}}\left(c_1y^++c_0\right). \tag{4.11}$$

To find the general solution of the homogeneous equation (4.11), we first solve the homogeneous part of the ordinary differential equation (4.11)

$$2M_1\frac{d^2U^{+(0)}}{dy^{+2}}-M_2U^{+(0)}=0. \tag{4.12}$$

Therefore, we obtain

$$\begin{aligned}2M_1r^2-M_2&=0\\2M_1r^2&=M_2\\r^2&=\frac{M_2}{2M_1}\\r&=\pm\sqrt{\frac{M_2}{2M_1}}.\end{aligned} \tag{4.13}$$

Then, the general solution $U_c^{+(0)}=w_1e^{\sqrt{\frac{M_2}{2M_1}}y^+}+w_2e^{-\sqrt{\frac{M_2}{2M_1}}y^+}$, where $\frac{M_2}{2M_1}=\frac{h^2\varepsilon^l}{2k_{11}}>0$. To find the particular solution of (4.11), we use the undetermined coefficient method. Since

$$U^{+(0)}=U_c^{+(0)}+U_p^{+(0)}$$

$$U^{+(0)}=w_1e^{\sqrt{\frac{M_2}{2M_1}}y^+}+w_2e^{-\sqrt{\frac{M_2}{2M_1}}y^+}+U_p^{+(0)}, \tag{4.14}$$

we show how to find of the solution $U_p^{+(0)}$ by using the method of differential equation. We start with the particular solution. Let

$$U_p^{+(0)} = a_1 y^+ + a_0 \tag{4.15}$$

Differentiating (4.15) with respect to y^+, we have

$$\left(U_p^{+(0)}\right)' = a_1 \text{ and } \left(U_p^{+(0)}\right)'' = 0. \tag{4.16}$$

Substituting (4.15) and (4.16) into (4.11), we obtain

$$-M_2 a_1 y^+ - M_2 a_0 = -M_3 + \frac{dp^+}{dx^+} - \frac{h^2\varepsilon^l}{k_{11}} c_1 y^+ - \frac{h^2\varepsilon^l}{k_{11}} c_0 \tag{4.17}$$

Using the method of comparing coefficients, we have

$$-M_2 a_1 = -\frac{h^2\varepsilon^l}{k_{11}} c_1 \text{ and } -M_2 a_0 = -M_3 + \frac{dp^+}{dx^+} - \frac{h^2\varepsilon^l}{k_{11}} c_0 .$$

Then we have

$$a_1 = \frac{1}{M_2}\frac{h^2\varepsilon^l}{k_{11}} c_1 \quad \text{and} \tag{4.18}$$

$$a_0 = \frac{M_3}{M_2} - \frac{1}{M_2}\frac{dp^+}{dx^+} + \frac{1}{M_2}\frac{h^2\varepsilon^l}{k_{11}} c_0. \tag{4.19}$$

Substituting (4.18) and (4.19) into (4.15) and then substituting (4.15) into (4.14), we obtain the general solution

$$U^{+(0)} = w_1 e^{\sqrt{\frac{M_2}{2M_1}}y^+} + w_2 e^{-\sqrt{\frac{M_2}{2M_1}}y^+} + \frac{1}{M_2}\frac{h^2\varepsilon^l}{k_{11}} c_1 y^+ + \frac{M_3}{M_2} - \frac{1}{M_2}\frac{dp^+}{dx^+} + \frac{1}{M_2}\frac{h^2\varepsilon^l}{k_{11}} c_0 \tag{4.20}$$

Applying the boundary condition (4.6) to (4.20), we have

$$0 = w_1 + w_2 + \frac{M_3}{M_2} - \frac{1}{M_2}\frac{dp^+}{dx^+} + \frac{1}{M_2}\frac{h^2\varepsilon^l}{k_{11}} c_0. \tag{4.21}$$

Then we obtain

$$w_2 = -w_1 - \frac{M_3}{M_2} + \frac{1}{M_2}\frac{dp^+}{dx^+} - \frac{1}{M_2}\frac{h^2\varepsilon^l}{k_{11}} c_0. \tag{4.22}$$

Substituting (4.22) into (4.20), we obtain the general solution in Ω_2 is

$$\begin{aligned} U^{+(0)} = {} & w_1 e^{\sqrt{\frac{M_2}{2M_1}}y^+} + \left(-w_1 - \frac{M_3}{M_2} + \frac{1}{M_2}\frac{dp^+}{dx^+} - \frac{1}{M_2}\frac{h^2\varepsilon^l}{k_{11}} c_0\right) e^{-\sqrt{\frac{M_2}{2M_1}}y^+} \\ & + \frac{1}{M_2}\frac{h^2\varepsilon^l}{k_{11}} c_1 y^+ + \frac{M_3}{M_2} - \frac{1}{M_2}\frac{dp^+}{dx^+} + \frac{1}{M_2}\frac{h^2\varepsilon^l}{k_{11}} c_0. \end{aligned} \tag{4.23}$$

Let $J_1 = \sqrt{\frac{M_2}{2M_1}}, J_2 = \frac{1}{M_2}\frac{dp^+}{dx^+}, J_3 = \frac{1}{M_2}\frac{h^2\varepsilon^l}{k_{11}}, J_4 = \frac{M_3}{M_2}, J_5 = \frac{1}{M_1}\frac{dp^+}{dx^+},$ and $J_6 = \frac{M_3}{M_1}$

(4.24)

all of which are constants. Therefore (4.23) can be rewritten as

$$U^{+(0)} = w_1 e^{J_1 y^+} - w_1 e^{-J_1 y^+} + \left(-J_4 + J_2 - J_3 c_0\right) e^{-J_1 y^+} + J_3 c_1 y^+ + J_4 - J_2 + J_3 c_0. \quad (4.25)$$

Considering the first-order term of ε of (4.6), we have

$$2M_1 \frac{d^2 U^{+(1)}}{dy^{+2}} - M_2 U^{+(1)} = 0. \quad (4.26)$$

Therefore, we obtain

$$\begin{aligned} 2M_1 r^2 - M_2 &= 0 \\ 2M_1 r^2 &= M_2 \\ r^2 &= \frac{M_2}{2M_1} \\ r &= \pm\sqrt{\frac{M_2}{2M_1}}, \end{aligned} \quad (4.27)$$

where $\frac{M_2}{2M_1} = \frac{h^2\varepsilon^l}{2k_{11}} > 0.$ We obtain the general solution

$$U^{+(1)} = w_3 e^{\sqrt{\frac{M_2}{2M_1}} y^+} + w_4 e^{-\sqrt{\frac{M_2}{2M_1}} y^+}. \quad (4.28)$$

Applying the boundary condition (4.7) into (4.28), we have

$$0 = w_3 + w_4.$$

Then we obtain

$$w_4 = -w_3. \quad (4.29)$$

Substituting (4.29) into (4.28), we obtain the first-order solution in Ω_2 is

$$U^{+(1)} = w_3 e^{\sqrt{\frac{M_2}{2M_1}} y^+} - w_3 e^{-\sqrt{\frac{M_2}{2M_1}} y^+},$$

or

$$U^{+(1)} = w_3 e^{J_1 y^+} - w_3 e^{-J_1 y^+}, \quad (4.30)$$

where $w_1, w_2, w_3,$ and w_4 are constants.

4.1.2 Asymptotic expansion method of Stokes equation with the velocity to be a function of G

Similarly to the previous section, we calculate the velocity of the PCL fluid in domain Ω_1 using the asymptotic expansion method with the Stokes equation (3.25). We assume that

$$U^{+} = U^{+(0)} + \varepsilon U^{+(1)} + \varepsilon^2 U^{+(2)} + O\left(\varepsilon^3\right). \tag{4.31}$$

Therefore $$U^{+}\left(y^{+}\right) = U^{+(0)}\left(y^{+}\right) + \varepsilon U^{+(1)}\left(y^{+}\right) + \varepsilon^2 U^{+(2)}\left(y^{+}\right) + O\left(\varepsilon^3\right).$$

(4.32)

Substituting (3.31) into (4.32), we have

$$U^{+}(1) = U^{+(0)}(1) + \varepsilon U^{+(1)}(1) + \varepsilon^2 U^{+(2)}(1) + O\left(\varepsilon^3\right). \tag{4.33}$$

$$\frac{G}{U_0} = U^{+(0)}(0) + \varepsilon U^{+(1)}(0) + \varepsilon^2 U^{+(2)}(0) + O\left(\varepsilon^3\right).$$

(4.34)

Then we have $$U^{+(0)}(1) = \frac{G}{U_0}, U^{+(1)}(1) = 0 \text{ and } U^{+(2)}(1) = 0. \tag{4.35}$$

Therefore, the top boundary condition (3.31) and (3.32) becomes

$$U^{+(0)} = \frac{G}{U_0} \quad \text{at } y^{+} = 1$$

(4.36)

$$U^{+(1)} = 0 \quad \text{at } y^{+} = 1 \tag{4.37}$$

$$U^{+(0)} = D_0 \quad \text{at } y^{+} = 1 \tag{4.38}$$

$$U^{+(1)} = 0 \quad \text{at } y^{+} = 1 \tag{4.39}$$

In the case $y^{+} > \frac{y_{Stoke}}{h}$, we substitute (4.31) into (3.25). Therefore

$$2M_1 \frac{d^2\left(U^{+(0)} + \varepsilon U^{+(1)} + O\left(\varepsilon^2\right)\right)}{dy^{+2}} = \frac{dp^{+}}{dx^{+}} - M_3. \tag{4.40}$$

Considering the zeroth order term of ε , ε^0, we obtain

$$\frac{d^2U^{+(0)}}{dy^{+2}} = \frac{1}{2M_1}\frac{dp^{+}}{dx^{+}} - \frac{M_3}{2M_1}. \tag{4.41}$$

Since we assume that $\frac{dp^{+}}{dx^{+}}$ is a constant, integrating (4.41) twice, we have

$$U^{+(0)} = \left(\frac{1}{2M_1}\frac{dp^{+}}{dx^{+}} - \frac{M_3}{2M_1}\right)\frac{y^{+2}}{2} + w_5 y^{+} + w_6, \tag{4.42}$$

Where w_5 and w_6 are constants. Applying the boundary condition (4.36) to (4.42), we have

$$\frac{G}{U_0}=\frac{1}{2}\left(\frac{1}{2M_1}\frac{dp^+}{dx^+}-\frac{M_3}{2M_1}\right)+w_5+w_6. \tag{4.43}$$

Hence,
$$w_6=\frac{G}{U_0}-\frac{1}{2}\left(\frac{1}{2M_1}\frac{dp^+}{dx^+}-\frac{M_3}{2M_1}\right)-w_5. \tag{4.44}$$

Substituting (4.44) into (4.42), we obtain the general solution in Ω_1 is

$$U^{+(0)}=w_5\left(y^+-1\right)+\left(\frac{1}{2M_1}\frac{dp^+}{dx^+}-\frac{M_3}{2M_1}\right)\frac{y^{+2}}{2}+\frac{G}{U_0}-\frac{1}{2}\left(\frac{1}{2M_1}\frac{dp^+}{dx^+}-\frac{M_3}{2M_1}\right),$$

or

$$U^{+(0)}=w_5\left(y^+-1\right)+\left(\frac{1}{2}J_2-\frac{1}{2}J_6\right)\frac{y^{+2}}{2}+\frac{G}{U_0}-\frac{1}{2}\left(\frac{1}{2}J_5-\frac{1}{2}J_6\right). \tag{4.45}$$

Considering the first-order term of ε of (4.40), we have

$$2M_1\frac{d^2U^{+(1)}}{dy^{+2}}=0. \tag{4.46}$$

Integrating (4.46) twice, we have

$$U^{+(1)}=w_7y^++w_8, \tag{4.47}$$

where w_7 and w_8 are constants. Applying the boundary condition (4.37) to (4.47), we have

$$0=w_7+w_8.$$

Then we have

$$w_8=-w_7. \tag{4.48}$$

Substituting (4.48) into (4.47), we obtain the first-order solution in Ω_1 is

$$U^{+(1)}=w_7y^+-w_7. \tag{4.49}$$

Next, we determine the relation of the constants w_1 in the solution of Brinkman equation and w_5 in the solution of Stokes equation by using Beavers-Joseph boundary condition. Differentiating the solution $U^{+(0)}$ (4.25) in domain Ω_2 with respect to y^+ both sides, we have

$$\left.\frac{dU^{+(0)}}{dy^+}\right|_{y^+=\frac{y_{stoke}}{h}}=w_1J_1e^{J_1\frac{y_{stoke}}{h}}-J_1\left(-w_1-J_4+J_2-J_3c_0\right)e^{-J_1\frac{y_{stoke}}{h}}+J_3. \tag{4.50}$$

Differentiating the solution $U^{+(0)}$ (4.45) in domain Ω_1 with respect to y^+ both sides, we have

$$\left.\frac{dU^{+(0)}}{dy^+}\right|_{y^+=\frac{y_{stoke}}{h}} = w_5 + \left(\frac{1}{2}J_5 - \frac{1}{2}J_6\right)\frac{y_{stoke}}{h}, \tag{4.51}$$

where $y^+ = \frac{y_{stoke}}{h}$. Substituting (4.50) and (4.51) into (3.28), we obtain

$$\begin{aligned} &w_5 + \left(\frac{1}{2}J_5 - \frac{1}{2}J_6\right)\frac{y_{stoke}}{h} \\ &-\frac{1}{\varepsilon^l}\begin{bmatrix} w_1 J_1 e^{J_1\frac{y_{stoke}}{h}} \\ -J_1\left(-w_1 - J_4 + J_2 - J_3 c_0\right)e^{-J_1\frac{y_{stoke}}{h}} \\ +J_3 \end{bmatrix} = \frac{h\beta}{\sqrt{K^+ K_0}}U^{+(0)}\Big|_{y^+=\frac{y_{stoke}}{h}}. \end{aligned} \tag{4.52}$$

where $U^{+(0)}\Big|_{y^+=\frac{y_{stoke}}{h}}$ (on the right-hand side of (4.50) can be obtained from the PCL velocity in Ω_1 or Ω_2, or both. However, the velocity $\frac{h\beta}{\sqrt{K^+K_0}}U^{+(0)}\Big|_{y^+=\frac{y_{stoke}}{h}}$ is a slip velocity [13, 16]. Therefore, in this work, we considers the case that $U^{+(0)}\Big|_{y^+=\frac{y^-_{stoke}}{h}} = U^{+(0)}\Big|_{y^+=\frac{y^+_{stoke}}{h}}$. Substituting (4.45) into the right hand side of (4.52) we have

$$\begin{aligned} &w_5 + \left(\frac{1}{2}J_5 - \frac{1}{2}J_6\right)\frac{y_{stoke}}{h} - \frac{1}{\varepsilon^l}\left[w_1 J_1 e^{J_1\frac{y_{stoke}}{h}} - J_1\left(-w_1 - J_4 + J_2 - J_3 c_0\right)e^{-J_1\frac{y_{stoke}}{h}} + J_3\right] \\ &= \frac{h\beta}{\sqrt{K^+K_0}}\left[w_5\left(\frac{y_{stoke}}{h} - 1\right) + \left(\frac{1}{2}J_2 - \frac{1}{2}J_6\right)\frac{1}{2}\left(\frac{y_{stoke}}{h}\right)^2 + \frac{G}{U_0} - \frac{1}{2}\left(\frac{1}{2}J_5 - \frac{1}{2}J_6\right)\right]. \end{aligned} \tag{4.53}$$

$$\begin{aligned} &w_5 + \left(\frac{1}{2}J_5 - \frac{1}{2}J_6\right)\frac{y_{stoke}}{h} - \frac{1}{\varepsilon^l}\begin{bmatrix} w_1 J_1 e^{J_1\frac{y_{stoke}}{h}} + J_1 e^{-J_1\frac{y_{stoke}}{h}} w_1 + J_1 J_4 e^{-J_1\frac{y_{stoke}}{h}} \\ -J_1 J_2 e^{-J_1\frac{y_{stoke}}{h}} + J_1 J_3 c_0 e^{-J_1\frac{y_{stoke}}{h}} + J_3 \end{bmatrix} \\ &= \frac{h\beta}{\sqrt{K^+K_0}}\left[w_5\frac{y_{stoke}}{h} - w_5 + \left(\frac{1}{2}J_2 - \frac{1}{2}J_6\right)\frac{1}{2}\left(\frac{y_{stoke}}{h}\right)^2 + \frac{G}{U_0} - \frac{1}{2}\left(\frac{1}{2}J_5 - \frac{1}{2}J_6\right)\right]. \end{aligned} \tag{4.54}$$

$$w_5+\left(\frac{1}{2}J_5-\frac{1}{2}J_6\right)\frac{y_{stoke}}{h}-\frac{1}{\varepsilon^l}w_1J_1e^{J_1\frac{y_{stoke}}{h}}-\frac{1}{\varepsilon^l}J_1w_1e^{-J_1\frac{y_{stoke}}{h}}$$
$$-\frac{1}{\varepsilon^l}J_1J_4e^{-J_1\frac{y_{stoke}}{h}}+\frac{1}{\varepsilon^l}J_1J_2e^{-J_1\frac{y_{stoke}}{h}}-\frac{1}{\varepsilon^l}J_1J_3c_0e^{-J_1\frac{y_{stoke}}{h}}-\frac{1}{\varepsilon^l}J_3$$
$$=\frac{h\beta}{\sqrt{K^+K_0}}w_5\frac{y_{stoke}}{h}-\frac{h\beta}{\sqrt{K^+K_0}}w_5$$
$$+\frac{h\beta}{\sqrt{K^+K_0}}\left[\left(\frac{1}{2}J_2-\frac{1}{2}J_6\right)\frac{1}{2}\left(\frac{y_{stoke}}{h}\right)^2+\frac{G}{U_0}-\frac{1}{2}\left(\frac{1}{2}J_5-\frac{1}{2}J_6\right)\right].$$

(4.55)

$$w_5-\frac{h\beta}{\sqrt{K^+K_0}}w_5\frac{y_{stoke}}{h}+\frac{h\beta}{\sqrt{K^+K_0}}w_5$$
$$=\frac{h\beta}{\sqrt{K^+K_0}}\left[\left(\frac{1}{2}J_2-\frac{1}{2}J_6\right)\frac{1}{2}\left(\frac{y_{stoke}}{h}\right)^2+\frac{G}{U_0}-\frac{1}{2}\left(\frac{1}{2}J_5-\frac{1}{2}J_6\right)\right]$$
$$-\left(\frac{1}{2}J_5-\frac{1}{2}J_6\right)\frac{y_{stoke}}{h}+\frac{1}{\varepsilon^l}w_1J_1e^{J_1\frac{y_{stoke}}{h}}+\frac{1}{\varepsilon^l}J_1w_1e^{-J_1\frac{y_{stoke}}{h}}$$
$$+\frac{1}{\varepsilon^l}J_1J_4e^{-J_1\frac{y_{stoke}}{h}}-\frac{1}{\varepsilon^l}J_1J_2e^{-J_1\frac{y_{stoke}}{h}}+\frac{1}{\varepsilon^l}J_1J_3c_0e^{-J_1\frac{y_{stoke}}{h}}+\frac{1}{\varepsilon^l}J_3.$$

(4.56)

Then we have

$$w_5\left(1-\frac{h\beta}{\sqrt{K^+K_0}}\frac{y_{stoke}}{h}+\frac{h\beta}{\sqrt{K^+K_0}}\right)$$
$$=w_1\left(\frac{1}{\varepsilon^l}J_1e^{J_1\frac{y_{stoke}}{h}}+\frac{1}{\varepsilon^l}J_1e^{-J_1\frac{y_{stoke}}{h}}\right)-\left(\frac{1}{2}J_5-\frac{1}{2}J_6\right)\frac{y_{stoke}}{h}+\frac{1}{\varepsilon^l}J_1J_4e^{-J_1\frac{y_{stoke}}{h}}$$
$$-\frac{1}{\varepsilon^l}J_1J_2e^{-J_1\frac{y_{stoke}}{h}}+\frac{1}{\varepsilon^l}J_1J_3c_0e^{-J_1\frac{y_{stoke}}{h}}+\frac{1}{\varepsilon^l}J_3$$
$$+\frac{h\beta}{\sqrt{K^+K_0}}\left[\left(\frac{1}{2}J_2-\frac{1}{2}J_6\right)\frac{1}{2}\left(\frac{y_{stoke}}{h}\right)^2+\frac{G}{U_0}-\frac{1}{2}\left(\frac{1}{2}J_5-\frac{1}{2}J_6\right)\right].$$

(4.57)

We obtain

$$w_5=\frac{1}{\left(1-\frac{h\beta}{\sqrt{K^+K_0}}\frac{y_{stoke}}{h}+\frac{h\beta}{\sqrt{K^+K_0}}\right)}\left\{\begin{array}{l} w_1\left(\frac{1}{\varepsilon^l}J_1e^{J_1\frac{y_{stoke}}{h}}+\frac{1}{\varepsilon^l}J_1e^{-J_1\frac{y_{stoke}}{h}}\right)-\left(\frac{1}{2}J_5-\frac{1}{2}J_6\right)\frac{y_{stoke}}{h} \\ +\frac{1}{\varepsilon^l}J_1J_4e^{-J_1\frac{y_{stoke}}{h}}-\frac{1}{\varepsilon^l}J_1J_2e^{-J_1\frac{y_{stoke}}{h}} \\ +\frac{1}{\varepsilon^l}J_1J_3c_0e^{-J_1\frac{y_{stoke}}{h}}+\frac{1}{\varepsilon^l}J_3 \\ +\frac{h\beta}{\sqrt{K^+K_0}}\left[\begin{array}{l}\left(\frac{1}{2}J_2-\frac{1}{2}J_6\right)\frac{1}{2}\left(\frac{y_{stoke}}{h}\right)^2 \\ +\frac{G}{U_0}-\frac{1}{2}\left(\frac{1}{2}J_5-\frac{1}{2}J_6\right)\end{array}\right] \end{array}\right\}. \tag{4.58}$$

We now have the relation of the constants w_1 and w_5. Inserting (4.54) into (4.45), we have the solution of the Stokes equation depending on w_1. That is

$$U^{+(0)}=\left[\begin{array}{l}\frac{1}{\left(1-\frac{h\beta}{\sqrt{K^+K_0}}\frac{y_{stoke}}{h}+\frac{h\beta}{\sqrt{K^+K_0}}\right)}\left\{\begin{array}{l} w_1\left(\frac{1}{\varepsilon^l}J_1e^{J_1\frac{y_{stoke}}{h}}+\frac{1}{\varepsilon^l}J_1e^{-J_1\frac{y_{stoke}}{h}}\right)-\left(\frac{1}{2}J_5-\frac{1}{2}J_6\right)\frac{y_{stoke}}{h}+\frac{1}{\varepsilon^l}J_1J_4e^{-J_1\frac{y_{stoke}}{h}} \\ -\frac{1}{\varepsilon^l}J_1J_2e^{-J_1\frac{y_{stoke}}{h}}+\frac{1}{\varepsilon^l}J_1J_3c_0e^{-J_1\frac{y_{stoke}}{h}}+\frac{1}{\varepsilon^l}J_3 \\ +\frac{h\beta}{\sqrt{K^+K_0}}\left[\left(\frac{1}{2}J_2-\frac{1}{2}J_6\right)\frac{1}{2}\left(\frac{y_{stoke}}{h}\right)^2+\frac{G}{U_0}-\frac{1}{2}\left(\frac{1}{2}J_5-\frac{1}{2}J_6\right)\right]\end{array}\right\}y^+ \\ -\left[\frac{1}{\left(1-\frac{h\beta}{\sqrt{K^+K_0}}\frac{y_{stoke}}{h}+\frac{h\beta}{\sqrt{K^+K_0}}\right)}\left\{\begin{array}{l} w_1\left(\frac{1}{\varepsilon^l}J_1e^{J_1\frac{y_{stoke}}{h}}+\frac{1}{\varepsilon^l}J_1e^{-J_1\frac{y_{stoke}}{h}}\right)-\left(\frac{1}{2}J_5-\frac{1}{2}J_6\right)\frac{y_{stoke}}{h}+\frac{1}{\varepsilon^l}J_1J_4e^{-J_1\frac{y_{stoke}}{h}} \\ -\frac{1}{\varepsilon^l}J_1J_2e^{-J_1\frac{y_{stoke}}{h}}+\frac{1}{\varepsilon^l}J_1J_3c_0e^{-J_1\frac{y_{stoke}}{h}}+\frac{1}{\varepsilon^l}J_3 \\ +\frac{h\beta}{\sqrt{K^+K_0}}\left[\left(\frac{1}{2}J_2-\frac{1}{2}J_6\right)\frac{1}{2}\left(\frac{y_{stoke}}{h}\right)^2+\frac{G}{U_0}-\frac{1}{2}\left(\frac{1}{2}J_5-\frac{1}{2}J_6\right)\right]\end{array}\right\}\end{array}\right] \\ +\left(\frac{1}{2}J_2-\frac{1}{2}J_6\right)\frac{y^{+2}}{2}+\frac{G}{U_0}-\frac{1}{2}\left(\frac{1}{2}J_5-\frac{1}{2}J_6\right). \tag{4.59}$$

The solutions (4.59) of Stokes-Brinkman equations. The solution (4.25) and (4.45) are plotted in Figure 4.1. In the graph, we assume that the angles θ between the cilia and the horizontal plane are $40^\circ,50^\circ,60^\circ,70^\circ,80^\circ,90^\circ$ where the cilia have the highest velocity at $\theta=90^\circ$ during the forword stoke and stop beating at $\theta=40^\circ$ [36]. So at $\theta=40^\circ$ we do not need to calculate the velocity of the PCL fluid. The variables used in equations (4.25) and (4.45) are given in Table 4.1. The values of y_{Stoke} and K_p^+ are obtained from [21], and v^s is the velocities of the solid, cilia, where the maximum velocity of motile cilia value is assumed to occure at $\theta=90^\circ$ and v^s decreases and is terminated at $\theta=40^\circ$, h is the cilium height, U_0 is one cycle of ciliary beat, and ε^l

and β were obtained from [13]. We assume that the rate of pressure changes $\frac{dp^+}{dx^+}$ equals 1. The variable G at the top of the free-fluid domain equals 1. The variable w_1 in the equation (4.25) and (4.45) equals 0 because we aim to verify the solution if the solid velocities applied to the equation effect the results.

Table 4.1 Values of the variables in the solution of the Stokes-Brinkman equations

Variable	Value	Unit
h	7.5	$[\mu m]$
ρ	$992.2\times10^{(-15)}$	$\left[g/\mu m^3\right]$
μ	3×10^{-6}	$[g/\mu m\cdot s]$
g	$9.81\times10^{(6)}$	$\left[\mu m/s^2\right]$
U_0	1.00	$[\mu m/s]$
β	1	$[1]$
v^+	1	$[1]$
$\frac{dp^+}{dx^+}$	1	$[1]$
w_1	0	$[1]$
G	1	$[1]$

Table 4.2 Values of variables used in (4.59) used to plot Figure 4.1 for each angle θ

	50°	60°	70°	80°	90°
y_{Stoke}	0.7672	0.8638	0.9353	0.9818	1.0000
K^+	0.0012	0.0015	0.0016	0.0017	0.0018
ε^l	0.6717	0.7099	0.7331	0.7439	0.7487
v^s	0.0023	0.0024	0.0044	0.0049	0.0050

The asymptotic solution $U^{+(0)}$ (4.25) and (4.45) of the Stokes-Brinkman equation are shown in Figure 4.1. It can be noted that the velocities decrease with decreasing angles and the graph bends sharply in the porous medium region.

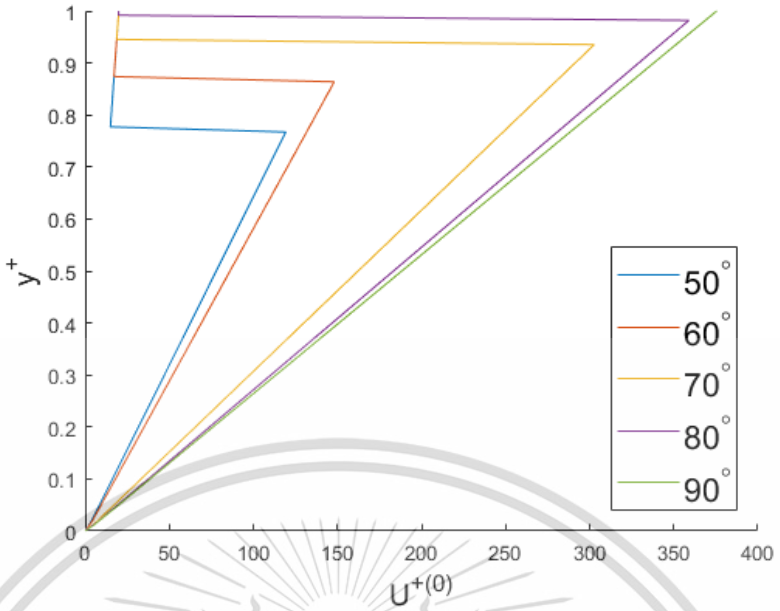

Figure 4.1 The asymptotic solution $U^{+(0)}$ of the Stokes-Brinkman equations from (4.25) and (4.45) with Beaver-Joseph boundary condition

4.1.3 Asymptotic expansion method of Stokes equation with boundary conditions illustrated in Figure 3.2

Applying the boundary condition (4.38) into (4.42), we have

$$D_0 = \frac{1}{2}\left(\frac{1}{2M_1}\frac{dp^+}{dx^+} - \frac{M_3}{2M_1}\right) + w_5 + w_6. \tag{4.60}$$

Then we have

$$w_6 = D_0 - \frac{1}{2}\left(\frac{1}{2M_1}\frac{dp^+}{dx^+} - \frac{M_3}{2M_1}\right) - w_5. \tag{4.61}$$

Substituting (4.61) into (4.42), we obtain the first-order solution in Ω_1 is

$$U^{+(0)} = \left(\frac{1}{2M_1}\frac{dp^+}{dx^+} - \frac{M_3}{2M_1}\right)\frac{y^{+2}}{2} + w_5 y^+ + D_0 - \frac{1}{2}\left(\frac{1}{2M_1}\frac{dp^+}{dx^+} - \frac{M_3}{2M_1}\right) - w_5, \tag{4.62}$$

or

$$U^{+(0)} = \left(\frac{1}{2}J_5 - \frac{1}{2}J_6\right)\frac{y^{+2}}{2} + w_5 y^+ + D_0 - \frac{1}{2}\left(\frac{1}{2}J_5 - \frac{1}{2}J_6\right) - w_5. \tag{4.63}$$

Now, we have another outer solution obtained from boundary condition (4.63) in the free-fluid domain which will be used in the Section 4.3.

4.2 Inner Solution

In this section, we find the solution in the inner region of the problem by using the asymptotic expansion. In the inner region for any variable f, we use $\overline{f}$ instead

of a physical variable f. For example, y^+. is written as $\bar{y}^+$ and U^+ is written as $\bar{U}^+$. Let

$$\bar{y}^+ = \frac{y^+ - y_{Stoke}}{\varepsilon}. \tag{4.64}$$

Then

$$\bar{U}^+\left(\bar{y}^+\right) = \bar{U}^+\left(\frac{y^+ - y_{Stoke}}{\varepsilon}\right). \tag{4.65}$$

Therefore,

$$\frac{d\bar{y}^+}{dy^+} = \frac{1}{\varepsilon}. \tag{4.66}$$

Thus,

$$\frac{d^2U^+}{dy^{+2}} = \frac{1}{\varepsilon^2}\frac{d^2\bar{U}^+}{d\bar{y}^{+2}} \tag{4.67}$$

Substituting (4.64) into (4.10), we have

$$H\left(\bar{y}^+\right) = \frac{h^2\varepsilon^l}{k_{11}}c_1\bar{y}^+\varepsilon + \frac{h^2\varepsilon^l}{k_{11}}c_1 y_{Stoke} + \frac{h^2\varepsilon^l}{k_{11}}c_0. \tag{4.68}$$

To solve the problem in the transition zone, the asymptotic expansion of (4.5) is

$$\begin{aligned} 2M_1\frac{1}{\varepsilon^2}\frac{d^2(\bar{U}^{+(0)} + \varepsilon\bar{U}^{+(1)} + o\left(\varepsilon^2\right)}{d\bar{y}^{+2}} - M_2\left(\bar{U}^{+(0)} + \varepsilon\bar{U}^{+(1)} + o\left(\varepsilon^2\right)\right) + M_3 \\ = \frac{dp^+}{dx^+} - \frac{h^2\varepsilon^l}{k_{11}}c_1\bar{y}^+\varepsilon - \frac{h^2\varepsilon^l}{k_{11}}c_1 y_{Stoke} - \frac{h^2\varepsilon^l}{k_{11}}c_0. \end{aligned} \tag{4.69}$$

Considering the order terms of ε, we have

$$O\left(\varepsilon^{-2}\right):\ 2M_1\frac{d^2\bar{U}^{+(0)}}{d\bar{y}^{+2}} = 0. \tag{4.70}$$

Since $M_1 = \frac{1}{\varepsilon^l}$, then we have

$$\frac{d^2\bar{U}^{+(0)}}{d\bar{y}^{+2}} = 0.$$

Therefore

$$\bar{U}^{+(0)} = m_1\bar{y}^+ + m_2, \tag{4.71}$$

where m_1 and m_2 are constants

$$O\left(\varepsilon^{-1}\right):\ 2M_1\frac{d^2\bar{U}^{+(1)}}{d\bar{y}^{+2}}=0 \tag{4.72}$$

Similarly for the case of $O\left(\varepsilon^{-2}\right)$, we obtain

$$\bar{U}^{+(1)}=m_3\bar{y}^{+}+m_4, \tag{4.73}$$

where m_3 and m_4 are constant.

$$O\left(\varepsilon^{0}\right):\ 2M_1\frac{d^2\bar{U}^{+(2)}}{d\bar{y}^{+2}}-M_2\bar{U}^{+(0)}+M_3=\frac{dp^{+}}{dx^{+}}-\frac{h^2\varepsilon^{l}}{k_{11}}c_1y_{Stoke}-\frac{h^2\varepsilon^{l}}{k_{11}}c_0 \tag{4.74}$$

Substituting (4.71) into (4.74), we have

$$2M_1\frac{d^2\bar{U}^{+(2)}}{d\bar{y}^{+2}}-M_2\left(m_1\bar{y}^{+}+m_2\right)+M_3=\frac{dp^{+}}{dx^{+}}-\frac{h^2\varepsilon^{l}}{k_{11}}c_1y_{Stoke}-\frac{h^2\varepsilon^{l}}{k_{11}}c_0. \tag{4.75}$$

Then we have

$$\frac{d^2\bar{U}^{+(2)}}{d\bar{y}^{+2}}=\frac{m_1M_2}{2M_1}\bar{y}^{+}+\frac{m_2M_2}{2M_1}-\frac{M_3}{2M_1}+\frac{1}{2M_1}\frac{dp^{+}}{dx^{+}}-\frac{1}{2M_1}\frac{h^2\varepsilon^{l}}{k_{11}}c_1y_{Stoke}-\frac{1}{2M_1}\frac{h^2\varepsilon^{l}}{k_{11}}c_0. \tag{4.76}$$

Therefor we obtain the second-order analytical solution

$$\bar{U}^{+(2)}=\frac{M_2}{12M_1}m_1\bar{y}^{+3}+\left(\frac{M_2m_2}{2M_1}-\frac{M_3}{2M_1}+\frac{1}{2M_1}\frac{dp^{+}}{dx^{+}}-\frac{h^2\varepsilon^{l}}{2M_1k_{11}}c_1y_{Stoke}-\frac{h^2\varepsilon^{l}}{2M_1k_{11}}c_0\right)\frac{\bar{y}^{+2}}{2}+m_5\bar{y}^{+}+m_6, \tag{4.77}$$

where m_5 and m_6 are constants. Hence, the zeroth, first and second-order analytical solutions can be expressed as

$$\bar{U}^{+(0)}=m_1\bar{y}^{+}+m_2, \tag{4.78}$$

$$\bar{U}^{+(1)}=m_3\bar{y}^{+}+m_4, \tag{4.79}$$

$$\bar{U}^{+(2)}=\frac{M_2}{12M_1}m_1\bar{y}^{+3}+\left(\frac{M_2m_2}{2M_1}-\frac{M_3}{2M_1}+\frac{1}{2M_1}\frac{dp^{+}}{dx^{+}}-\frac{h^2\varepsilon^{l}}{2M_1k_{11}}c_1y_{Stoke}-\frac{h^2\varepsilon^{l}}{2M_1k_{11}}c_0\right)\frac{\bar{y}^{+2}}{2}+m_5\bar{y}^{+}+m_6, \tag{4.80}$$

We now have the analytic solution of the inner region. The outer and inner solutions will be matched by using the matching conditions provide in the next section.

4.3 Matching condition

In this section, we match the outer and inner solutions by using Van Dyke's rule. Because at the interface between the two outer domains, the speed of the PCL fluid changes rapidly, the transition zone is occure between these two regions. This zone is called inner zone as shown in Figure 4.2. The transition zone occure at $y = y_{Stoke}$.

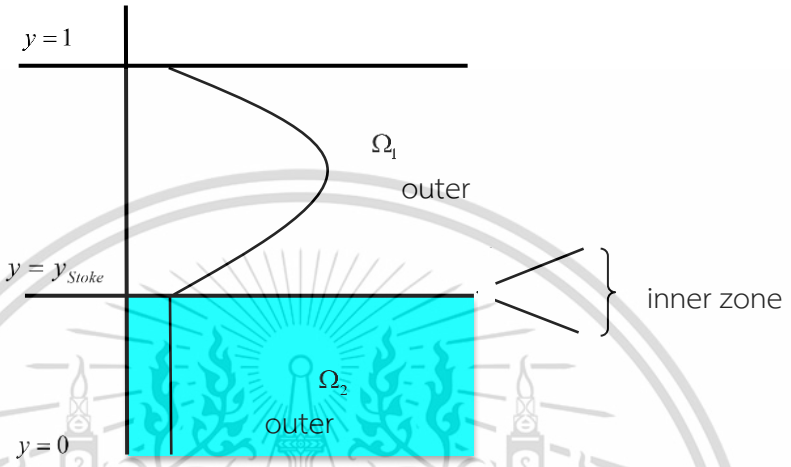

Figure 4.2 PCL fluid flow in outer and inner zones

We derive matching conditions to match the variables in the solutions of the outer and inner regions. The matching condition used in this work are developed from Van Dyke's rule [3, 34],

$$\lim_{\bar{y}^+ \to \pm\infty} \bar{f}\left(\bar{y}^+\right) = \lim_{y^+ \to y^{\pm}_{Stoke}} f\left(y^+\right). \tag{4.81}$$

With the outer and inner variables,

$$f\left(y^+, \varepsilon\right) = f^{(0)}\left(y^+\right) + \varepsilon f^{(1)}\left(y^+\right) + o\left(\varepsilon^2\right) \tag{4.82}$$

$$\bar{f}\left(\bar{y}^+, \varepsilon\right) = \bar{f}^{(0)}\left(\bar{y}^+\right) + \varepsilon \bar{f}^{(1)}\left(\bar{y}^+\right) + o\left(\varepsilon^2\right), \tag{4.83}$$

we find the matching condition of $f^{(0)}$ by substituting (4.68) and (4.69) into (4.67). Therefore,

$$\lim_{y^+ \to y^{\pm}_{Stoke}} \left[f^{(0)}\left(y^+\right) + \varepsilon f^{(1)}\left(y^+\right) + O\left(\varepsilon^2\right) \right] = \lim_{\bar{y}^+ \to \pm\infty} \left[\bar{f}^{(0)}\left(\bar{y}^+\right) + \varepsilon \bar{f}^{(1)}\left(\bar{y}^+\right) + O\left(\varepsilon^2\right) \right]. \tag{4.84}$$

We suppose that $\lim_{y^+ \to y^{\pm}_{Stoke}} f^{(i)}\left(y^+\right)$ and $\lim_{\bar{y}^+ \to \pm\infty} f^{(i)}\left(y^+\right)$ exist, $i = 0,1,2,\ldots$ Then, considering the zeroth order term of ε, we have

$$\lim_{\bar{y}^+ \to \pm\infty} \bar{f}^{(0)}\left(\bar{y}^+\right) = \lim_{y^+ \to y^{\pm}_{Stoke}} f^{(0)}\left(y^+\right). \tag{4.85}$$

Next, we find another matching condition by applying the Tayloy's series expansion to each $f^{(i)}$ in (4.82) around the point y^{+}_{Stoke} or y^{-}_{Stoke}, where the superscript plus and minus signs mean the right and left sides of y_{Stoke} and we assume that $f^{(i)}\left(y^{+}\right), i=0,1,2,3,...$ are continuous at $y=y_{Stoke}$ so that

$$f^{(i)}\left(y^{+}_{Stoke}\right)=\lim_{y^{+}\to y^{\pm}_{Stoke}} f^{(i)}\left(y^{+}\right), i=0,1,2,3,... \tag{4.86}$$

Therefore,

$$f\left(y^{+},\varepsilon\right)=\lim_{y^{+}\to y^{\pm}_{Stoke}}\left[f^{(0)}\left(y^{+}\right)+\varepsilon f^{(1)}\left(y^{+}\right)+O\left(\varepsilon^{2}\right)\right]$$

$$f\left(y^{+},\varepsilon\right)=\lim_{y^{+}\to y^{\pm}_{Stoke}}\left\{\begin{array}{l}\left[\begin{array}{l}f^{(0)}\left(y^{+}\right)+\dfrac{\left(y^{+}-y^{\pm}_{Stoke}\right)}{1!}\dfrac{df^{(0)}\left(y^{+}\right)}{dy^{+}}+\dfrac{\left(y^{+}-y^{\pm}_{Stoke}\right)^{2}}{2!}\dfrac{d^{2}f^{(0)}\left(y^{+}\right)}{dy^{+}}\\ +O\left(y^{+}-y^{\pm}_{Stoke}\right)^{3}\end{array}\right]\\ +\varepsilon\left[f^{(1)}\left(y^{+}\right)+\dfrac{\left(y^{+}-y^{\pm}_{Stoke}\right)}{1!}\dfrac{df^{(1)}\left(y^{+}\right)}{dy^{+}}+O\left(y^{+}-y^{\pm}_{Stoke}\right)^{2}\right]+O\left(\varepsilon^{2}\right)\end{array}\right\} \tag{4.87}$$

$$f\left(y^{+},\varepsilon\right)=\left[\begin{array}{l}\lim\limits_{y^{+}\to y^{\pm}_{Stoke}} f^{(0)}\left(y^{+}\right)+\lim\limits_{y^{+}\to y^{\pm}_{Stoke}}\dfrac{\left(y^{+}-y^{\pm}_{Stoke}\right)}{1!}\dfrac{df^{(0)}\left(y^{+}\right)}{dy^{+}}\\ +\lim\limits_{y^{+}\to y^{\pm}_{Stoke}}\dfrac{\left(y^{+}-y^{\pm}_{Stoke}\right)^{2}}{2!}\dfrac{d^{2}f^{(0)}\left(y^{+}\right)}{dy^{+}}\lim\limits_{y^{+}\to y^{\pm}_{Stoke}} O\left(y^{+}-y^{\pm}_{Stoke}\right)^{3}\end{array}\right]$$
$$+\varepsilon\left[\begin{array}{l}\lim\limits_{y^{+}\to y^{\pm}_{Stoke}} f^{(1)}\left(y^{+}\right)+\lim\limits_{y^{+}\to y^{\pm}_{Stoke}}\dfrac{\left(y^{+}-y^{\pm}_{Stoke}\right)}{1!}\dfrac{df^{(1)}\left(y^{+}\right)}{dy^{+}}\\ +\lim\limits_{y^{+}\to y^{\pm}_{Stoke}} O\left(y^{+}-y^{\pm}_{Stoke}\right)^{2}\end{array}\right]+O\left(\varepsilon^{2}\right) \tag{4.88}$$

Then, we have

$$f\left(y^{+},\varepsilon\right)=\left[\begin{array}{l}\lim\limits_{y^{+}\to y^{\pm}_{Stoke}} f^{(0)}\left(y^{+}\right)+\left(y^{+}-y^{\pm}_{Stoke}\right)\lim\limits_{y^{+}\to y^{\pm}_{Stoke}}\dfrac{df^{(0)}\left(y^{+}\right)}{dy^{+}}\\ +\dfrac{\left(y^{+}-y^{\pm}_{Stoke}\right)^{2}}{2}\lim\limits_{y^{+}\to y^{\pm}_{Stoke}}\dfrac{d^{2}f^{(0)}\left(y^{+}\right)}{dy^{+}}+O\left(y^{+}-y^{\pm}_{Stoke}\right)^{3}\end{array}\right]$$
$$+\varepsilon\left[\lim_{y^{+}\to y^{\pm}_{Stoke}} f^{(1)}\left(y^{+}\right)+\left(y^{+}-y^{\pm}_{Stoke}\right)\lim_{y^{+}\to y^{\pm}_{Stoke}}\frac{df^{(1)}\left(y^{+}\right)}{dy^{+}}+O\left(y^{+}-y^{\pm}_{Stoke}\right)^{2}\right] \tag{4.89}$$
$$+O\left(\varepsilon^{2}\right).$$

Substituting (4.64) into (4.89), we have

$$
\begin{aligned}
f\left(y^{+},\varepsilon\right) = & \lim_{y^{+}\to y^{\pm}_{Stoke}} f^{(0)}\left(y^{+}\right) + \varepsilon\bar{y}^{+} \lim_{y^{+}\to y^{\pm}_{Stoke}} \frac{df^{(0)}\left(y^{+}\right)}{dy^{+}} \\
& + \frac{\left(\varepsilon\bar{y}^{+}\right)^{2}}{2} \lim_{y^{+}\to y^{\pm}_{Stoke}} \frac{d^{2}f^{(0)}\left(y^{+}\right)}{dy^{+}} + O\left(\varepsilon\bar{y}^{+}\right)^{3} \\
& + \varepsilon\left[\lim_{y^{+}\to y^{\pm}_{Stoke}} f^{(1)}\left(y^{+}\right) + \varepsilon\bar{y}^{+} \lim_{y^{+}\to y^{\pm}_{Stoke}} \frac{df^{(1)}\left(y^{+}\right)}{dy^{+}} + O\left(\varepsilon\bar{y}^{+}\right)^{2}\right] \\
& + O\left(\varepsilon^{2}\right).
\end{aligned}
\tag{4.90}
$$

Differentiating (4.90) with respect to $\bar{y}^{+}$, taking $y^{+}\to y^{\pm}_{Stoke}$ both sides and omitting the big O, then, we obtain

$$
\begin{aligned}
\lim_{y^{+}\to y^{\pm}_{Stoke}} \frac{df\left(y^{+},\varepsilon\right)}{d\bar{y}^{+}} = & \varepsilon \lim_{y^{+}\to y^{\pm}_{Stoke}} \frac{df^{(0)}\left(y^{+}\right)}{dy^{+}} + \varepsilon^{2}\bar{y}^{+} \lim_{y^{+}\to y^{\pm}_{Stoke}} \frac{d^{2}f^{(0)}\left(y^{+}\right)}{dy^{+}} \\
& + \varepsilon^{2} \lim_{y^{+}\to y^{\pm}_{Stoke}} \frac{df^{(1)}\left(y^{+}\right)}{dy^{+}},
\end{aligned}
\tag{4.91}
$$

where in this work we assume that the function f is continuous enough so that the differentiation can be switched with the limit. To find the matching condition for the first derivative of the function f and $\bar{f}$, we differentiate (4.83) with respect to $\bar{y}^{+}$ and taking limit $\bar{y}^{+}\to\pm\infty$ on both sides, we obtain

$$
\lim_{\bar{y}^{+}\to\pm\infty} \frac{d\,\bar{f}\left(\bar{y}^{+},\varepsilon\right)}{d\,\bar{y}^{+}} = \lim_{\bar{y}^{+}\to\pm\infty} \left[\frac{d\,\bar{f}^{(0)}\left(\bar{y}^{+}\right)}{d\,\bar{y}^{+}} + \varepsilon\frac{d\,\bar{f}^{(1)}\left(\bar{y}^{+}\right)}{d\,\bar{y}^{+}} + \varepsilon^{2}\frac{d\,\bar{f}^{(2)}\left(\bar{y}^{+}\right)}{d\,\bar{y}^{+}}\right].
\tag{4.92}
$$

Since we assume that the differentiation can be switched with the limit, from (4.81), we have

$$
\lim_{y^{+}\to y^{\pm}_{Stoke}} \frac{df\left(y^{+},\varepsilon\right)}{d\bar{y}^{+}} = \lim_{\bar{y}^{+}\to\pm\infty} \frac{d\bar{f}\left(\bar{y}^{+},\varepsilon\right)}{d\bar{y}^{+}}.
$$

From (4.81), it demonstrates that (4.91) and (4.92) are equal. Then, we get

$$
\begin{aligned}
& \varepsilon \lim_{y^{+}\to y^{\pm}_{Stoke}} \frac{df^{(0)}\left(y^{+}\right)}{dy^{+}} + \varepsilon^{2}\bar{y}^{+} \lim_{y^{+}\to y^{\pm}_{Stoke}} \frac{d^{2}f^{(0)}\left(y^{+}\right)}{dy^{+}} + \varepsilon^{2} \lim_{y^{+}\to y^{\pm}_{Stoke}} \frac{df^{(1)}\left(y^{+}\right)}{dy^{+}} \\
& \qquad = \lim_{\bar{y}^{+}\to\pm\infty} \left[\frac{d\,\bar{f}^{(0)}\left(\bar{y}^{+}\right)}{d\,\bar{y}^{+}} + \varepsilon\frac{d\,\bar{f}^{(1)}\left(\bar{y}^{+}\right)}{d\,\bar{y}^{+}} + \varepsilon^{2}\frac{d\,\bar{f}^{(2)}\left(\bar{y}^{+}\right)}{d\,\bar{y}^{+}}\right].
\end{aligned}
\tag{4.93}
$$

Collecting the same order of ε in (4.93), we obtain

$$\varepsilon^0 : \lim_{\bar{y}^+ \to \pm\infty} \frac{d\,\bar{f}^{(0)}\left(\bar{y}^+\right)}{d\,\bar{y}^+} = 0, \tag{4.94}$$

$$\varepsilon^1 : \lim_{\bar{y}^+ \to \pm\infty} \frac{d\,\bar{f}^{(1)}\left(\bar{y}^+\right)}{d\,\bar{y}^+} = \lim_{y^+ \to y^{\pm}_{Stoke}} \frac{df^{(0)}\left(y^+\right)}{dy^+}, \tag{4.95}$$

$$\varepsilon^2 : \lim_{\bar{y}^+ \to \pm\infty} \frac{d\,\bar{f}^{(2)}\left(\bar{y}^+\right)}{d\,\bar{y}^+} = \bar{y}^+ \lim_{y^+ \to y^{\pm}_{Stoke}} \frac{d^2 f^{(0)}\left(y^+\right)}{dy^+} + \lim_{y^+ \to y^{\pm}_{Stoke}} \frac{df^{(1)}\left(y^+\right)}{dy^+}. \tag{4.96}$$

We now have matching conditions at the free-fluid/ porous-medium interface. The zeroth-order solution for the Stokes-Brinkman equations are provided in the next section.

4.4 The Zeroth-Order Solution

In this section, we couple the zeroth-order solutions of the governing equations (3.19) and (3.25) by using the matching conditions provided in Section 4.3. Before using the matching conditions, we differentiate the zeroth-order and first-order inner solutions (4.78) and (4.79) with respect to $\bar{y}^+$ and taking the limit $y^+ \to +\infty$ on both sides, we obtain

$$\lim_{\bar{y}^+ \to +\infty} \frac{d\bar{U}^{+(0)}}{d\bar{y}^+} = m_1, \tag{4.97}$$

and

$$\lim_{\bar{y}^+ \to +\infty} \frac{d\bar{U}^{+(1)}}{d\bar{y}^+} = m_3, \tag{4.98}$$

respectively. According to the matching condition (4.94), we have $m_1 = 0.$ Then, from (4.78), we obtain

$$\bar{U}^{+(0)} = m_2. \tag{4.99}$$

Next, we provide the matching process of the outer solutions in domain Ω_2 and Ω_1. Differentiating the zeroth-order outer solutions (4.23) and (4.62) for the outer regions Ω_2 and Ω_1 respectively, with respect to y^+, and taking the limit $y^+ \to y^+_{Stoke}$ on both sides, we obtain

$$\begin{aligned}\lim_{y^+ \to y^+_{Stoke}} \frac{dU^{+(0)}}{dy^+} = {} & w_1 \sqrt{\frac{M_2}{2M_1}} e^{\sqrt{\frac{M_2}{2M_1}} y^+_{Stoke}} + w_1 \sqrt{\frac{M_2}{2M_1}} e^{-\sqrt{\frac{M_2}{2M_1}} y^+_{Stoke}} \\ & - \sqrt{\frac{M_2}{2M_1}} \left(-\frac{M_3}{M_2} + \frac{1}{M_2} \frac{dP^+}{dx^+} - \frac{h^2 \varepsilon^l}{M_2 k_{11}} c_0 \right) e^{-\sqrt{\frac{M_2}{2M_1}} y^+_{Stoke}} \\ & + \frac{h^2 \varepsilon^l}{M_2 k_{11}} c_1.\end{aligned} \tag{4.100}$$

$$\lim_{y^+ \to y^+_{Stoke}} \frac{dU^{+(0)}}{dy^+} = \left(\frac{1}{2} - \frac{M_3}{2}\right) y^+_{Stoke} + w_3, \tag{4.101}$$

respectively. Substituting (4.98) and (4.100) into (4.95), we obtain

$$\begin{aligned} m_3 = {} & w_1 \sqrt{\frac{M_2}{2M_1}} e^{\sqrt{\frac{M_2}{2M_1}} y^+_{Stoke}} + w_1 \sqrt{\frac{M_2}{2M_1}} e^{-\sqrt{\frac{M_2}{2M_1}} y^+_{Stoke}} \\ & - \sqrt{\frac{M_2}{2M_1}} \left(-\frac{M_3}{M_2} + \frac{1}{M_2} \frac{dP^+}{dx^+} - \frac{1}{M_2} \frac{h^2 \varepsilon^l}{k_{11}} c_0 \right) e^{-\sqrt{\frac{M_2}{2M_1}} y^+_{Stoke}} \\ & + \frac{1}{M_2} \frac{h^2 \varepsilon^l}{k_{11}} c_1, \end{aligned} \tag{4.102}$$

in region Ω_2. Similarly, substituting (4.98) and (4.101) into (4.95), we have

$$m_3 = \left(\frac{1}{2} - \frac{M_3}{2}\right) y^+_{Stoke} + w_3, \tag{4.103}$$

in region Ω_1. Since equation (4.102) is equal to (4.103), we then have

$$\begin{aligned} w_3 = {} & -\left(\frac{1}{2} - \frac{M_3}{2}\right) y^+_{Stoke} + w_1 \left(\sqrt{\frac{M_2}{2M_1}} e^{\sqrt{\frac{M_2}{2M_1}} y^+_{Stoke}} + \sqrt{\frac{M_2}{2M_1}} e^{-\sqrt{\frac{M_2}{2M_1}} y^+_{Stoke}} \right) \\ & - \sqrt{\frac{M_2}{2M_1}} \left(-\frac{M_3}{M_2} + \frac{1}{M_2} \frac{dp^+}{dx^+} - \frac{1}{M_2} \frac{h^2 \varepsilon^l}{k_{11}} c_0 \right) e^{-\sqrt{\frac{M_2}{2M_1}} y^+_{Stoke}} + \frac{1}{M_2} \frac{h^2 \varepsilon^l}{k_{11}} c_1. \end{aligned} \tag{4.104}$$

Define

$$z_1 = \sqrt{\frac{M_2}{2M_1}}, z_2 = \frac{1}{2} - \frac{M_3}{2}, z_3 = \frac{1}{2M_1} \frac{dp^+}{dx^+} - \frac{M_3}{2M_1}, z_4 = -\frac{M_3}{M_2} + \frac{1}{M_2} \frac{dp^+}{dx^+} - \frac{1}{M_2} \frac{h^2 \varepsilon^l}{k_{11}} c_0 \quad \text{and} \quad z_5 = \frac{1}{M_2} \frac{h^2 \varepsilon^l}{k_{11}} c_1, \tag{4.105}$$

which are known constants. Applying (4.105) to (4.104) and (4.23), this yields

$$w_3 = -z_2 y^+_{Stoke} + w_1 \left(z_1 e^{z_1 y^+_{Stoke}} + z_1 e^{-z_1 y^+_{Stoke}} \right) - z_1 z_4 e^{-z_1 y^+_{Stoke}} + z_5. \tag{4.106}$$

and

$$\left[U^{+(0)}\right]^{(p)} = w_1 e^{z_1 y^+} - w_1 e^{-z_1 y^+} + z_4 e^{-z_1 y^+} + z_5 y^+ - z_4; \; 0 < y^+ < y_{Stoke}, \tag{4.107}$$

respectively, where $\left[U^{+(0)}\right]^{(p)}$ means the zeroth-order solution in the porous-medium domain Ω_2. Substituting (4.105) and (4.106) into (4.62), we have

$$\begin{aligned} \left[U^{+(0)}\right]^{(f)} = {} & \frac{z_2 y^{+2}}{2} + D_0 - \frac{z_2}{2} \\ & + \left[-z_2 y^+_{Stoke} + w_1 \left(z_1 e^{z_1 y^+_{Stoke}} + z_1 e^{-z_1 y^+_{Stoke}} \right) - z_1 z_4 e^{-z_1 y^+_{Stoke}} + z_5 \right] \left(y^+ - 1 \right); \; y_{Stoke} < y^+ < 1, \end{aligned} \tag{4.108}$$

Where $\left[U^{+(0)}\right]^{(f)}$ means the zeroth-order solution in the free-fluid domain. Now, we obtain $\left[U^{+(0)}\right]^{(p)}$ and $\left[U^{+(0)}\right]^{(f)}$ in term of w_1.

To illustrate our results, the solution (4.107) and (4.108) are plotted in Figure 4.3, where the angles between the cilia and the horizontal plane considered in this work are $40^\circ, 50^\circ, 60^\circ, 70^\circ, 80^\circ$ and 90°, respectively. In this research, we assume that the cilia have the highest velocity at $\theta = 90^\circ$ and stop beating at $\theta = 40^\circ$. The values of the variables used in (4.107) and (4.108) are presented in Tables 4.3 and 4.4. The values in Table 4.3 are used for all angles θ and the values of the variables in Table 4.4 are different for each angle θ which are obtained from [7, 35], where they have obtained the data from an biological experiment [36].

Table 4.3 Values of the variables applied to the solution (4.107) to plot Figure 4.2.

Variable	Value	Unit	Variable	Value	Unit
c_0	0	$[1]$	U_0	1	$[\mu m/s]$
h	7.5	$[\mu m]$	K_0	1	$[\mu m^2]$
ρ	992.2×10^{-15}	$[g/\mu m^3]$	$\frac{dp^+}{dx^+}$	1	$[1]$
μ	3×10^{-6}	$[g/\mu m\cdot s]$	w_1	0	$[1]$
g	9.81×10^{6}	$[\mu m/s^2]$			

Since the solid phases in the experimental are static, we have to find set v^s to be zero inour solution and choose a value of w_1 so that our solutions are matched with the experimental data. So we choose $w_1 = 0.$

Table 4.4 Values of the variables used to plot Figure 4.2 for each angle θ.

Variable	50°	60°	70°	80°	90°
y_{Stoke}	0.7672	0.8638	0.9353	0.9818	1.0000
K^+	0.0012	0.0015	0.0016	0.0017	0.0018
ε^l	0.6717	0.7099	0.7331	0.7439	0.7487
c_1	1.2	1.4	1.6	1.8	2

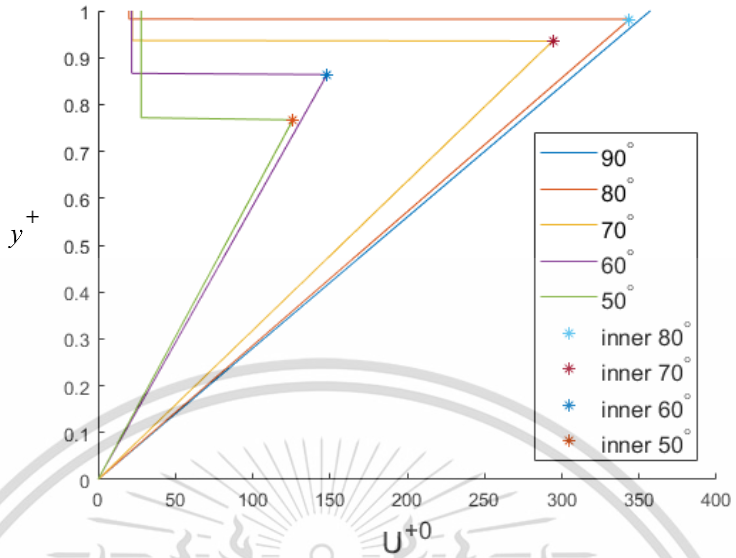

Figure 4.3 The asymptotic solution $U^{+(0)}$, equations (4.107), outer solution in the porous medium domain and (4.108), outer solution in the free-fluid region and inner solution (4.99)

Figure 4.3 shows the velocity of the PCL fluid with different angles θ in domain Ω_2. The highest velocity is occurred at $\theta = 90^\circ$ as expected. This is because, in this study, we assume that the maximum velocity of cilia occurs at $\theta = 90^\circ$. Notice that the velocities decrease when the angles between the cilia and the horizontal plane decreases. The star is the solution in the inner zone, the interface between the free-fluid/ porous-medium domain. The oblique line represents the solution in the porous medium domain, the horizontal line is the line that lies between the free-fluid domain and the porous medium domain, and the vertical line represent the solution in the free-fluid domain. Note that, the solution in the porous medium is small and rapidly large in the free-fluid domain. The star is the solution in the inner zone.

4.5 Comparison with an Experimental Study

In this section, we compare the mass flow rate Φ of our result with the study of Beavers and Joseph [30], where

$$\Phi = \frac{M_f - M_p}{M_p}, \tag{4.109}$$

where M_f is the mass flow rate in the free-fluid region and M_p is the mass flow rate in the porous medium. In this study M_f is the zeroth-order solution in the free-fluid domain when the velocity of solid phases is zero

$$M_f=\left[U^{+(0)}\right]^{(f)}A_f=\left\{\begin{array}{l}\frac{1}{2}\left(\frac{\varepsilon^l}{2}-\frac{\varepsilon^l h^2\rho g^+ g_0}{2\mu U_0}\right)y^{+2}+D_0-\frac{1}{2}\left(\frac{\varepsilon^l}{2}-\frac{\varepsilon^l h^2\rho g^+ g_0}{2\mu U_0}\right)\\ +\left[\begin{array}{l}-\left(\frac{\varepsilon^l}{2}-\frac{\varepsilon^l h^2\rho g^+ g_0}{2\mu U_0}\right)y^+{}_{Stoke}+w_1\left(\sigma\sqrt{\frac{\varepsilon^l}{2K^+}}e^{\sigma\sqrt{\frac{\varepsilon^l}{2K^+}}y^+{}_{Stoke}}+\sigma\sqrt{\frac{\varepsilon^l}{2K^+}}e^{-\sigma\sqrt{\frac{\varepsilon^l}{2K^+}}y^+{}_{Stoke}}\right)\\ -\sigma\sqrt{\frac{\varepsilon^l}{2K^+}}\left(-\frac{K_0K^+\rho g^+ g_0}{\mu U_0}+\frac{K^+}{\sigma}\frac{dp^+}{dx^+}\right)e^{-\sigma\sqrt{\frac{\varepsilon^l}{2K^+}}y^+{}_{Stoke}}\end{array}\right]\left(y^+-1\right)\end{array}\right\}A_f;\ y_{Stoke}<y^+<1,$$

and

$$M_p=\left[U^{+(0)}\right]^{(p)}A_p=\left[\begin{array}{l}w_1e^{\sigma\sqrt{\frac{\varepsilon^l h}{2K_0}}y^+}-w_1e^{-\sigma\sqrt{\frac{\varepsilon^l h}{2K_0}}y^+}+\left(-\frac{K_0K^+\rho g^+ g_0}{\mu U_0}+\frac{K^+}{\sigma}\frac{dp^+}{dx^+}\right)e^{-\sigma\sqrt{\frac{\varepsilon^l h}{2K_0}}y^+}\\ +\frac{K_0K^+\rho g^+ g_0}{\mu U_0}-\frac{K^+}{\sigma}\frac{dp^+}{dx^+}\end{array}\right]A_p;\ 0<y^+<y_{Stoke},$$

where unit of M_f and M_p are mass per time and unit of Φ is 1. In the BJ study, they have carried out the experiment to measure the flow rate of a long porous block and a small uniform gap immediately above the block, while in this study, we analytically find the mass flow rate of the fluid flow in the PCL in human lung by using the asymptotic expansion method. The porous medium in the experimental study are stationary porous blocks, while the porous medium in this study is the ciliary layer, which is a motion medium. Therefore, we compare our solution with the experimental data at only one porosity and the solid velocity is set to be zero. Since Beavers and Joseph provide the data, the mass flow rate, only on the free-fluid domain, as the result, only the solution on the free-fluid domain is compared.

Applying the zeroth-order solutions (4.107) - (4.108) provided in Section 4.4 to (4.109), the mass flow rate obtained from both equations is

$$\Phi=\frac{\left\{\begin{array}{l}\frac{1}{2}\left(\frac{1}{2}-\frac{\sigma^2K_0\rho g^+ g_0}{2\mu U_0}\right)\sigma^2K_0+D_0-\frac{1}{4}\left(1-\frac{\sigma^2K_0\rho g^+ g_0}{\mu U_0}\right)\\ +\left[\begin{array}{l}-\left(\frac{1}{2}-\frac{\sigma^2K_0\rho g^+ g_0}{2\mu U_0}\right)y^+{}_{Stoke}+w_1\left(\sigma\sqrt{\frac{1}{2K^+}}e^{\sigma\sqrt{\frac{1}{2K^+}}y^+{}_{Stoke}}+\sigma\sqrt{\frac{1}{2K^+}}e^{-\sigma\sqrt{\frac{1}{2K^+}}y^+{}_{Stoke}}\right)\\ +\sigma\sqrt{\frac{1}{2K^+}}\left(\frac{\rho g^+ g_0K_0K^+}{\mu U_0}+\frac{h^2}{\sigma^2K_0}\right)e^{-\sigma\sqrt{\frac{1}{2K^+}}y^+{}_{Stoke}}\end{array}\right]\left(\sigma\sqrt{K_0}-1\right)\end{array}\right\}A_f}{\left\{w_1e^{\sigma^2\sqrt{\frac{\varepsilon^l K_0}{2K^+}}}-w_1e^{-\sigma^2\sqrt{\frac{\varepsilon^l K_0}{2K^+}}}-\left(\frac{\rho g^+ g_0K_0K^+}{\mu U_0}+\frac{h^2}{\sigma^2K_0}\right)e^{-\sigma^2\sqrt{\frac{\varepsilon^l K_0}{2K^+}}}+\frac{\rho g^+ g_0K_0K^+}{\mu U_0}+\frac{h^2}{\sigma^2K_0}\right\}A_p}-1,$$

(4.110)

where $\sigma=\frac{y^+}{\sqrt{K_0}}$ and $y_{Stoke}\le y^+\le 1$. To compare the result with the experimental data, we use the same values of the variables as in the experiment. The dynamic viscosity and the density of water are $8.9\times10^{(-4)}\ \left[Pa\cdot s\right]$ and $997\ \left[kg/m^3\right]$, respectively [20]. The gravity g^+g_0 is $9.8\,[m/s^2]$. The length of the free-fluid domain ranges from

3.37046×10^{-4} to 1, where y_{Stoke} is assumed to be 3.37046×10^{-4}. The porosity is 0.78 and the characteristic permeability K_0 is 7.1×10^{-9}. The values of other variables used in (4.110) are $K^+ = \frac{k_{11}}{K_0}$, $k_{11}=0.4$, $w_1=-2.5$, $U_0=1$, $D_0=1$ and h = 7.5, and Φ is normalized by 10^4.

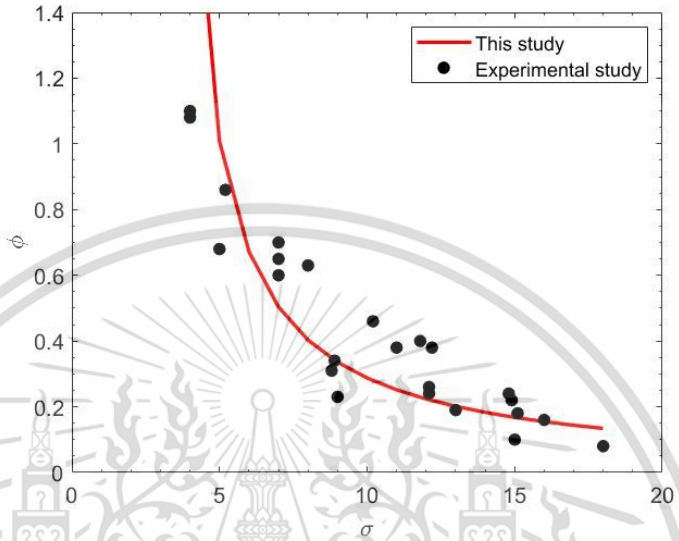

Figure 4.4 The mass flow rate in this study and the experimental data [30]

Figure 4.4 shows the comparison of the mass flow rate in this study (solid line), when the velocity of the solid phases are set to be zero, through the free-fluid domains as a function of σ, and the mass flow rate in the experimental study of Beavers and Joseph [30]. Beaver-Joseph experiment determined the mass flow rate in the free-fluid domain and the solid in the porous medium domain is a non-movable solid. However, the solids in this work are moving solids. Therefore, in order to be able to compare the results we have to set the velocity of solids to be zero. Since the experiment provide the flow only the free-fluid region, we compare the results only in this zone. Because the resulting solution still has the variable w_1 attached, in order to confirm that the solution we get tend to be consistent with the experimental results. We can find a value of w_1 that make the mass flow rate curve more likely to be close to the experimental results. It can be seen that the solution obtained in this work has an edge value placed at the junction area. As can be seen from Figure 4.4, the solution of our study (solid line) is in a good agreement with the experimental data of Beavers and Joseph literature [30].

In Chapter 5, we will use the solution found in this chapter to find the boundary condition at the free-fluid/ porous-medium interface.

Chapter 5
Boundary conditions at the Free-Fluid/Porous Medium interface

The boundary condition at the free-fluid/ porous-medium interface with the Beaver-Joseph boundary condition may not appropriated for our research problem. In this chapter we find the boundary condition at the free-fluid/ porous-medium interface by solving the two solutions (4.107) and (4.108) in the two domains. Based on solution (4.107) we obtain

$$w_1 = \frac{1}{\left(e^{z_1 y^+} - e^{-z_1 y^+}\right)}\left\{\left[U^{+(0)}\right]^{(p)} - z_4 e^{-z_1 y^+} - z_5 y^+ + z_4\right\}. \tag{5.1}$$

Substituting (5.1) in (4.108), then we have the boundary condition at the free-fluid/ porous-medium interface is

$$\begin{aligned}\left[U^{+(0)}\right]^{(f)} = {} & \frac{z_2 y^{+2}}{2} + D_0 - \frac{z_2}{2} + \left[-z_2 y^+_{Stoke} - z_1 z_4 e^{-z_1 y^+_{Stoke}} + z_5\right]\left(y^+ - 1\right) \\ & + \left[\frac{1}{\left(e^{z_1 y^+} - e^{-z_1 y^+}\right)}\left\{\begin{array}{l}\left[U^{+(0)}\right]^{(p)} \\ -z_4\left(e^{-z_1 y^+} - 1\right) \\ -z_5 y^+\end{array}\right\}\right]\left(z_1 e^{z_1 y^+_{Stoke}} + z_1 e^{-z_1 y^+_{Stoke}}\right)\left(y^+ - 1\right).\end{aligned} \tag{5.2}$$

The equation (5.2) is the new boundary condition at the interface that represents the different of $\left[U^{+(0)}\right]^{(f)}$ and $\left[U^{+(0)}\right]^{(p)}$ but this is the form of velocity profile.

Next we provide another boundary condition at the free-fluid/ porous-medium interface. Differentiating the zeroth-order solutions (4.107) and (4.108) both sides, we have

$$\frac{d\left[U^{+(0)}\right]^{(P)}}{dy^+} = w_1 J_1 e^{J_1 y^+} + w_1 J_1 e^{-J_1 y^+} - z_1 J_1 e^{-z_1 y^+} + z_2, , \tag{5.3}$$

$$\begin{aligned}\frac{d\left[U^{+(0)}\right]^{(f)}}{dy^+} = {} & w_1\left(J_1 e^{J_1 y^+_{Stoke}} + J_1 e^{-J_1 y^+_{Stoke}}\right) - J_1 z_1 e^{-J_1 y^+_{Stoke}} \\ & + z_2 - z_3\, y^+_{Stoke} + z_4 y^+,\end{aligned} \tag{5.4}$$

respectively, from (5.3), we obtain

$$w_1 = \frac{1}{\left(J_1 e^{J_1 y^+} + J_1 e^{-J_1 y^+}\right)}\left\{\frac{d\left[U^{+(0)}\right]^{(P)}}{dy^+} + z_1 J_1 e^{-z_1 y^+} - z_2\right\}. \tag{5.5}$$

Substituting (5.5) in (5.4), therefore we obtain another boundary condition at the free-fluid/ porous-medium interface, which is

$$\frac{d\left[U^{+(0)}\right]^{(f)}}{dy^{+}} - \frac{\left(e^{z_1 y^{+}_{Stoke}} + e^{-z_1 y^{+}_{Stoke}}\right)}{\left(e^{z_1 y^{+}} + e^{-z_1 y^{+}}\right)}\left[\frac{d\left[U^{+(0)}\right]^{(P)}}{dy^{+}} + z_1 z_4 e^{-z_1 y^{+}} - z_5\right] = z_2\left(y^{+} - y^{+}_{Stoke}\right) z_1 z_4 e^{-z_1 y^{+}_{Stoke}} + z_5, \tag{5.6}$$

Thus, we obtain two boundary conditions at the free-fluid/ porous-medium interface, which are proper for the fluid flow in the PCL due to the movement of cilia.

Next, we compare the obtained solutions with the boundary conditions (5.2) and (5.6) with the results with the Beaver-Joseph boundary condition.

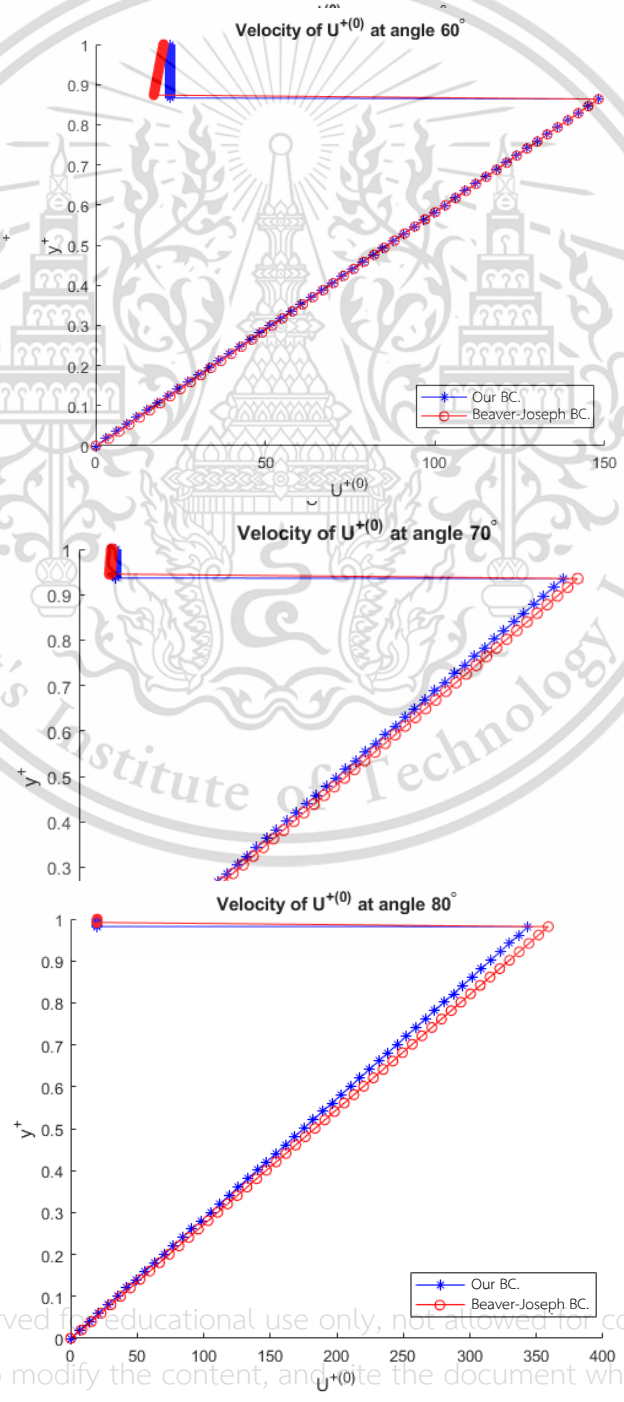

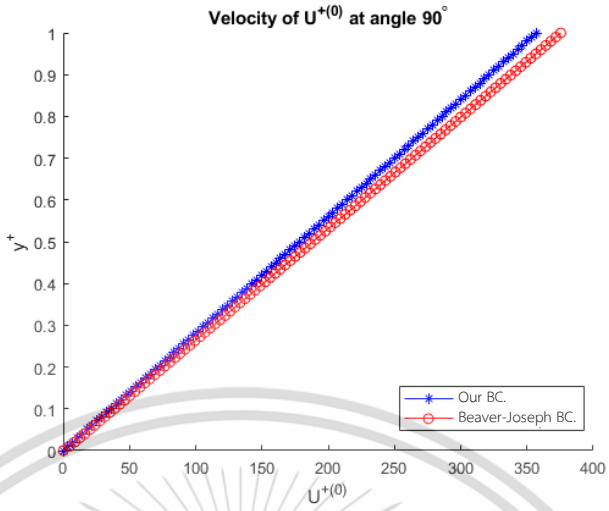

Figure 4.5 Comparison between the velocity of PCL fluid with Beaver-Joseph boundary condition at the interface and the velocity of the PCL fluid with our boundary condition at the interface

Figure 4.5 shows the velocities of the PCL fluid in different angle θ that the cilia make with the horizontal plane. The red line graph shows the velocity of the PCL fluid using the Beaver-Joseph boundary condition at the free-fluid/ porous-medium interface. The blue line is the velocity of the PCL fluid with the boundary conditions (5.2) and (5.6). It notes that the graphs of the velocities of the PCL fluid are similar. Although they are not completely overlap, but they are not very different, which is demonstrated in each degree. In the porous-medium domain the velocity of the PCL fluid due to the movement of cilia with Beaver-Joseph boundary condition and the velocity of the PCL fluid with the boundary conditions (5.2) and (5.6) are small difference. At the angle 50°, the velocity with boundary conditions (5.2) and (5.6) is greater than the one using Beaver-Joseph boundary condition. The curve overlaps completely at the angle 60°, and notice that at the angle greater than 60° the velocity of the PCL fluid with the boundary conditions (5.2) and (5.6) is less than the velocity of the PCL fluid with Beaver-Joseph boundary condition. In the free-fluid domain the velocity of the PCL fluid with the boundary conditions (5.2) and (5.6) is larger than the velocity in the PCL fluid with Beaver-Joseph boundary condition at every angle θ that the cilia make with the horizontal plane accept at $\theta = 90^\circ$ the solution is overlap.

Chapter 6
Conclusion

The movement of the cilia in the PCL layer plays an important role in the clearance of mucus and in preventing foreign materials from entering the lower respiratory tract. Determining the velocity of the PCL fluid flow in motile cilia is necessary for a better understanding of the clearance mechanism. The velocity of PCL fluid can be determined using an ordinary differential equation (ODE), which requires boundary conditions. This research quantifies the boundary conditions at the interface between the porous-medium and free-fluid regions

We divided our work into two parts. In the first part, the velocity in the PCL fluid due to the movement of cilia with Beaver-Joseph boundary condition is determined. Because of the movement of cilia, the first part is separated into two details depending on the angle θ. The cilia perpendicular to the horizontal plane and the cilia move forward and form an angle $\theta, \theta < 90^\circ$ with the horizontal plane. When the cilia move forward and form an angle $\theta, \theta < 90^\circ$ with the horizontal plane, the PCL can be divided into two domains, while the PCL has only one domain when $\theta = 90^\circ$. The layer containing cilia is called a porous medium domain and the layer above the cilia is called a free-fluid domain. The governing equation used in the work is the Stokes-Brinkman equation. In the free-fluid domain (Ω_1), we use the Stokes equation and in the porous medium domain (Ω_2), we use the Brinkman equation. The boundary condition at the bottom of the domain is $u = 0$ at $y = 0$, the top of the domain is $u = G$ at $y = h$, and the Beaver-Joseph boundary condition is applied at the interface between the free-fluid/porous medium domain. The velocity of the PCL fluid due to the movement of cilia are obtained by using the matched asymptotic expansion The solutions are the velocity of PCL fluid in the layer containing cilia with different angle θ $\left(50^\circ, 60^\circ, 70^\circ, 80^\circ, 90^\circ\right)$, respectively. The asymptotic solution of the Stokes-Brinkman equations (4.25) and (4.45) is shown in Figure 4.1. The second part is to determine the boundary condition at the free-fluid/ porous medium interface is suitable for this problem. To find the boundary condition at the interface suitable for the problem, we divide domains into inner and outer zones and find the solutions for these two regions and then use Van Dyke's conditions to match these two solutions. We derive matching conditions to match the solutions of the outer and inner regions. The outer zone are the free-fluid domain and porous medium domain, and the inner zone is the transition zone at interface between the free-fluid/porous medium domain. The results are illustrated in Figure 4.3 with different angles, $\theta = 40^\circ, 50^\circ, 60^\circ, 70^\circ, 80^\circ, 90^\circ$, that the cilia make with the horizontal plane. The variables employed to plot the graph of the

solutions are shown in Tables 4.3 and 4.4. The velocity of the PCL fluid reaches its maximum value when $\theta = 90^{\circ}$ and decreases when θ decreases, which satisfies our assumption that the highest velocity of cilia occurs when the cilia are perpendicular to the horizontal plane and the cilia velocities decrease with decreasing angle θ. The first boundary condition is the relationship between the two zeroth-ordered solutions in the two domains while the second boundary condition is the derivative of those two solutions. The limitation of this study is that the asymptotic expansion method applied in this study is good for a linear equation, but it is not easy to find the solutions for nonlinear equations. The disadvantage of this study is that we calculate the zeroth-order approximation solution, where the other orders are cut off. We compare our solution with the experimental data of Beaver-Joseph by observing the mass flow rate. The solution in domain Ω_1 of our study is in good agreement with the experimental data in the Beaver-Joseph literature when the solid phase are set to be zero. After that, we find the boundary condition at the free-fluid/ porous-medium interface appropriate for our research problem. Then we compare the solution that uses the Beaver-Joseph condition at the interface between the free-fluid/ porous-medium domain and the solution with our boundary conditions (5.2) in Figure 4.5 the graphs of the velocities of the PCL fluid are similar which is demonstrated in each degree. We conclude the work in this thesis in the flowchart below

We use the normalized of the Stokes–Brinkman equations: Brinkman equation (3.19) and Stokes equation (3.25) to determine the velocity of PCL fluid. The normalized boundary conditions used at the bottom of the domain Ω_2 is (3.30), the top boundary condition is (3.31), and the Beaver-Joseph boundary condition (3.28) is employed at the porous medium/free-fluid interface.

We obtain the velocity of PCL fluid: the zero-order solutions (4.25) and (4.45) of the porous medium domain in the outer zone and the free-fluid domain, respectively. Then, we apply the Beaver-Joseph boundary condition (3.28) at the porous medium/free-fluid interface and obtain the zero-order solution (4.59) in the whole domain.

We use the normalization of the Stokes–Brinkman equations: Brinkman equation (3.19) and Stokes equation (3.25) with the bottom boundary condition (3.30), and the top boundary condition (3.32).

We obtain the velocity of PCL fluid, the zero-order solutions (4.25) and (4.63) in the porous medium domain and the free-fluid domain, respectively. We obtain the velocity of PCL fluid, the zero-order solution (4.78) in the inner zone.

We match the outer and inner zone by using conditions (4.94) - (4.96), then we obtain the zero-order solution (4.107) and (4.108) in the porous medium domain and the free-fluid domain, respectively.

We match the outer and inner zone by using conditions (4.94) - (4.96), then we obtain the zero-order solution (4.107) and (4.108) in the porous medium domain and the free-fluid domain, respectively.

Comparison of the zero-order solution with the experimental of Beaver-Joseph in the pattern of mass flow rate Φ, the mass flow rate in our study is the equation (4.110) (shown in Figure 4.4).

Compare our matched solutions with the results that use the Beaver-Joseph condition at the interface between the free-fluid/ porous-medium domain as shown

Nomenclature

variable	definition	unit	equation
a_0	a constant		(4.15)
a_1	a constant		(4.15)
c_0	a constant		(4.10)
c_1	a constant		(4.10)
$H(y^+)$	a function of y^+		(3.18)
D_0	a constant		(3.32)
$\frac{dp}{dx}$	the pressure gradient	$\left[\frac{dp}{dx}\right]=\frac{M}{L^2T^2}$	(3.3)
g	the gravity	$[g]=\frac{L}{T^2}$	(3.1)
g_0	characteristic gravity	$[g_0]=\frac{L}{T^2}$	(3.13)
h	the characteristic length	$[h]=L$	Fig 3.1
K_0	characteristic permeability	$[K_0]=L^2$	(3.13)
K^+	dimensionless permeability	$[K^+]=1$	(3.13)
$k_{11}{}^{-1}$	the inverse of the permeability tensor	$\left[k_{11}{}^{-1}\right]=\frac{1}{L^2}$	(3.3)
k_{11}	a permeability tensor	$[k_{11}]=L^2$	(3.13)
M_1	a constant		(3.18)
M_2	a constant		(3.18)
M_3	a constant		(3.18)
m_1	a constant		(4.71)
m_2	a constant		(4.71)
m_3	a constant		(4.73)
m_4	a constant		(4.73)
M_f	the mass flow rate in the free-fluid region	$[M_f]=\frac{M}{T}$	(4.109)
M_P	the mass flow rate in the porous medium	$[M_P]=\frac{M}{T}$	(4.109)
p	pressure	$[p]=\frac{M}{LT^2}$	(3.1)
U_0	a volumetric average velocity in a porous medium	$[U_0]=\frac{L}{T}$	(2.5.12)
U^+	dimensionless average velocity		(3.13)
$\bar{U}^+$	dimensionless velocity in the inner region		(4.65)

variable	definition	unit	Equation
$U^{+(0)}$	dimensionless the zeroth-order solution of the outer region		(4.1)
$U^{+(1)}$	dimensionless the first-order solution of the outer region		(4.1)
v^l	the velocity of the liquid phase	$\left[v^l\right]=\frac{L}{T}$	(3.1)
v^S	the velocity of the solid phases	$\left[v^s\right]=\frac{L}{T}$	(3.1)
w_1	a constant		(4.14)
w_3	a constant		(4.28)
w_5	a constant		(4.42)
w_7	a constant		(4.47)
y^+	dimensionless y		(3.13)
y^+	dimensionless y in the inner region		(4.64)
y_{Stoke}	The height of the porous medium domain	$\left[y_{Stoke}\right]=L$	Fig 1.2
y^+_{Stoke}	y_{Stoke} in free-fluid region	$\left[y^+_{Stoke}\right]=L$	(3.12)
y^-_{Stoke}	y_{Stoke} in porous medium region	$\left[y^-_{Stoke}\right]=L$	(3.12)
z_1	a constant		(4.105)
z_2	a constant		(4.105)
z_3	a constant		(4.105)
z_4	a function depending on ε^l and k_{11}		(4.105)
z_5	a function depending on ε^l and k_{11}		(4.105)
Ω	periciliary layer (PCL)	$\left[\Omega\right]=L^2$	Fig 1.2
Ω_1	free-fluid domain	$\left[\Omega_1\right]=L^2$	Fig 1.2
Ω_2	porous medium	$\left[\Omega_2\right]=L^2$	Fig 1.2
ε^l	a porosity	$\left[\varepsilon^l\right]=1$	(3.1)
ρ	the fluid density	$[\rho]=\frac{M}{L^3}$	(3.1)
μ	a dynamic viscosity	$[\mu]=\frac{M}{LT}$	(3.1)
Φ	the mass flow rate in the total domain	$\left[\Phi\right]=1$	(4.109)

where L,T and M represent length, time and mass, respectively.

References

[1] A. E. Tilley, M. S. Walters, R. Shaykhiev, and R. G. Cryatal, "Cilia Dysfunction in Lung Disease", HHS Public Access. *Annual Review of Physiology*. Vol. 77: 379-406, doi: 10.1146/annurev-physiol-021014-071931, 2015.

[2] B. Button, L. H. Cai, C. Ehre, M. Kesimer, D. B. Hill, J. K. Sheehan, R. C. Boucher, and M. Rubinstein, "A Periciliary Brush Promotes the Lung Health by Separating the Mucus layer from Airway Epithelia". *Science*. Vol. 337: 937-941, doi: 10.1126/science.1223012, 2012.

[3] M. Chandesris, and D. Jamet, "Boundary Conditions at a Planar Fluid-Porous Interface for a Poiseuille Flow". *International journal of Heat and Mass Transfer*. Vol 49, P. 2137-2150, doi: 10.1016/j.ijheatmasstransfer.2005.12.010, 2006.

[4] F. J. Valdes-Parada, and D. Lasseux, "A Novel One-domain Approach for Modelling Flow in a Fluid-Porous System Including Inertia and Slip Effects". *Physics of Fluids.* Vol.33, Issue 2, doi: 10.1063/5.0036812, 2020.

[5] S. Poopra, and K. Wuttanachamsri, "The Velocity of PCL Fluid in Human Lungs with Beaver and Joseph Boundary Condition by Using Asymptotic Expansion Method". *Mathematics 2019*, Vol. 7, Issue 6, P. 567, doi: 10.3390/math7062567, 2019.

[6] K. Wuttanachamsri, "Free Interface at the Tips of Cilia in the One-Dimensional Periciliary Layer". Journal of Mathematics. Vol. 8, Issue 11, doi:10:3390/math8111961, 2020.

[7] K. Wuttanachamsri, and L. Schreyer, "Effects of Cilia movement on Fluid Velocity: II Numerical Solutions Over a Fixed Domain". *Transport in Porous Media*. Vol. 134, P. 471-489, doi: 10.1007/511242-020-01455-4, 2020.

[8] T. Carraro, C. Goll, A. Marciniak-Czochra, and A. Mikelic, "Pressure Jump Interface Law for The Stokes-Darcy Coupling: Comfirmation by Direct Numerical Simulations". *Journal of Fluid Mechanics.* Vol. 732, P.510-536, doi:10.1017/ jfm.2013.416, 2013.

[9] S. B. Naqvi, and A. Bottaro, "Interfacial conditions Between a Free-Fluid \ Region and a Porous Medium". *International Journal of Multiphase Flow.* Vol. 141, doi: 10.1016/ j.ijmultiphaseflow.2021.103585, 2021.

References (Continue)

[10] M. Ehrhardt, "An Introduction to Fluid-Porous Interface Coupling". *In book: Progress in Computational Physics.* Vol 2: 2 coupled Fluid Flow in Energy, Biology and Enviromental Research P. 3-12, doi: 10.2174/9781608052547 11201010003, 2012.

[11] J. Ballenger, "Experimental Effect of Cigarette Smoke on Human Respiratory Cilia". *The New England Journal of Medicine.* Vol. 263, P. 832-835, doi: 10.1056/NEJM196010272631704, 1960.

[12] H. Machemer, "Ciliary Activity and The Origin of Metachrony in Paramecium: Effects of Increasd Viscocity". *The Journal of Experimental Biology.* Vol. 57, P.239-259, doi: 10.1242/jeb.57.1.239, 1972.

[13] D.J. Smith, A.A. Smith, and J.R. Blake, "Mathematical Embryology: The Fluid Mechanics of Nodal Cilia". *The Journal of Engineering Mathematics.* doi: 10.48550/arXiv.1007.1691, 2010.

[14] G.R. Fulford, and J.R. Blake. "Muco – Ciliary Transport in The Lung". *The Journal of Theoretical Biology.* Vol. 86, P. 381-402, doi: 10.1016/s0022-5193(86)80098-4, 1986.

[15] M. King, M. Agarwal, and J.B. Shukla. "A Planar Model For Mucociliary Transport: Effect of Mucus Viscoelasticity". *The Journal of Biorheology*. Vol. 30, P. 49-61, PMID: 8374102, 1993.

[16] T.E. Gray, K. Guzman, C.W. Davis. L.H. Abdullah, and P. nettesheim. "Mucociliary Differentiation of Serially Passaged Normal Human Tracheabronchial Epithelial Cells". *American Journal of Respiratory Cell and Molecular Biology.* Vol. 14, P. 104-112, doi: 10.1165/ajrcmb.14.1.8534481, 1996

[17] H. Rahmoune, and K.L. Shephard. "State of Airway Surface Liquid on Guinea Pig Trachea". *Journal of Applied Physiology.* Vol. 6, P.2020-2024, doi: 10.1152/jappl.1995.78.6, 2020.

[18] B. Spungin, and A. Silberberg. "Stimulation of Mucus Secretion, Ciliary Activity, and Transport in Frog Palate Epithelium". *The American Journal of Physiology.* Vol. 247, P.299-308, doi: 10.1152/ajpcell.1984.247.5.C299, 1984.

[19] S.M. Serafini, and E.D. Michaelson. "Length and Distribution of Cilia in Human and Canine Airways". *Bulletin Europeen De Physiopayhologie Respiratoire.* Vol. 13, P.551-559, PMID: 912142 1977.

References (Continue)

[20] N.G. Toremalm. “The Daily Amount of Tracheo-Bronchial Secretions in Man. A Method For Continuous Tracheal Aspiration in Laryngectomized and Tracheotomized Patients”. *Acta Oto-Laryngologica. Supplementum.* P.43-53, doi: 10.3109/00016486009122392, 1960.

[21] P.G. Jayathilake, Z. Tan, D.V. Le, H.P. Lee, and B.C. Khoo. “Three-Dimensional Numerical Simulations of Human Pulmonary Cilia in The Periciliary Liquid Layer By The Immersed Boundary Method”. *Computers & Fluids Sciencedirect*. Vol. 67, P.130-137, doi: 10.1016/j.compfluid.2012.07.016, 2012.

[22] H. Matsui, S.H. Randell, S.W. Peretti, C.W. Davis, and R.C. Boucher. “Coordinated Clearance of Periciliary Liquid and Mucus From Airway Surfaces”. *The Journal of Clinical Investigation.* Vol. 102(6), P.1125-1131, doi: 10.1172/JCI2687, 1998.

[23] F. J. Valdes-Parada, and D. Lasseux, “A Novel One-domain Approach for Modelling Flow in a Fluid-Porous System Including Inertia and Slip Effects”. *Physics of Fluids.* Vol.33, Issue 2, doi: 10.1063/5.0036812, 2020.

[24] T. Carraro, C. Goll, A. Marciniak-Czochra, and A. Mikelic, “Pressure Jump Interface Law for The Stokes-Darcy Coupling: Comfirmation by Direct Numerical Simulations”. *Journal of Fluid Mechanics.* Vol. 732, P.510-536, doi:10.1017/ jfm.2013.416, 2013.

[25] S. B. Naqvi, and A. Bottaro, “Interfacial conditions Between a Free-Fluid Region and a Porous Medium”. *International Journal of Multiphase Flow.* Vol. 141, doi: 10.1016/ j.ijmultiphaseflow.2021.103585, 2021.

[26] G. Du, and L. Zu, “Local and Parallel Finite Element Method for the Mixed Navier-Stokes/Darcy Model with Beaver-Joseph Interface Conditions”. *Acta Mathematica Scientia.* Vol. 37, Issue 5, P. 1331-1347, doi: 10.1016/s0252-9602(17)30076-0, 2017.

[27] J. A. Ochoa–Tapia, and S. Whitaker, “Momentum Transfer at the Boundary between a Porous Medium and a Homogeneous Fluid – II”. *International Journal of Heat and Mass Transfer.* Vol. 38, Issue 14, P.2635–2646, doi: 10.1016/0017-9310(94)00346-w, 1995.

[28] B. Goyeau, D. Lhuillie, D. Gobin, and M. G. Velarde, “Momentum Transport at a Fluid – Porous Interface”. *International Journal of Heat and Mass Transfer.* Vol. 46, Issue 21, P.4071 – 4081, doi: 10.1016/s0017-9310(03)00241-2, 2003.

References (Continue)

[29] S. Whitaker, "Flow in Porous Media I: A Theoretical Derivation of Darcy's law". *Transport in Porous Media.* Vol 1: 3–25, doi: 10.1007/BF01036523, 1986.

[30] G. S. Beaver, and D. D. Joseph, "Boundary Conditions at a Naturally Permeable Wall". *Journal of Fluid Mechanics.* Vol. 30, Issue 1, P.197-207, doi: 10.1017/s0022112067001375, 1967.

[31] M. Sahraoui, and M. Kaviany, "Slip and No-Slip Velocity Boundary Conditions at Interface of Porous, Plain Media". *International journal of Heat and Mass Transfer.* Vol. 3, Issue 4, P. 5: 927-943, doi: 10.1016/0017-9310(92)90258-T, 1992.

[32] K. Chamsri. "Formulation of a Well-Posed Stokes-Brinkman Problem With a Permeability Tensor". *International Sciencetific Journal of Mathematics.* Vol. 1, P.1-7, 2015.

[33] J. H. Cushman, L. Bennethum, and B. Hu, "A Primer on Upscaling Tools for Porous Media". Advances in Water Resources. Vol. 25, Issue 8, P. 1043-1067, doi: 10.1016/50309-1708(02)00047-7, 2002.

[34] J. Kevorkian, and J. D. Cole, "Introduction to Perturbation Methods". Applied Mathematical Science, Vol. 34, Springer-Verlag, Berlin and New York, 1981.

[35] K. Chamsri, and L. S. Bennthum, "Permeability of Fluid Flow Through a Periodic Array of Cylinders". Applied Mathematical Modelling. Vol. 39 P. 244-254, doi: 10.1016/j.apm.2014.05.024, 2015.

[36] P. R. Sears, K. Thomson, M. R. Knowles, and C. W. Davis, "Human Airway Ciliary Dynamics". American Journal of Physiology Lung Cellular and Molecular Physiology. Vol. 3, P. 170-183, doi: 10.1152/ajplung.00105, 2012.

[37] P. Zhu, "An Introduction to Matched Asymptotic Expansion". Basque Center for Applied Mathematics and Ikerbasque Foundation for Science. Nov., 2009.

[38] "Perturbation method", 18 July 2022, Http://www.math.unm.edu/ courses/Ma 570/text.pdf.

[39] K. Chamsri, "Modeling the Flow of PCL Fluid Due to the Movement of Lung Cilia". Doctor of Philosophy Applied Mathematics. University of Colorado Denver., 2012

[40] P.Zhu, "An Introduction to Matched Asyptotic Expamsions". Basque center for Applied Mathematics and Ikerbasque Foundation for Science., 2009

[41] "Little Oh Notation (o)", 3 April 2022, https://www.tutorialspoint.com/little-oh-notation-o

[42] "Big O and Little O Definitin", 3 April 2022, Http://www.baeldung.com/cs/big-o-vs-little-o-notation,

Appendices

Appendix A
Research Papers

mathematics

MDPI

Article

The Velocity of PCL Fluid in Human Lungs with Beaver and Joseph Boundary Condition by Using Asymptotic Expansion Method

Sudaporn Poopra * and Kanognudge Wuttanachamsri

Department of Mathematics, Faculty of Science, King Mongkut's Institute of Technology Ladkrabang, Bangkok 10520, Thailand; kanognudge.wu@kmitl.ac.th

* Correspondence: 57605022@kmitl.ac.th; Tel.: +66-0890-342-375

Received: 17 April 2019; Accepted: 23 May 2019; Published: 24 June 2019

check for updates

Abstract: Humans breathe air into the respiratory system through the trachea, but with all the pollutants in our environment (both outside and inside), the air we breathe may not be clean. When that is so, the respiratory system secretes mucus to trap dirt that is inhaled through the nostrils. The respiratory tract contains hair-like structures in the epithelial tissue, called cilia: These wave back and forth to help expel particles of dust, dirt, mucus, and contaminants from the body. Cilia are found in this layer (a porous medium) and the fluid in this layer is called the periciliary layer (PCL). This study aims to determine the velocity of the PCL fluid flow in motile cilia. Usually, fluids move due to pressure changes, but in this study, the velocity of solids or of the cilia moves the PCL fluid. Stokes-Brinkman equations are used to determine the velocity of PCL fluid flow when cilia form an angle with the horizontal plane. The Beavers and Joseph boundary condition is applied in this study. The asymptotic expansion method is adapted in order to determine the velocity of PCL from the movement of the cilia.

Keywords: periciliary layer; moving solid phases; asymptotic expansion method; Stokes–Brinkman equations

1. Introduction

The human body contains numerous cilia, which are omnipresent inside and outside of the body. Cilia are hair-like organelles that provide locomotion to liquids throughout the body. This study focuses on cilia inside the body, particularly in the respiratory system. The human respiratory system is illustrated in Figure 1, with labeling of the nose, trachea, and lungs. We breathe in and out all the time, and as we inhale, some dust and pathogens will enter the body. However, the human body has a defense mechanism to protect against these foreign particles. In a closer look at the immune system, a diagram representing a cross-section of the trachea is displayed in Figure 2, and Figure 3 shows a close-up view of the trachea.

Figure 3 shows the platform of the innate immune system of the throat cells, which consists of three layers: The air layer, the mucus layer, and the periciliary layer (PCL). Cilia are found in the PCL layer. The function of the cilia is to filter out dust and other inhaled foreign particles. Cilia work as a part of the immune system, protecting the body against pathogens in the air. Goblet cells (vital component cells of the immune system) secrete mucus to trap the inhaled particles and cilia help to transport these particles out of the body by cilia-generated flow. To calculate the mucus velocity, the velocity of PCL fluid is measured to determine the bottom boundary of the mucus layer.

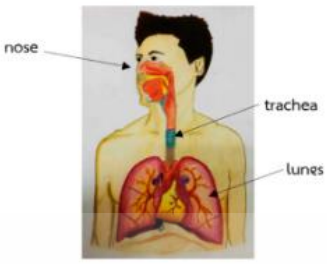

Figure 1. The human respiratory system.

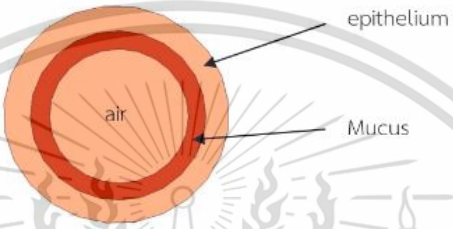

Figure 2. A cross-section of the trachea.

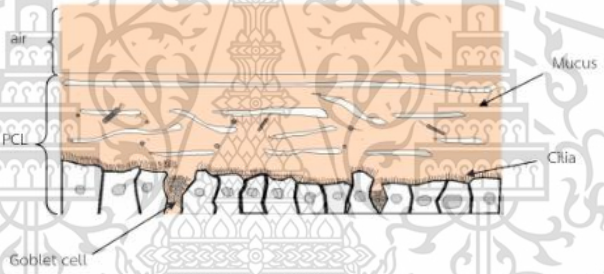

Figure 3. Platform of the innate immune system.

Numerical studies on the PCL and mucus layers have been carried out by several researchers. For example, Machemer [1] observed the ciliary system and found that frequency of peristomal cilia decreases with increasing viscosity, which leads to an increase of the average wavelength from 10.7 at 1 cP to 14.3 at 40 cP. Smith et al. [2] developed a new model for the nodal flow, utilizing the regularized stokeslet method. Fulford and Blake [3] studied a two-layer Newtonian fluid model for muco-ciliary transportation in the lung, and discovered that the viscosity of the upper mucous layer is much greater than the viscosity of the lower periciliary layer. Jayathilake et al. [4] developed a three-dimensional numerical model to simulate human pulmonary cilia motion in the PCL using the immersed boundary method combined with the projection method. Their numerical results indicated that the phase differences of cilia—in both stream-wise and span-wise directions—resulted in the maximum PCL velocity in the stream-wise direction.

Another approach on the study of the PCL and mucus layers is experimental study, which has been examined by a number of researchers. For example, Serafini and Michaelson [5] determined ciliary length and the percentage of ciliated cells from six mongrel dogs and ten humans. Matsui et al. [6]

studied the movements of mucus and PCL liquid in airway surfaces, using conventional and confocal microscopy of fluorescent microspheres photoactivated fluorescent dyes and well-differentiated human tracheobronchial epithelial cell cultures that exhibited spontaneous, radial mucociliary transport. Their findings showed that the entire PCL liquid was transported at approximately the same rate as mucus, 39 ± 24.7 and 39.8 ± 4.2 μm/s. Moreover, they found that the removal of the mucus layer reduced PCL transport by >80%, 4.8 ± 0.6 μm/s, which is close to the value predicted by theoretical analyses of the ciliary beat cycle. Therefore, it has been suggested that the movement of PCL liquid depends on the transport of mucus.

Although the study of PCL and mucus layers, both numerical and experimental studies, has been investigated extensively, these studies covered only movement, length, and direction of cilia; the research on velocity of cilia in the PCL layer is limited. In general, the asymptotic expansion method is used to examine the PCL fluid flow order to determine the velocity of PCL fluid. Cilia in the PCL layer are shown in Figure 4; cilia making a 90° angle with the horizontal plane are displayed in Figure 4a, while cilia at an angle of less than 90° are illustrated in Figure 4b. The domain Ω_1 is the PCL with an absence of cilia. The second domain, Ω_2 is the PCL containing cilia.

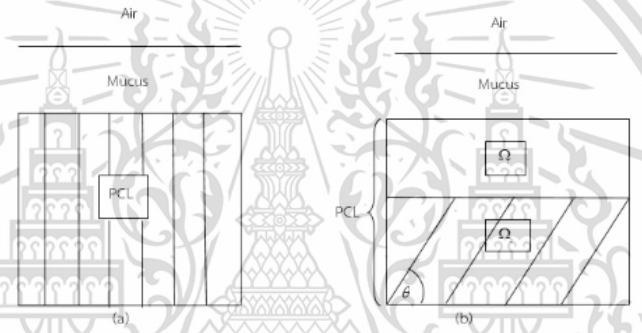

Figure 4. Cartoon picture of cilia (**a**) cilia are perpendicular to the horizontal plane; (**b**) cilia make angle $\theta, \theta < 90^{\circ}$ with the horizontal plane.

As the domain Ω_2 contains both liquid and solid phases, it is considered to be a porous medium. For the mathematical model used in the free fluid and the porous medium domains, some studies have used Navier-Stokes in the free fluid layer and Darcy in the porous medium [7], or Stokes equation in the free fluid layer and the Brinkman equation in the porous medium [8,9]. The Beavers-Joseph condition has been widely used in many numerical studies as well as to compare solutions, especially between a porous medium and a free fluid domain. For example, Francisco et al. [10] derived boundary conditions that complete the statement of a two-domain approach for a one-dimensional momentum transport in a system containing a porous medium and free fluid under a constant pressure gradient. These boundary conditions involve a jump in both the velocity and the viscous stress and are thus expressed in terms of jump coefficients.

In this paper, we use the Stokes equation in the free fluid region and the Brinkman equation in the porous medium in order to analytical study the Stoke–Brinkman equations. The asymptotic expansion method has been widely used in a number of studies [11–13]. Chandesris and Jamet [14] found the boundary condition at the interface between the porous medium and the free fluid based on the Poiseuille flow over a permeable block. The problem was solved using the matched asymptotic expansion method, therefore, both a heterogeneous transition zone and a homogeneous zone between the two homogeneous regions (porous medium and free fluid) were considered. The two homogeneous regions were described using volume averaged transport equation, with the assumption

that this equation still holds in the heterogeneous transition zone by considering variable porosity and permeability.

However, to the authors' knowledge, no study to date has used asymptotic expansion related to the velocity of the cilia in the model. The model used in the present study involves the velocity of solid helping to move the PCL fluid. In this study, we provide the velocity of the PCL fluid by using asymptotic expansion due to the movement of cilia where the Beaver–Joseph boundary condition is employed at the free fluid/porous medium interface.

In Section 2, we write n-dimensional Stokes–Brinkman equations in one dimension by using the indicial notation. The dimensionization of the governing equations is derived in Section 3. The solutions of the Stokes–Brinkman equations are computed with the asymptotic expansion method in Section 4. In Section 5, we determine the relation of the constants. We describe result and discussion in Section 6, and in Section 7 we draw our conclusions.

2. Mathematical Model and Boundary Conditions

In this section, we introduce our governing equations: the n-dimensional Stokes–Brinkman equations and the boundary conditions used in the PCL.

2.1. Stokes–Brinkman Equations

The n-dimensional Stokes–Brinkman equations were derived using an upscaling method, which is a method that helps to change the equations from a microscopic scale to a macroscopic scale. Then, we simplified the equations to one dimension by using an indicial notation. The macroscale Stokes–Brinkman equations [12] and the continuity equation [12] in n dimension are

$$\mu \mathrm{k}^{-1} \cdot \left(\varepsilon^l \mathrm{v}^l\right) + \nabla p - \frac{\mu}{\varepsilon^l} \Delta\left(\varepsilon^l \mathrm{v}^l\right) = \rho \mathrm{g} + \mu \mathrm{k}^{-1} \cdot \varepsilon^l \mathrm{v}^s + \frac{\mu}{\varepsilon^l} \nabla f, \tag{1}$$

$$\nabla \cdot \left(\varepsilon^l \mathrm{v}^l\right) = f, \tag{2}$$

respectively, where the function $f = \frac{-\varepsilon^{\cdot l}}{(1-\varepsilon^l)} + \nabla \cdot \varepsilon^l \mathrm{v}^s$; μ is a dynamic viscosity; k^{-1} is the inverse of the permeability tensor; ε^l is the porosity; v^l and v^S are the velocities of the liquid and solid phases, respectively; p is the pressure; ρ is the fluid density; g is gravity; and $\varepsilon^{\cdot l}$ is the material time derivative of the porosity with respect to the solid phase, $\varepsilon^{\cdot l} = \frac{\partial \varepsilon^l}{\partial t} + \mathrm{v}^s \cdot \nabla \varepsilon^l$. Equation (1) is the Brinkman equation. Without the first and fifth terms in the equation, it is a Stokes equation. Thus, in general, Equation (1) is called a Stokes–Brinkman equations. Applying the indicial notation to the Stokes–Brinkman equations we obtain

$$\mu \mathrm{k}_{\mathrm{ij}}^{-1}\left(\varepsilon^l v^l{}_j\right) + p_{,i} - \frac{\mu}{\varepsilon^l}\left(\varepsilon^l v_1{}^l\right)_{,jj} = \rho \mathrm{g}_\mathrm{i} + \mu \mathrm{k}_{\mathrm{ij}}^{-1} \varepsilon^l v_j{}^s + \frac{\mu}{\varepsilon^l} f_{,i}, i = 1, 2, 3, \ldots, n \tag{3}$$

$$\varepsilon^l v^l_{i,i} = f, i = 1, 2, 3, \ldots, n \tag{4}$$

where the repeat index indicates the summation. Substituting Equation (4) into the last term of Equation (3), for the one-dimensional domain, we have

$$\mu \mathrm{k}_{11}^{-1} \varepsilon^l v_1{}^l + p_{,1} - \frac{\mu}{\varepsilon^l}\left(\varepsilon^l v_1{}^l\right)_{,11} = \rho \mathrm{g}_1 + \mu \mathrm{k}_{11}^{-1}\left(\varepsilon^l v_1{}^s\right) + \frac{\mu}{\varepsilon^l}\left(\varepsilon^l v_{1,1}{}^l\right)_{,1} \tag{5}$$

Note that $\left(\varepsilon^l v_{1,1}{}^l\right)_{,1} = \left(\varepsilon^l v_1{}^l\right)_{,11}$. Simplifying Equation (5) yields

$$\frac{2\mu}{\varepsilon^l}\left(\varepsilon^l v_1{}^l\right)_{,11} - \mu \mathrm{k}_{11}^{-1}\left(\varepsilon^l v_1{}^l\right) + \rho \mathrm{g}_1 = p_{,1} - \mu \mathrm{k}_{11}^{-1}\left(\varepsilon^l v_1{}^s\right) \tag{6}$$

In this study, we assume that the solid velocity depends on only the Y direction; the fluid flow along the x-axis; and the pressure depends on the X direction. As a result, Equation (6) becomes

$$\frac{2\mu}{\varepsilon^l}\frac{d^2\left(\varepsilon^l {v_1}^l\right)}{dy^2} - \mu {k_{11}}^{-1}\left(\varepsilon^l {v_1}^l\right) + \rho g_1 = \frac{dp}{dx} - \mu {k_{11}}^{-1}\left(\varepsilon^l {v_1}^s\right) \tag{7}$$

Equation (7) is a Brinkman equation, which is used in the domain containing cilia.
In region Ω_1, we use a Stokes equation,

$$\frac{2\mu}{\varepsilon^l}\frac{d^2\left(\varepsilon^l {v_1}^l\right)}{dy^2} + \rho g_1 = \frac{dp}{dx} - \mu {k_{11}}^{-1}\left(\varepsilon^l {v_1}^s\right) \tag{8}$$

The continuity equation applied in this region is

$$\frac{\partial\left(\varepsilon^l v^l\right)}{\partial y} = 0 \tag{9}$$

For the free fluid region, we use a Stokes equation in domain Ω_1. The equation is actually the Brinkman equation, without the permeability term.

Notice that we have two different and adjacent domains. Therefore, a boundary used at the interface is special. In this work we applied the Beavers–Joseph boundary condition at the interface between the free fluid region and the porous medium domain.

2.2. Boundary Conditions

No free fluid exists in the PCL when the cilia are perpendicular to the horizontal plane. Figure 5a shows that the PCL has only domain Ω_2. Figure 5b shows our domains Ω_1 and Ω_2; the boundary condition between Ω_1 and Ω_2 is at y_{Stoke} at the tips of the cilia. Note that y_{Stoke} depends on the angle θ. We used 3 boundary conditions in this study $u = 0$ at $y = 0$, $u = G$ at $y = h$ and y_{Stoke} Beavers–Joseph boundary condition at y_{Stoke}.

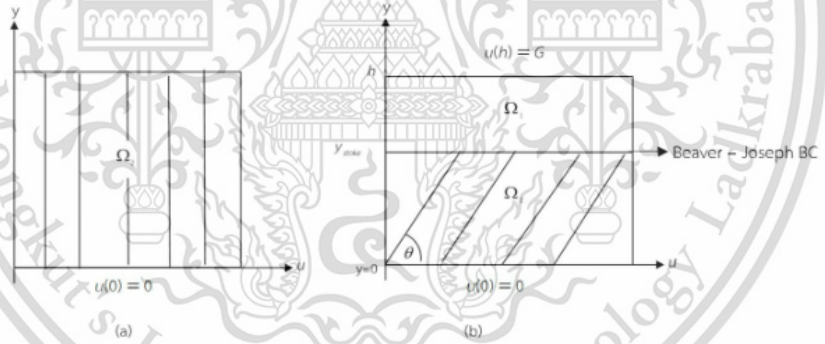

Figure 5. Cilia making the angle $\theta, 40^\circ \leq \theta \leq 90^\circ$, with the horizontal plane. (**a**) cilia are perpendicular to the horizontal plane; (**b**) cilia make angle with the horizontal plane.

Let $u = \varepsilon^l {v_1}^l$. We now have the system of equations with the unknown u and boundary conditions;

$$u = 0 \text{ at } y = 0 \tag{10}$$

$$u = G \text{ at } y = h \tag{11}$$

$$\left.\frac{du}{dy}\right|_{y=y^+{}_{stoke}} - \frac{1}{\varphi_p}\left.\frac{du}{dy}\right|_{y=y^-_{stoke}} = \frac{\beta}{\sqrt{K}}u|_{y=y_{stoke}} \text{ at } y = y_{Stoke} \tag{12}$$

where β is a dimensionless parameter of the order of one; ε^l is porosity of the porous medium; y_{Stoke} is length of porous medium; and G is a function depending on X and the angle θ.

3. Dimensionless Stokes–Brinkman Equations

In this section, we normalize the Stokes–Brinkman equations by introducing the following new variables.

$$y^+ = \frac{y}{h},\ U^{+(0)} = \frac{u}{U_0}, v^+ = \frac{v_1^s}{U_0}, x^+ = \frac{x}{h}, K^+ = \frac{k_{11}}{K_0}, P^+ = p\frac{h}{U_0\mu} \text{ and } g^+ = \frac{g}{g_0} \tag{13}$$

where h is the characteristic length; U_0 is volumetric average velocity in the porous medium; K_0 is characteristic permeability; and g_0 is characteristic gravity.

3.1. Dimensionless of Brinkman Equation

We normalize the Brinkman equation, of Equation (7) by substituting Equation (13) for Equation (7). We then have

$$\frac{2}{\varepsilon^l}\frac{d^2U^{+(0)}}{dy^{+2}} - \frac{h^2}{K_0K^+}U^{+(0)} + \frac{h^2\rho g^+ g_0}{\mu U_0} = \frac{dP^+}{dx^+} - \frac{h^2\varepsilon^l v^+}{K_0K^+} \tag{14}$$

Equation (14) can be rewritten as

$$2M_1\frac{d^2U^{+(0)}}{dy^{+2}} - M_2U^{+(0)} + M_3 = \frac{dP^+}{dx^+} - H\left(y^+\right), \tag{15}$$

where $M_1 = \frac{1}{\varepsilon^l}, M_2 = \frac{h^2}{K_0K^+}, M_3 = \frac{h^2\rho g^+ g_0}{\mu U_0}$ are constants and

$$H\left(y^+\right) = \frac{h^2\varepsilon^l v^+}{K_0K^+} \text{ is a function of } y^+. \tag{16}$$

3.2. Dimensionless Stokes Equation

We normalize the Stokes Equation (8) by substituting Equation (13) for Equation (8). We then obtain

$$\frac{2}{\varepsilon^l}\frac{d^2U^{+(0)}}{d(y^+)^2} = \frac{dP^+}{dx^+} - \frac{h^2\rho g^+ g_0}{\mu U_0} \tag{17}$$

Equation (17) can be rewritten as

$$2M_1\frac{d^2U^+}{dy^{+2}} = \frac{dP^+}{dx^+} - M_3 \tag{18}$$

where M_1 and M_3 are the constants defined in Equation (16).

3.3. Dimensionless Boundary Conditions

In this section we normalize the boundary conditions at the free fluid/porous medium interface used in our domain.

Substituting Equation (13) for Equation (12) we have

$$\left.\frac{dU^{+(0)}}{dy^+}\right|_{y^+=\frac{y_{stoke}}{h}} - \frac{1}{\varphi_p}\left.\frac{dU^{+(0)}}{dy^+}\right|_{y^+=\frac{y_{stoke}}{h}} = \frac{h\beta}{\sqrt{K_p^+K_0}}U^{+(0)}\Big|_{y^+=\frac{y_{stoke}}{h}}. \tag{19}$$

Next, we normalize the bottom and top boundary conditions by substituting Equation (13) for Equation (10) and Equation (11), giving us

$$U^{+(0)} = 0 \text{ at } y^+ = 0. \tag{20}$$

$$U^{+(0)} = \frac{G}{U_0} \text{ at } y^+ = 1. \tag{21}$$

respectively.

We have now normalized the Stokes–Brinkman equations and the boundary conditions. Consequently, the system of equations used in the next sections and the boundary conditions are

$$2M_1 \frac{d^2U^{+(0)}}{dy^{+2}} - M_2 U^{+(0)} + M_3 = \frac{dP^+}{dx^+} - H\left(y^+\right) \text{ in } \Omega_2 \tag{22}$$

$$2M_1 \frac{d^2U^+}{dy^{+2}} = \frac{dP^+}{dx^+} - M_3 \text{ in } \Omega_1 \tag{23}$$

$$U^{+(0)} = 0 \text{ at } y^+ = 0. \tag{24}$$

$$U^{+(0)} = \frac{G}{U_0} \text{ at } y^+ = 1. \tag{25}$$

$$\left.\frac{dU^{+(0)}}{dy^+}\right|_{y^+ = \frac{y_{Stoke}}{h}} - \frac{1}{\varphi_p}\left.\frac{dU^{+(0)}}{dy^+}\right|_{y^+ = \frac{y_{Stoke}}{h}} = \frac{h\beta}{\sqrt{K_p^+ K_0}} U^{+(0)}\Big|_{y^+ = \frac{y_{Stoke}}{h}} \text{ at } y^+ = \frac{y_{Stoke}}{h}. \tag{26}$$

4. Asymptotic Expansion Method of the Stokes–Brinkman Equations

As mentioned in Section 2, we have two different domains where the domain Ω_1, is the region where $y > y_{Stoke}$ and the region Ω_2 is the layer where $y < y_{Stoke}$. In this section, we find the analytical solution of the governing equations with the asymptotic expansion. Section 4.1 shows the result of the Brinkman equation and Section 4.2 shows the result of the Stokes equation.

4.1. Asymptotic Expansion Method of the Brinkman Equation

Using the method of asymptotic expansion, we assume that

$$U^+ = U^{+(0)} + \varepsilon U^{+(1)} + \varepsilon^2 U^{+(2)} + \ldots \tag{27}$$

In the case $y^+ < \frac{y_{Stoke}}{h}$, we substitute Equation (27) for Equation (22), giving us

$$2M_1 \frac{d^2\left(U^{+(0)} + \varepsilon U^{+(1)} + o\left(\varepsilon^2\right)\right)}{dy^{+2}} - M_2\left(U^{+(0)} + \varepsilon U^{+(1)} + o\left(\varepsilon^2\right)\right) + M_3 = \frac{dP^+}{dx^+} - H\left(y^+\right) \tag{28}$$

Considering the zeroth-order of ε^0; we obtain

$$2M_1 \frac{d^2U^{+(0)}}{dy^{+2}} - M_2 U^{+(0)} + M_3 = \frac{dP^+}{dx^+} - H\left(y^+\right) \tag{29}$$

Since $H(y^+)$, the velocity of cilia, is a known source term in this work, we assume that it is a linear function. That is

$$H\left(y^+\right) = \frac{h^2 \varepsilon^I}{k_{11}}\left(c_1 y^+ + c_0\right)$$

where c_0 and c_1 are constants. Thus, Equation (29) becomes

$$2M_1\frac{d^2U^{+(0)}}{dy^{+2}} - M_2U^{+(0)} = -M_3 + \frac{dP^+}{dx^+} - \frac{h^2\varepsilon^l}{k_{11}}\left(c_1y^+ + c_0\right) \tag{30}$$

First, we find the general solution of the homogeneous Equation (30). Solving the homogeneous part of the ordinary differential equation

$$2M_1\frac{d^2U^{+(0)}}{dy^{+2}} - M_2U^{+(0)} = 0. \tag{31}$$

We obtain the general solution ${U_c}^{+(0)} = w_1e^{\sqrt{\frac{h^2\varepsilon^l}{2K_0K^+}}y^+} + w_2e^{-\sqrt{\frac{h^2\varepsilon^l}{2K_0K^+}}y^+}$. To find the particular solution of Equation (30), we use the method of undetermined coefficients. Therefore, the solution of the differential equation is

$$U^{+(0)} = w_1e^{\sqrt{\frac{M_2}{2M_1}}y^+} + w_2e^{-\sqrt{\frac{M_2}{2M_1}}y^+} + \frac{h^2\varepsilon^l}{M_2k_{11}}c_1y^+ + \frac{M_3}{M_2} - \frac{dP^+}{M_2dx^+} + \frac{h^2\varepsilon^l}{M_2k_{11}}c_0. \tag{32}$$

Let

$$J_1 = \sqrt{\frac{M_2}{2M_1}}, J_2 = \frac{dP^+}{M_2dx^+}, J_3 = \frac{h^2\varepsilon^l}{M_2k_{11}}, J_4 = \frac{M_3}{M_2}, J_5 = \frac{dP^+}{M_1dx^+}, \text{ and } J_6 = \frac{M_3}{M_1} \tag{33}$$

all of which are constants. Therefore Equation (32) can be rewritten as

$$U^{+(0)} = w_1e^{J_1y^+} + w_2e^{-J_1y^+} + J_3c_1y^+ + J_4 - J_2 + J_3c_0. \tag{34}$$

Applying Equation (24) to Equation (34), we have

$$w_2 = J_2 - J_4 - J_3c_0 - w_1 \tag{35}$$

which yields

$$U^{+(0)} = w_1e^{J_1y^+} - w_1e^{-J_1y^+} + (J_2 - J_4 - J_5c_0)e^{-J_1y^+} + J_3c_1y^+ + J_4 - J_2 + J_3c_0. \tag{37}$$

We now have the solution of the Brinkman equation.

4.2. Asymptotic Expansion Method of Stokes Equation

Similar to the previous section, we calculate the velocity of the PCL fluid in domain Ω_1 using the asymptotic expansion method with the Stokes Equation (23). We assume that

$$U^+ = U^{+(0)} + \varepsilon U^{+(1)} + \varepsilon^2U^{+(2)} + \ldots \tag{37}$$

In the case $y^+ > \frac{y_{Stoke}}{h}$, we substitute Equation (37) for Equation (23). Therefore

$$2M_1\frac{d^2(U^{+(0)} + \varepsilon U^{+(1)} + o\left(\varepsilon^2\right)}{dy^{+2}} = \frac{dP^+}{dx^+} - M_3. \tag{38}$$

Considering the zeroth-order term of ε, ε^0, we obtain

$$\begin{array}{c} \frac{d^2U^{+(0)}}{dy^{+2}} = \frac{1}{2M_1}\frac{dP^+}{dx^+} - \frac{M_3}{2M_1} \\ \text{or } \frac{d^2U^{+(0)}}{dy^{+2}} = \frac{1}{2}J_5 - \frac{1}{2}J_6. \end{array} \tag{39}$$

As we assume that $\frac{dP^+}{dx^+}$ is a constant, by integrating Equation (39) twice, we have

$$U^{+(0)} = \frac{\left(\frac{1}{2}J_5 - \frac{1}{2}J_6\right)y^{+2}}{2} + w_3 y^+ + w_4 \tag{40}$$

Applying the boundary condition (25) to Equation (40), we obtain

$$\begin{gathered}\frac{G}{U_0} = \frac{\left(\frac{1}{2}J_5 - \frac{1}{2}J_6\right)}{2} + w_3 + w_4. \text{ Hence } w_4 = \frac{G}{U_0} - \frac{\left(\frac{1}{2}J_5 - \frac{1}{2}J_6\right)}{2} - w_3. \\ \text{Then } U^{+(0)} = \frac{\left(\frac{1}{2}J_5 - \frac{1}{2}J_6\right)y^{+2}}{2} + w_3 y^+ + \frac{G}{U_0} - \frac{\left(\frac{1}{2}J_5 - \frac{1}{2}J_6\right)}{2} - w_3.\end{gathered} \tag{41}$$

We can find the solutions at and Ω_2, yet the constants w_1 and w_3 of the Stokes–Brinkman equation are unknown.

5. The Relation between the Constants

In this section, we determine the relation of the constants w_1 and w_3 with Beavers–Joseph boundary condition. Substituting Equation (36) and Equation (41) for Equation (26), we obtain

$$\left(\frac{1}{2}J_5 - \frac{1}{2}J_6\right)\frac{y_{Stoke}}{h} + w_3 - \frac{1}{\varphi_p}w_1 J_1 e^{J_1}\frac{y_{Stoke}}{h} - \frac{1}{\varphi_p}w_1 J_1 e^{-J_1}\frac{y_{Stoke}}{h} + \frac{1}{\varphi_p}J_1(J_2 - J_4 - J_3 c_0)e^{-J_1}\frac{y_{Stoke}}{h} - \frac{1}{\varphi_p}J_3 c_1 = \frac{h\beta}{\sqrt{K_p^+ K_0}}U^+\Big|_{y^+ = \frac{y_{stoke}}{h}}, \tag{42}$$

where $U^+\Big|_{y^+ = \frac{y_{stoke}}{h}}$ (on the right-hand side of Equation (42)) can be obtained from the PCL velocity in $\Omega_1\Omega_2$, or both. However, the velocity $\frac{h\beta}{\sqrt{K_p^+ K_0}}U^+\Big|_{y^+ = \frac{y_{stoke}}{h}}$ is a slip velocity [13,14]. Therefore, in this work, we consider the case that $U^+\Big|_{y^+ = \frac{y_{Stoke}}{h}} = U^+\Big|_{y^+ = \frac{y_{stoke}}{h}^+}$.

Substituting Equation (41) for the right-hand side of Equation (42) and simplifying, we have

$$w_3 = \frac{1}{\left(1 - \frac{h\beta}{\sqrt{K_p^+ K_0}}\frac{y_{Stoke}}{h} + \frac{h\beta}{\sqrt{K_p^+ K_0}}\right)}\left[\begin{array}{l} w_1\left(\frac{1}{\varphi_p}J_1 e^{J_1}\frac{y_{Stoke}}{h} + \frac{1}{\varphi_p}J_1 e^{-J_1}\frac{y_{Stoke}}{h}\right) + \frac{h\beta}{\sqrt{K_p^+ K_0}}\frac{\left(\frac{1}{2}J_5 - \frac{1}{2}J_6\right)\left(\frac{y_{Stoke}}{h}\right)^2}{2} + \frac{h\beta}{\sqrt{K_p^+ K_0}}\frac{G}{U_0} \\ - \frac{h\beta}{\sqrt{K_p^+ K_0}}\frac{\left(\frac{1}{2}J_5 - \frac{1}{2}J_6\right)}{2} - \left(\frac{1}{2}J_5 - \frac{1}{2}J_6\right)\frac{y_{Stoke}}{h} - \frac{1}{\varphi_p}J_1(J_2 - J_4 - J_3 c_0)e^{-J_1}\frac{y_{Stoke}}{h} + \frac{1}{\varphi_p}J_3 c_1 \end{array}\right]. \tag{43}$$

We now have the relation between the constants w_1 and w_3. Inserting Equation (42) into Equation (41), we have the solution of the Stokes equation depending on w_1. That is

$$\begin{aligned} U^{+(0)} = {} & \frac{\left(\frac{1}{2}J_5 - \frac{1}{2}J_6\right)y^{+2}}{2} + \left\{\frac{1}{\left(1 - \frac{h\beta}{\sqrt{K_p^+ K_0}}\frac{y_{Stoke}}{h} + \frac{h\beta}{\sqrt{K_p^+ K_0}}\right)}\left[\begin{array}{l} w_1\left(\frac{1}{\varphi_p}J_1 e^{J_1}\frac{y_{Stoke}}{h} + \frac{1}{\varphi_p}J_1 e^{-J_1}\frac{y_{Stoke}}{h}\right) + \frac{h\beta}{\sqrt{K_p^+ K_0}}\frac{\left(\frac{1}{2}J_5 - \frac{1}{2}J_6\right)\left(\frac{y_{Stoke}}{h}\right)^2}{2} + \frac{h\beta}{\sqrt{K_p^+ K_0}}\frac{G}{U_0} \\ - \frac{h\beta}{\sqrt{K_p^+ K_0}}\frac{\left(\frac{1}{2}J_5 - \frac{1}{2}J_6\right)}{2} - \left(\frac{1}{2}J_5 - \frac{1}{2}J_6\right)\frac{y_{Stoke}}{h} - \frac{1}{\varphi_p}J_1(J_2 - J_4 - J_3 c_0)e^{-J_1}\frac{y_{Stoke}}{h} + \frac{1}{\varphi_p}J_3 c_1 \end{array}\right]\right\}y^+ \\ & + \frac{G}{U_0} - \frac{\left(\frac{1}{2}J_5 - \frac{1}{2}J_6\right)}{2} - \left\{\frac{1}{\left(1 - \frac{h\beta}{\sqrt{K_p^+ K_0}}\frac{y_{Stoke}}{h} + \frac{h\beta}{\sqrt{K_p^+ K_0}}\right)}\left[\begin{array}{l} w_1\left(\frac{1}{\varphi_p}J_1 e^{J_1}\frac{y_{Stoke}}{h} + \frac{1}{\varphi_p}J_1 e^{-J_1}\frac{y_{Stoke}}{h}\right) + \frac{h\beta}{\sqrt{K_p^+ K_0}}\frac{\left(\frac{1}{2}J_5 - \frac{1}{2}J_6\right)\left(\frac{y_{Stoke}}{h}\right)^2}{2} + \frac{h\beta}{\sqrt{K_p^+ K_0}}\frac{G}{U_0} \\ - \frac{h\beta}{\sqrt{K_p^+ K_0}}\frac{\left(\frac{1}{2}J_5 - \frac{1}{2}J_6\right)}{2} - \left(\frac{1}{2}J_5 - \frac{1}{2}J_6\right)\frac{y_{Stoke}}{h} - \frac{1}{\varphi_p}J_1(J_2 - J_4 - J_3 c_0)e^{-J_1}\frac{y_{Stoke}}{h} + \frac{1}{\varphi_p}J_3 c_1 \end{array}\right]\right\}. \end{aligned} \tag{44}$$

We now obtain the general solution of the Stokes–Brinkman equations, depending only the constant w_1 with the asymptotic expansion method, in which the Beavers–Joseph condition is employed at the free fluid/ porous medium interface.

6. Results and Discussion

The solutions of Stokes–Brinkman equations, Equation (36) and Equation (44), calculated in Sections 4 and 5 are plotted on a graph and discussed in this section. To plot the graph, we assume that the graphs θ between the cilia and the horizontal plane are $40°, 50°, 60°, 70°, 80°, 90°$ where the cilia have the highest velocity at $\theta = 90°$ during the forward stroke and stop beating at $\theta = 40°$. So, at $\theta = 40°$ we do not need to calculate the velocity of the PCL. The variables used in Equation (44) are given in Tables 1 and 2. The values of y_{Stoke} and $K_p{}^+$ are obtained from [4], and v^s is the velocities of

the solid, cilia, where the maximum velocity of motile cilia value is assumed at $\theta = 90°$ in descending order of degree, terminating at $\theta = 40°$, h is the cilium height, U_0 is one cycle of ciliary beat, and φ_p and β were obtained from [2]. We assume that the rate of pressure changes $\frac{dP^+}{dx^+}$ equals 1. The boundary condition at the top of the free fluid domain equals 1. The variable w_1 in Equation (44) equals 0 because in this study we aim to verify if the solid velocities applied to the equation are valid, the solutions correlate with the variable velocity employed, where the maximum velocity is assumed at $\theta = 90°$ and decreases with decreasing angles.

Table 1. Variable of the experimental data in the solution of the Stoke–Brinkman equations.

Variable	Value	Unit
h	7.5	$[\mu m]$
ρ	992.2×10^{-15}	$\left[N/m^2\right]$
μ	3×10^{-6}	$\left[ML^{-1}T^{-2}\right]$
g	9.81×10^{6}	$[\mu m]$
U_0	1.00	$[\mu m]$
β	1	[1]
v^+	1	[1]
$\frac{dP^+}{dx^+}$	1	[1]
w_1	0	[1]
G	1	[1]

Table 2. Values of variables used in Equation (44) used to plot Figure for each angle θ.

Variable	50°	60°	70°	80°	90°
y_{Stoke}	0.7672	0.8638	0.9353	0.9818	1.0000
K_{P^+}	0.0012	0.0015	0.0016	0.0017	0.0018
ε^1	0.6717	0.7099	0.7331	0.7439	0.7487
v^s	0.0023	0.0024	0.0044	0.0049	0.0050

These solutions are the velocity of PCL fluid in the layer containing cilia with different angle θ ($50°, 60°, 70°, 80°, 90°$), respectively. It can be noted that the velocity decrease with decreasing angles and bends sharply at the seam of the porous medium and the free fluid region. The asymptotic solution $U^{+(0)}$ of the Stoke–Brinkman Equation (44) is shown in Figure 6 (the code is given in Appendix A here).

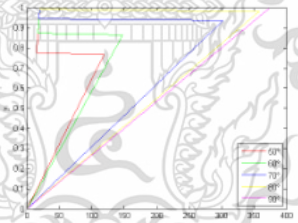

Figure 6. The asymptotic solution $U^{+(0)}$ of the Stoke–Brinkman equations.

The asymptotic expansion method is the tool for finding analytical approximate solutions to complicated practical problems, for example, the problem in ordinary differential equations in terms of regular perturbation and singular perturbation. We construct different asymptotic solutions inside and outside the region of rapid change and match them together to determine a global solution. Other methods used for finding exact and approximate solutions for linear and nonlinear partial differential equations is the homotopy perturbation method which is only a special case of the homotopy analysis

method. The basic ideas of the homotopy perturbation method is a coupling of the traditional perturbation method and homotopy in topology deforms continuously the problem in hand to a simple one which can be easily solved. The advantage of this method is that it can be applied to various nonlinear problems, and the disadvantage is that we should suitably choose an initial guess, or infinite iterations are required [15]. The asymptotic expansion method and the homotopy perturbation method are principally based on a Taylor series with respect to an embedding parameter.

Another method used to describe the samples with porous media, is the fractal derivative model. This method is developed from fractal calculus for calculating the solution of problem phenomena in porous media or hierarchical structures [16]. For instance, in a study by Wang, Shi, He, and Li [17], to find an optimal hair length of a polar bear for thermal protection, which helps maintain a normal body temperature, by using a fractal derivative model of one-dimensional heat conduction along the hair. The basic ideas of the fractal calculus begin from Fourier's law of thermal conduction, which can be expressed as $q = k\frac{\Delta T}{\Delta x}$, where q is the heat flux, k is the material's conductivity, and $\frac{\Delta T}{\Delta x}$ is the temperature gradient, but the asymptotic expansion method is adopted to determine the velocity of ciliary motion that moves foreign particles out of the body.

While the asymptotic expansion method can be used to study the interface between the porous media region and the free fluid region, the homotopy perturbation method and the fractal derivative model are only adopted for the porous media domain. These three approaches are the tools for finding analytical approximate solutions to the problem in ordinary differential equations or partial differential equations. Another difference is that the asymptotic expansion method can be applied to solve linear ordinary differential equations and perturbation equations. On the other hand, the homotopy perturbation method and the fractal derivative model are used to derive the solutions to nonlinear ordinary differential equations or partial differential equations.

7. Conclusions

In this article, we studied the fluid flow in the periciliary layer (PCL) of the respiratory tract using the of asymptotic expansion method to determine the velocity of PCL fluid. The PCL is divided into two domains: the free fluid and the porous medium domains. The free fluid domain is the upper layer of the PCL from cilia are absent. The porous medium domain is the lower layer of PCL and contains cilia. The Stokes equation is employed in the free fluid domain and the Brinkman equation is applied in the porous medium. The Beavers–Joseph boundary condition is employed at the interface between the porous medium and the free fluid region. We assume that the velocity of the PCL fluid at the bottom of the porous medium domain (at $y = 0$) is zero and the velocity of the PCL fluid in the porous medium depends on angle θ. The boundary condition at the top of the free fluid domain is assumed to be a function of G, where G depends on X and the angle θ. The explicit formula of velocity of PCL fluid $U^{+(0)}$ is obtained by applying asymptotic expansion to the Stokes–Brinkman equations.

Author Contributions: Conceptualization, S.P. and K.W.; methodology, S.P.; software, S.P.; validation, K.W. and S.P.; formal analysis, S.P.; investigation, S.P.; resources, S.P.; data curation, K.W.; writing—original draft preparation, S.P.; writing—review and editing, K.W.; visualization, S.P.; supervision, K.W.; project administration, K.W.; funding acquisition, S.P.

Funding: This research received no external funding.

Acknowledgments: The authors would to thank Rachada Pongprairat and Krongkaew Mighanetara for advice and support.

Conflicts of Interest: The authors declare no conflict of interest.

Nomenclature

Variable	Meaning	Unit
μ	a dynamic viscosity	$\left[\frac{L^2}{T}\right]$
	the inverse of the permeability tensor	$\left[\frac{1}{L^2}\right]$
ε^l	a porosity	$[1]$
v^l	the velocities of the liquid	$\left[\frac{L}{T}\right]$
v^S	the velocities of the solid	$\left[\frac{L}{T}\right]$
p	pressure	$\left[\frac{M}{LT^2}\right]$
$\varepsilon^{\cdot l}$	the material time derivative of the porosity with respect to the solid phase	$\left[\frac{L}{T}\right]$
h	the characteristic length	$\left[\frac{L}{T}\right]$
U_0	a volumetric average velocity in a porous medium	$\left[\frac{L}{T}\right]$
K_0	characteristic permeability	$\left[L^2\right]$
g_0	characteristic gravity	$\left[\frac{L}{T^2}\right]$
g	gravity	$\left[\frac{L}{T^2}\right]$

where L = length, T = time and M = mass.

Appendix A

```
%=========================================================================
   %================= This Program for Compute the Solutions ================
   %=========================================================================
   clear all;
clc;
format long;
%% Set Value
yStoke = [0.7672 0.8638 0.9353 0.9818 1.0];
K11 = [0.0012 0.0015 0.0016 0.0017 0.0018];
Eps = [0.6716 0.7099 0.7331 0.7439 0.7487];
c = [0 0.0023; 0 0.0024;0 0.0044; 0 0.0049; 0 0.0050];
c = c*10^(5);
h = 7.5;
Rho = 992.2*10^(-15);
Mu = 3*power(10,-6);
g = 9.81*10^(6);
u0 = 0.05;
Beta = 1;
h = 7.5;
Kp = K11;
vPlus = 100;
dPplus = 10;
w1 = 0;
G = 1;
gram = [0 -0.05 0.06 0.16 -0.3];
% phiP = 1-6.*gram;
phiP = Eps;
angle = 50:10:90;
% Left and Right Boundary of Part 1 and 2
% Step Size of Y
noY = 50;
yy1 = [linspace(0,yStoke(1),noY); linspace(0,yStoke(2),noY);...
          linspace(0,yStoke(3),noY); linspace(0,yStoke(4),noY);...
        linspace(0,yStoke(5),noY)];
y1 = linspace(0,yStoke(5),noY+noY);
yy2 = [linspace(yStoke(1)+0.01,1,noY); linspace(yStoke(2)+0.01,1,noY);...
        linspace(yStoke(3)+0.01,1,noY); linspace(yStoke(4)+0.01,1,noY)];
```

```
y = [yy1(1:4,:) yy2; y1];
nData = length(yStoke);
% Color and Style Orders of line in each figure
Col = {'r'; 'g'; 'b'; 'y'; 'm'};
Style = {'-'; '-'; '-'; '-'; '-'};
% Parameter of part 1
M1 = 1./Eps;
M2 = (h^(2))./(K11);
M3 = ((h^(2))*Rho*g)/(Mu*u0);
J1 = sqrt(M2./(2*M1));
J2 = dPplus./M2;
J3 = (h^(2).*Eps)./(M2.*K11);
J4 = M3./M2;
%% Define and Compute the solutions
for i = 1 : nData
    % Part 1
    t1 = J2(i)-J4(i)-(J3(i)*c(i,1));
    t2 = J3(i)*c(i,2);
    % Computation of part 1
    j = 1;
    if i ~= nData
for y1p = 1 : noY
            uu1(i,j) = w1*exp(J1(i)*yy1(i,y1p))-w1*exp(-J1(i)*yy1(i,y1p))...
                  +t1*exp(-J1(i)*yy1(i,y1p))+t2*yy1(i,y1p)-t1;
            j = j+1;
        end
    else
        for y1p = 1 : noY
            uu1(i,j) = w1*exp(J1(i)*yy1(i,y1p))-w1*exp(-J1(i)*yy1(i,y1p))...
                  +t1*exp(-J1(i)*yy1(i,y1p))+t2*yy1(i,y1p)-t1;
            j = j+1;
        end
        j = 1;
        for y1p = 1 : 2*noY
            u1(1,j) = w1*exp(J1(i)*y1(1,y1p))-w1*exp(-J1(i)*y1(1,y1p))...
                  +t1*exp(-J1(i)*y1(1,y1p))+t2*y1(1,y1p)-t1;
            j = j+1;
        end
    end
    % Part 2
    f1 = exp(J1(i)*(yStoke (i)/h));
    f2 = exp(-J1(i)*(yStoke (i)/h));
    f3 = yStoke (i)/h;
    f4 = G/u0;
    f5 = ((1/2)*J2(i)-(1/2)*J4(i));
    f6 = 1/phiP(i);
    f7 = (h*Beta)/sqrt(Kp(i));
    if i ~= nData
        j = 1;
        % Computation of part 2 : Case 3 eq 4.23
        for y2p = 1 : noY
            s4(i,j) = (1/(1-f7*f3+f7))*((w1*(f6*J1(i)*f1+f6*J1(i)*f2))...
                      +((f7*f5*f3^2)/2)+f7*f4-((f7*f5)/2)...
                     -f5*f3-(f6*J1(i)*t1*f2)+(f6*J3(i)*c(i,2)));
            uu4(i,j) = ((f5/2)*(yy2(i,y2p))^2)+(s4(i,j)*yy2(i,y2p))...
                    +f4-(f5/2)-s4(i,j);
            j = j+1;
        end
        nPlot2{i,1} = [num2str((10*i)+40),'\circ'];
    end
    nPlot1{i,1} = [num2str((10*i)+40),'\circ'];
end
UU2 = cat(2,uu1(1:4,:),uu2(1:4,:));
UU3 = cat(2,uu1(1:4,:),uu3(1:4,:));
UU4 = cat(2,uu1(1:4,:),uu4(1:4,:));
U2 = cat(1,UU2,u1);
U3 = cat(1,UU3,u1);
```

```
U4 = cat(1,UU4,u1);
%% Plot Graph
% Plot Graph of each part
% part 1
figure();
plot(uu1(1,:),yy1(1,:),'r',uu1(2,:),yy1(2,:),'g',uu1(3,:),yy1(3,:),'b'...
      ,uu1(4,:),yy1(4,:),'y',uu1(5,:),yy1(5,:),'m');
  % case 3
   figure();
  plot(uu4(1,:),yy2(1,:),'r',uu4(2,:),yy2(2,:),'g',uu4(3,:),yy2(3,:),'b'...
        ,uu4(4,:),yy2(4,:),'y');
  xlabel('u')
   ylabel('y')
   title('The solution of u and y when y^{+} > y_{stoke} : case 3')
   legend(nPlot2,-1);
  % Plot Graph of all degree
   l = length(y);
   % case 3
   figure();
  plot(U4(1,:),y(1,:),'r',U4(2,:),y(2,:),'g',U4(3,:),y(3,:),'b'...
        ,U4(4,:),y(4,:),'y',U4(5,:),y(5,:),'m')
   xlabel('u')
   ylabel('y')
   % title(['The relation between u and y when y^{+} < y_ {stoke} '...
        %      'and y^{+} > y_{stoke} : case 3'])
   legend(nPlot1,4);
  saveas(gcf,'CompareSolStokeCase3.fig')
```

References

1. Machemer, H. Ciliary activity and the origin of metachrony in paramecium: Effects of increasd viscocity. *J. Exp. Biol.* **1972**, *57*, 239–259. [PubMed]
2. Smith, D.J.; Smith, A.A.; Blake, J.R. Mathematical embryology: The fluid mechanics of nodal cilia. *J. Eng. Math.* **2011**, *70*, 255–279. [CrossRef]
3. Fulford, G.R.; Blake, J.R. Muco–ciliary transport in the lung. *J. Thero. Biol.* **1986**, *121*, 381–402. [CrossRef]
4. Jayathilake, P.G.; Tan, Z.; Le, D.V.; Lee, H.P.; Khoo, B.C. Three-dimensional numerical simulations of human pulmonary cilia in the periciliary liquid layer by the immersed boundary method. *Comput. Fluids Sciencedirect.* **2012**, *67*, 130–137. [CrossRef]
5. Serafini, S.M.; Michaelson, E.D. Length and distribution of cilia in human and canine airways. *Bull. Eur. Pysiopathol. Respir.* **1977**, *13*, 551–559.
6. Matsui, H.; Randell, S.H.; Peretti, S.W.; Davis, C.W.; Boucher, R.C. Coordinated clearance of periciliary liquid and mucus from airway surfaces. *J. Clin. Investig.* **1998**, *102*, 1125–1131. [CrossRef] [PubMed]
7. Neale, G.; Nader, W. Practical significance of Brinkman's extension of Darcy slaw: Coupled parallel flows within a channel and a bounding porous medium. *Can. J. Chem. Eng.* **1974**, *52*, 475–478. [CrossRef]
8. Ochoa, J.A.; Whitaker, S. Momentum transfer at the boundary between a porous medium and a homogeneous fluid—I. Theoretical development. *Int. J. Heat Mass Transf.* **1995**, *38*, 2635–2646. [CrossRef]
9. Ochoa, J.A.; Whitaker, S. Momentum transfer at the boundary between a porous medium and a homogeneous fluid—II. Comparison with experiment. *Int. J. Heat Mass Transfer* **1995**, *38*, 2647–2655. [CrossRef]
10. Valdes-Parada, F.J.; Aguilar-Madera, C.G.; Ochoa-Tapia, J.A.; Goyeau, B. Velocity and stress jump conditions between a porous medium and a fluid. *Adv. Water Resour.* **2013**, *62*, 327–339. [CrossRef]
11. Chamsri, K. Formulation of a well-posed Stoke-Brinkman Problem with a Permeability Tensor. *J. Math.* **2015**, *1*, 1–7.
12. Wuttanachamsri, K.; Schreyer, L. Effects of the Cilia movement on fluid Velocity for fixed Domain. submitted.
13. Sears, P.R.; Thomson, K.; Knowles, M.R.; Davis, C.W. Human Airway Ciliary Dynamics. *Am. J. Physiol. Lung Cell. Mol. Physiol.* **2012**, *704*, L170–L183. [CrossRef] [PubMed]
14. Chandesris, M.; Jamet, D. Boundary conditions at a planar fluid-porous interface for a Poiseuille flow. *Int. J. Heat Mass Transf.* **2006**, *49*, 2137–2150. [CrossRef]

15. Homotopy Perturbation Method. Available online: www.shodhganga.inflibnet.ac.in/bitstream/10603/37622/9/09_chapter%202.pdf (accessed on 15 May 2019).
16. He, J.-H. Fractal calculus and its geometrical explanation. *Results Phys.* **2018**, *10*, 272–276. [CrossRef]
17. Fractal Calculus and Its Application to Explanation of Biomechanism of Polar Bear Hairs. Available online: www.Worldsciencetific (accessed on 3 May 2019).

Hindawi
Mathematical Problems in Engineering
Volume 2022, Article ID 1390486, 12 pages
https://doi.org/10.1155/2022/1390486

Research Article

On the Asymptotic Boundary Condition at the Free-Fluid/Porous-Medium Interface in Periciliary Layer due to the Ciliary Movement

Sudaporn Poopra and Kanognudge Wuttanachamsri

Department of Mathematics, School of Science, King Mongkut's Institute of Technology Ladkrabang, Bangkok 10520, Thailand

Correspondence should be addressed to Sudaporn Poopra; ordinary_555@hotmail.com

Received 17 November 2021; Revised 24 January 2022; Accepted 12 February 2022; Published 8 March 2022

Academic Editor: Rafał Stanisławski

The purpose of this study is to study the movement of the periciliary (PCL) fluid due to the ciliary locomotion. In this research, because the bundle of cilia is considered instead of a single cilium, Stokes–Brinkman equations in a macroscopic scale are employed to find the velocity of the PCL fluid. When the cilia are perpendicular to the horizontal plane, the PCL consists of only the cilia. The inclination of cilia (cilia make an angle $\theta(\theta < 90^\circ)$ to the horizontal plane) results in two different domains in the PCL, the regions comprising and not comprising cilia. The main objective of this study is to determine the appropriate boundary conditions of the velocity between these two regions where the PCL fluid is moved by self-propelled cilia rather than the pressure gradient. A matched asymptotic expansion method is applied to the Stokes–Brinkman equations to determine the constraints. Two boundary conditions at the interface are obtained and the velocity of the PCL fluid at the top of PCL can be used to be the boundary conditions at the bottom of the mucus layer to determine the velocity of mucus. This model can help engineers to build devices to treat patients who have problem with the respiratory system. Applications include modeling fluid flow through filters such as engine filter and rice fields.

1. Introduction

Breathing is one of the most important bodily functions that keep us alive. When we breathe air in through the nose it is not just oxygen but also small substances containing particles and pathogens that pass through lungs. However, the respiratory system has filters to trap and remove the strange pathogens, thus allowing us to breathe without irritation. The filters lining the bronchus within the respiratory system are called cilia, hair-like structure, scattered throughout the ciliated cells, which are vital components of the immune system. Beside cilia, there are goblet cells scattering among the ciliated cells in the respiratory system. One of the primary functions of the goblet cells is to secrete mucus to trap the particles or microorganisms that pass through our respiratory system. Then mucus forms a layer at the tips of cilia. The cilia aid in transporting these foreign particles out of the body by sweeping the mucus upwards towards the throat. The tips of the cilia make contact with the mucus layer on the forward stroke and bend sideways and backwards on the reverse stroke. Essentially, this causes the mucus to be propelled only in the forward direction on the forward stroke [1]. The excreted mucus is ejected through the vocal cords and into the pharynx. The primary innate defense mechanism is called mucociliary clearance [2]. Under optimal lung conditions, cilia beat at 12 to 15 Hz in coordinated waves propelling mucus at 4 to 20 mm/min [1].

Figure 1 shows a small portion of the trachea cross section. Inside the segment there exist three main layers, air, mucus, and the periciliary layers (PCL). The PCL is a moist layer composed of cilia covering the ciliated cells. The fluid in this layer is called PCL fluid. Below the PCL is epithelial cells. Goblet cells secret mucus to trap the strange particles entering the body to protect the lungs from contaminants

found in the epithelium. Among the goblet cells, there exist ciliated cells, where cilia are found on the top and wave in a rhythmic or pulsating motion and use that motion to keep passage ways free of mucus or foreign particles.

In this work, we determine the velocity of the PCL fluid due to the movement of cilia. We consider that the movement of cilia results in two different patterns in the PCL as shown in Figure 2. The left of Figure 2 shows the cilia perpendicular to the horizontal plane. The PCL has only one domain, which contains only cilia. When the cilia move forward and form an angle $\theta, \theta < 90^\circ$ with the horizontal plane, the PCL can be divided into two domains, the layer containing cilia and the layer above the cilia as shown on the right of Figure 2. Since the PCL layer consists of the PCL fluid, assisting to treat the cilia to operate normally, and the solid phases, cilia, this part in PCL is considered as a porous medium. The layer above the cilia in the PCL is called free-fluid domain, as shown on the right of Figure 2. The PCL domain is denoted by $\omega = \omega_1 \cup \omega_2$ where ω_1 is the free-fluid region above the porous layer ω_2 when the cilia form an angle $\theta, \theta < 90^\circ$ with the horizontal plane. With the perpendicular case, we have only ω_2. The variable y_{Stoke} is the height of the domain ω_2. Notice that y_{Stoke} changes according to the angle θ. In this study, the first aim is to figure out the velocity of the PCL fluid in both domains to determine the boundary conditions between the domains ω_1 and ω_2.

Mathematical models used to calculate the velocity in the free-fluid region and the porous medium are numerous [3–8]. The equation applied in the free-fluid region was described by the Stokes equation or Navier–Stokes equations, while flow in the porous-medium region was usually modeled by using Darcy's Law or Brinkman equations [6, 8–13]. In general, the Brinkman model is used for the porous media with high porosity [14]. Examples of flow in free-fluid region are diverse. For instance, Abbas et al. [15] studied the effect of the flow for an incompressible liquid with nonlinear differential equations. For flow in a porous medium, Ado-Elkhair et al. [16] presented the influence of the magnetic field and Darcy medium on oscillatory wavy walled (Peristalsis) flow due to the cilia motion by using a Adomian decomposition method (ADM) with a system of nonlinear partial differential equations. Zaher et al. [17] studied the effect of the ciliated walls in the uterine tube to strengthen the sperm to reach the egg. They used Darcy model with an oscillating wall and non-Newtonian magnetized fluid. An Adomian analysis method was employed to solve the equation. The illustrations of simultaneous flow in both free-fluid and porous regions are various; for example, Valdes-Parada and Lasseux [10] provided a new approach for modeling flow in porous and free-fluid domains based on Beaver and Joseph (BJ) configuration by using Darcy's Law and Navier–Stokes equation. Carraro et al. [12] figured out a high-precision simulation of the slow viscous flow over a porous bed by applying a finite element method to Stokes equation in free-fluid domain and Darcy's Law in porous bed. Naqvi and Bottaro [13] studied boundary conditions between an isotropic porous-medium and a free-fluid region by using the Stokes-like equation and homogenization theory. Du and Zu [18] proposed a local and parallel finite element method to the mixed Navier-Stokes/Darcy model with the Beaver–Joseph interface condition for an incompressible fluid flow. Wuttanachamsri [6] used one-dimensional Stokes–Brinkman equations to find the shape of free interface between a porous-medium and a free-fluid region.

The two-layer configuration that uses different equations in different domains requires proper boundary conditions at the interface between the free-fluid and porous-medium regions. The difficulty in determining boundary conditions results from the fact that the orders of the corresponding differential operators are often different [14]. The boundary conditions at the interface between the porous-medium and the free-fluid regions had been studied by several authors [10, 19–23]. For example, Beavers and Joseph [22] proposed a slip boundary condition based on repeated experiments with a Poiseuille flow over a permeable porous block. Sahraoui and Kaviany [23] determined an appropriate hydrodynamic boundary condition at the interface between a porous-medium and a plain domain using the pressure correction method. Valdes-Parada and Lasseux [10] studied three different boundary conditions: creeping flow under no-slip conditions, inertial flow no-slip conditions, and creeping flow with slip conditions with Navier-Stokes–Darcy equations. The solutions were calculated by using Direct Numerical Simulation (DNS).

Although the boundary conditions had been investigated extensively by many researchers, the studies of boundary conditions at the interface between the free-fluid region and the porous medium in the human lungs are limited. This study aims to determine the boundary conditions at the interface between the free-fluid region and the porous medium in PCL by using the method of matched asymptotic expansion, which has been used widely by considerable researchers. For example, Chandesris and Jamet [9] studied the Poiseuille flow over a permeable block by using the method of matched asymptotic expansion and determined the boundary conditions at the top of the permeable block. Poopra and Wuttanachamsri [11] calculated the velocity of the PCL fluid with the BJ boundary condition when cilia formed angles with the horizontal plane by using the asymptotic expansion method.

The results in the reviewed literature, however, are not appropriated for our research problem. In most of the studies, solid phases in the porous domain are stationary. In our study, on the contrary, cilia in the porous domain are mobile. Although Poopra and Wuttanachamsri [11] studied the PCL with self-propelled solid phases, they did not seek for matching conditions to match the solutions at the transition zone at the free-fluid/porous-medium interface and they did not provide a proper boundary condition at the interface, which was practical to the problem. Thus, this research has been conducted to figure out the boundary conditions suiting for the problem.

We first provide our mathematical model and boundary conditions at the top and bottom of our domain in dimensionless forms in Section 2. Second, the velocity of the PCL fluid is calculated by using the asymptotic expansion method in Sections 3.1 and 3.2. Third, because unknown

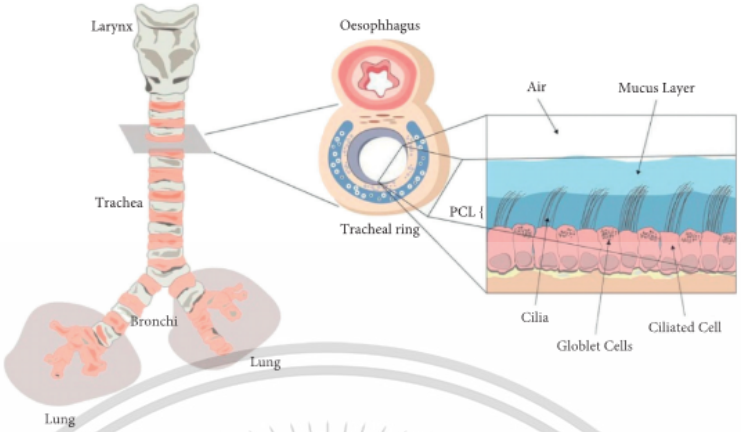

Figure 1: PCL, mucus, and air layers in the respiratory tracts.

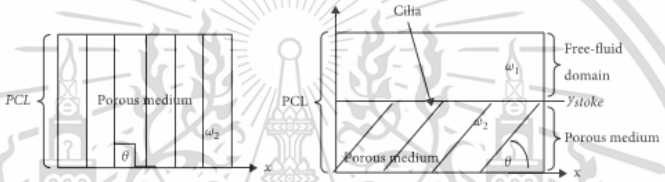

Figure 2: From left to right, the cilia are perpendicular and form an angle θ, $\theta < 90^{\circ}$ with the horizontal plane, respectively.

constants occurred during finding the asymptotic solutions, matching conditions presented in Section 3.3 are needed to match the outer and inner results presented in Sections 3.1 and 3.2. Fourth, the zeroth-order solution after applying the matching conditions to the inner and outer results is shown in Section 3.4. Next, to verify our solutions, comparisons of our results with experimental data are described in Section 4. Then, the boundary conditions at the free-fluid/porous-medium interface for this problem are illustrated in Section 5. Finally, the conclusion is drawn in the last section.

2. Mathematical Model and Boundary Conditions

We provide the governing equations, the Stokes–Brinkman equations, and their normalized models, in a one-dimensional domain and boundary conditions in this section. Because we consider the movement of the carpet of cilia (not just the movement of a single cilium), the equations used are in a macroscopic scale obtained from the Hybrid Mixture Theory (HMT), which is an upscaling method of changing a microscale equation to be a macroscale equation [24].

2.1. Stokes–Brinkman Equations. In this section, we provide the Stokes–Brinkman equations derived in [7] in a macroscopic scale in the one-dimensional domain ω. That is,

$$\frac{2\mu}{\varepsilon^l}\frac{d^2\left(\varepsilon^l v^l\right)}{dy^2} - \mu k_{11}^{-1}\left(\varepsilon^l v^l\right) + \rho g = \frac{dP}{dx} - \mu k_{11}^{-1}\left(\varepsilon^l v^s\right), \tag{1}$$

where μ is the dynamic viscosity, k_{11}^{-1} is the inverse of the permeability tensor, ε^l is the porosity, v^l and v^s are the velocities of the liquid and solid phases, respectively, p is pressure, g is gravity, and ρ is the fluid density. We assume that the fluid flows along the x-axis. With the macroscopic scale, we project the average variables on the y-axis. That is, other variables depend on only the y-direction and in the y-direction the pressure gradient is zero and dP/dx is a constant. The Stokes equation is equation (1) without the terms consisting of the permeability k_{11} and $\varepsilon^l = 1$. That is,

$$2\mu\frac{d^2\left(v^l\right)}{dy^2} + \rho g = \frac{dP}{dx}, \tag{2}$$

and the Brinkman equation is equation (1). Therefore (1) is called Stokes–Brinkman equations. The Brinkman equation used in ω_2 has been normalized in [11], which is

$$2\ell_1\frac{d^2U^+}{dy^{+2}} - \ell_2U^+ + \ell_3 = \frac{dP^+}{dx^+} - B(y^+), \tag{3}$$

and the normalized Stokes equation is

$$2\frac{d^2U^+}{dy^{+2}} + \ell_3 = \frac{dP^+}{dx^+}, \tag{4}$$

where $\ell_1 = 1/\varepsilon^l, \ell_2 = h^2/K_0K^+$, $\ell_3 = h^2\rho g^+ g_0/\mu U_0$, h is the characteristic length, U_0 is a volumetric average velocity in the porous medium, K_0 is characteristic permeability, g_0 is characteristic gravity, and $B(y^+) = h^2\varepsilon^l\nu^+/K_0K^+$ where the normalized variables

$$y^+ = \frac{y}{h}, U^+ = \frac{\varepsilon^l v^l}{U_0}, v^+ = \frac{v^s}{U_0}, x^+ = \frac{x}{h}, \quad K^+ = \frac{k_{11}}{K_0}, P^+ = P\frac{h}{U_0\mu} \text{ and } g^+ = \frac{g}{g_0}. \tag{5}$$

For the Stokes equation, the variable $U^+ = v^l/U_0$ because $\varepsilon^l = 1$. In this study, we assume that the velocity of cilia is linear, that is,

$$B(y^+) = \frac{h^2\varepsilon^l}{k_{11}}(a_1y^+ + a_0), \tag{6}$$

where a_0 and a_1 are constants. Next, we provide the boundary conditions at the top and the bottom of the domains used in this research.

2.2. Boundary Conditions. Because cilia are immobilized at the bottom of the domain, we assume that the PCL fluid has a no-slip condition at $y = 0$. That is,

$$U^+ = 0 \text{ at } y^+ = 0. \tag{7}$$

For the boundary condition at the top of the domain, we assume that the velocity is bounded by a constant. That is,

$$\lim_{y^+\to 1} U^+(y^+) = D_0, \tag{8}$$

where D_0 is a constant as illustrated in Figure 3.

For the special cases of the boundary condition, Vanaki et al. [25] used

$$U^+ = 0 \text{ at } y^+ = 0, \quad \frac{\partial U^+}{\partial y} = 0 \text{ at } y^+ = 1, \tag{9}$$

and U^+ is periodic on the left and right sides of the boundaries for the study of the movement of the PCL fluid in case of diseased and healthy conditions. Liron and Meyer [26] studied the PCL flow at $y^+ = 1$ by using the boundary condition $\partial U^+/\partial y = 0$. In this study, we use bounded boundary at $y^+ = 1$ so that one may apply this study to other related problems.

We now have the normalized Stokes–Brinkman equations and boundary conditions. Next, we find the solution U^+ by using the method of matched asymptotic expansion in Section 3.

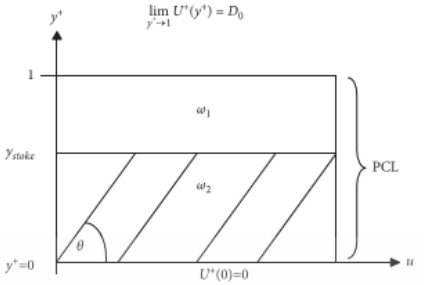

FIGURE 3: Boundary conditions used in this study.

3. Asymptotic Solutions

In this section we employ the method of asymptotic expansion to find the solutions in both domains ω_1 and ω_2. Because there exists a transition layer at the free-fluid/porous-medium interface, the approximation of this part of the domain is called inner solution. The approximation of other parts of the domain ω is named outer solution. Then the solutions are combined through matching conditions provided in Section 3.3. The inner and outer solutions, derived in [11], are briefly introduced in Sections 3.1 and 3.2. The zeroth-order results after applying the matching conditions are provided in Section 3.4.

3.1. Outer Solutions. In this section, we briefly provide the outer solutions found in [11] in two different domains, ω_1 and ω_2, by using the method of asymptotic expansion. The solutions in domain ω_2 and ω_1 are obtained by substituting

$$U^+ = U^{+(0)} + \varepsilon U^{+(1)} + \varepsilon^2U^{+(2)} + O(\varepsilon^3), \tag{10}$$

into (3) and (4), respectively. Thus, we have the zeroth-order and first-order solutions for the outer region ω_2 with the boundary condition (7) are

$$U^{+(0)} = w_1e^{\sqrt{\ell_2/2\ell_1}y^+} - w_1e^{-\sqrt{\ell_2/2\ell_1}y^+} + \left(\frac{\ell_3}{\ell_2} + \frac{1}{\ell_2}\frac{dP^+}{dx^+} - \frac{h^2\varepsilon^l}{\ell_2k_{11}}a_0\right)e^{-\sqrt{\ell_2/2\ell_1}y^+} + \frac{h^2\varepsilon^l}{\ell_2k_{11}}a_1y^+ + \frac{\ell_3}{\ell_2} - \frac{1}{\ell_2}\frac{dP^+}{dx^+} + \frac{h^2\varepsilon^l}{\ell_2k_{11}}a_0, \tag{11}$$

$$U^{+(1)} = w_5e^{\sqrt{\ell_2/2\ell_1}y^+} - w_5e^{-\sqrt{\ell_2/2\ell_1}y^+}, \tag{12}$$

respectively, where w_1 and w_5 are constants, and the zeroth-order and first-order solutions for the outer region ω_1 with the boundary condition (8) are

$$U^{+(0)} = \frac{(1/2 - \ell_3/2)y^{+2}}{2} + w_3 y^+ + D_0 - \frac{(1/2 - \ell_3/2)}{2} - w_3, \tag{13}$$

$$U^{+(1)} = w_7 y^+ + D_0 - w_7, \tag{14}$$

respectively, where w_3 and w_7 are constants. Next, we provide the solution in the inner region.

3.2. Inner Solutions. In this section, we provide the inner solutions in the transition zone between the porous medium and the free-fluid domain. In the inner region, for any variable f, we use $\overline{f}$ instead of a physical variable f. For example, y^+ in the inner region is $\overline{y}^+$ and U^+ in the inner region is $\overline{U}^+$. Define

$$\overline{y}^+ = \frac{y^+ - y_{\text{Stoke}}}{\varepsilon} \text{ and } \overline{U}^+(\overline{y}^+) = U^+\left(\frac{y^+ - y_{\text{Stoke}}}{\varepsilon}\right). \tag{15}$$

Applying (15) to (3) with the properties, obtained from (15),

$$\frac{\mathrm{d}\overline{y}^+}{\mathrm{d}y^+} = \frac{1}{\varepsilon} \text{ and } \frac{d^2U^+}{\mathrm{d}y^{+2}} = \frac{1}{\varepsilon^2}\frac{d^2\overline{U}^+}{\mathrm{d}\overline{y}^{+2}}, \tag{16}$$

and using the same process of finding the outer solution, we have the zeroth-, first-, and second-order solutions as follows:

$$\overline{U}^{+(0)} = m_1\overline{y}^+ + m_2, \tag{17}$$

$$\overline{U}^{+(1)} = m_3\overline{y}^+ + m_4, \tag{18}$$

$$\overline{U}^{+(2)} = \frac{\ell_2}{12\ell_1}m_1\overline{y}^{+3} + \left(\frac{\ell_2 m_2}{2\ell_1} - \frac{\ell_3}{2\ell_1'} + \frac{1}{2\ell_1}\frac{\mathrm{d}P^+}{\mathrm{d}x^+} - \frac{h^2\varepsilon'}{2\ell_1'k_{11}}a_1 y_{\text{Stoke}} - \frac{h^2\varepsilon'}{2\ell_1'k_{11}}a_0\right)\frac{\overline{y}^{+2}}{2} + m_5\overline{y}^+ + m_6, \tag{19}$$

where m_1, m_2, m_3, and m_4 are constants. The outer and inner solutions will be matched by using the matching conditions provided in the next section.

3.3. Matching Conditions. In this section, we derive matching conditions to match the variables defined in the outer and inner regions. The matching condition used in this work is developed from Van Dyke's rule [9, 27]. With the outer and inner variables,

$$f(y^+, \varepsilon) = f^{(0)}(y^+) + \varepsilon f^{(1)}(y^+) + o(\varepsilon^2). \tag{20}$$

$$\overline{f}(\overline{y}^+, \varepsilon) = \overline{f}^{(0)}(\overline{y}^+) + \varepsilon\overline{f}^{(1)}(\overline{y}^+) + o(\varepsilon^2), \tag{21}$$

and applying Van Dyke's rule matching principle, we have

$$\lim_{\overline{y}^+ \to \pm\infty} \overline{f}(\overline{y}^+) = \lim_{y^+ \to y^\pm_{\text{Stoke}}} f(y^+). \tag{22}$$

We find the matching condition of $f^{(0)}$ by substituting (20) and (21) into (22). Therefore,

$$\lim_{y^+ \to y^\pm_{\text{Stoke}}} \left[f^{(0)}(y^+) + \varepsilon f^{(1)}(y^+) + O(\varepsilon^2)\right] = \lim_{\overline{y}^+ \to \pm\infty} \left[\overline{f}^{(0)}(\overline{y}^+) + \varepsilon\overline{f}^{(1)}(\overline{y}^+) + O(\varepsilon^2)\right]. \tag{23}$$

We suppose that $\lim_{y^+ \to y^\pm_{\text{Stoke}}} f^{(i)}(y^+)$ and $\lim_{\overline{y}^+ \to \pm\infty} f^{(i)}(y^+)$ exist, $i = 0, 1, 2, \ldots$ Then, considering the zeroth-order term of ε, we have

$$\lim_{\overline{y}^+ \to \pm\infty} \overline{f}^{(0)}(\overline{y}^+) = \lim_{y^+ \to y^\pm_{\text{Stoke}}} f^{(0)}(y^+). \tag{24}$$

Next, we find another matching condition by applying Taylor's series expansion to (20) around the point $y^\pm_{\text{Stoke}}$ or y_{Stoke}, where the superscript plus and minus signs mean the right and left sides of y_{Stoke} and we assume that $f^{(i)}(y^+), i = 0, 1, 2, 3, \ldots$ are continuous at $y = y_{\text{Stoke}}$ so that

$$f^{(i)}(y^\pm_{\text{Stoke}}) = \lim_{y^+ \to y^\pm_{\text{Stoke}}} f^{(i)}(y^+), i = 0, 1, 2, 3, \ldots. \tag{25}$$

Then, we have

$$f(y^+, \varepsilon) = \left[\lim_{y^+ \to y^\pm_{\text{Stoke}}} f^{(0)}(y^+) + (y^+ - y^\pm_{\text{Stoke}}) \lim_{y^+ \to y^\pm_{\text{Stoke}}} \frac{\mathrm{d}f^{(0)}(y^+)}{\mathrm{d}y^+} + \frac{(y^+ - y^\pm_{\text{Stoke}})^2}{2} \lim_{y^+ \to y^\pm_{\text{Stoke}}} \frac{d^2 f^{(0)}(y^+)}{\mathrm{d}y^+} + O(y^+ - y^\pm_{\text{Stoke}})^3\right] + \varepsilon\left[\lim_{y^+ \to y^\pm_{\text{Stoke}}} f^{(1)}(y^+) + (y^+ - y^\pm_{\text{Stoke}}) \lim_{y^+ \to y^\pm_{\text{Stoke}}} \frac{\mathrm{d}f^{(1)}(y^+)}{\mathrm{d}y^+} + O(y^+ - y^\pm_{\text{Stoke}})^2\right] + O(\varepsilon^2). \tag{26}$$

Substituting (15) into (26), we obtain

$$f(y^+,\varepsilon) = \lim_{y^+ \longrightarrow y^{\pm}_{\text{Stoke}}} f^{(0)}(y^+) + \varepsilon\overline{y}^+ \lim_{y^+ \longrightarrow y^{\pm}_{\text{Stoke}}} \frac{\mathrm{d}f^{(0)}(y^+)}{\mathrm{d}y^+} + \frac{(\varepsilon\overline{y}^+)^2}{2} \lim_{y^+ \longrightarrow y^{\pm}_{\text{Stoke}}} \frac{d^2 f^{(0)}(y^+)}{\mathrm{d}y^+} + \mathrm{O}(\varepsilon\overline{y}^+)^3 + \varepsilon\left[\lim_{y^+ \longrightarrow y^{\pm}_{\text{Stoke}}} f^{(1)}(y^+) + \varepsilon\overline{y}^+ \lim_{y^+ \longrightarrow y^{\pm}_{\text{Stoke}}} \frac{\mathrm{d}f^{(1)}(y^+)}{\mathrm{d}y^+} + \mathrm{O}(\varepsilon\overline{y}^+)^2\right] + \mathrm{O}(\varepsilon^2). \tag{27}$$

Differentiating (27) with respect to $\overline{y}^+$, taking $y^+ \longrightarrow y^{\pm}_{\text{Stoke}}$ on both sides, and omitting the big O, then, we obtain

$$\lim_{y^+ \longrightarrow y^{\pm}_{\text{Stoke}}} \frac{\mathrm{d}f(y^+,\varepsilon)}{\mathrm{d}\overline{y}^+} = \varepsilon \lim_{y^+ \longrightarrow y^{\pm}_{\text{Stoke}}} \frac{\mathrm{d}f^{(0)}(y^+)}{\mathrm{d}y^+} + \varepsilon^2\overline{y}^+ \lim_{y^+ \longrightarrow y^{\pm}_{\text{Stoke}}} \frac{d^2 f^{(0)}(y^+)}{\mathrm{d}y^+} + \varepsilon^2 \lim_{y^+ \longrightarrow y^{\pm}_{\text{Stoke}}} \frac{\mathrm{d}f^{(1)}(y^+)}{\mathrm{d}y^+}, \tag{28}$$

where in this work we assume that the function f is continuous enough so that the differentiation can be switched with the limit. To find the matching condition for the first derivative of the functions f and $\overline{f}$, we differentiate (21) with respect to $\overline{y}^+$ and taking limit $\overline{y}^+ \longrightarrow \pm\infty$ on both sides, we obtain

$$\lim_{\overline{y}^+ \longrightarrow \pm\infty} \frac{\mathrm{d}\overline{f}(\overline{y}^+,\varepsilon)}{\mathrm{d}\overline{y}^+} = \lim_{\overline{y}^+ \longrightarrow \pm\infty}\left[\frac{\mathrm{d}\overline{f}^{(0)}(\overline{y}^+)}{\mathrm{d}\overline{y}^+} + \varepsilon\frac{\mathrm{d}\overline{f}^{(1)}(\overline{y}^+)}{\mathrm{d}\overline{y}^+} + \varepsilon^2\frac{\mathrm{d}\overline{f}^{(2)}(\overline{y}^+)}{\mathrm{d}\overline{y}^+}\right]. \tag{29}$$

Since we assume that the differentiation can be switched with the limit, from (22), we have

$$\lim_{y^+ \longrightarrow y^{\pm}_{\text{Stoke}}} \frac{\mathrm{d}f(y^+,\varepsilon)}{\mathrm{d}\overline{y}^+} = \lim_{\overline{y}^+ \longrightarrow \pm\infty} \frac{\mathrm{d}\overline{f}(\overline{y}^+,\varepsilon)}{\mathrm{d}\overline{y}^+}. \tag{30}$$

This fact demonstrates that (28) and (29) are equal. Then, we get

$$\varepsilon \lim_{y^+ \longrightarrow y^{\pm}_{\text{Stoke}}} \frac{\mathrm{d}f^{(0)}(y^+)}{\mathrm{d}y^+} + \varepsilon^2\overline{y}^+ \lim_{y^+ \longrightarrow y^{\pm}_{\text{Stoke}}} \frac{d^2 f^{(0)}(y^+)}{\mathrm{d}y^+} + \varepsilon^2 \lim_{y^+ \longrightarrow y^{\pm}_{\text{Stoke}}} \frac{\mathrm{d}f^{(1)}(y^+)}{\mathrm{d}y^+} = \lim_{\overline{y}^+ \longrightarrow \pm\infty}\left[\frac{\mathrm{d}\overline{f}^{(0)}(\overline{y}^+)}{\mathrm{d}\overline{y}^+} + \varepsilon\frac{\mathrm{d}\overline{f}^{(1)}(\overline{y}^+)}{\mathrm{d}\overline{y}^+} + \varepsilon^2\frac{\mathrm{d}\overline{f}^{(2)}(\overline{y}^+)}{\mathrm{d}\overline{y}^+}\right]. \tag{31}$$

Collecting the same order of ε in (31), we obtain

$$\varepsilon^0: \lim_{\overline{y}^+ \longrightarrow \pm\infty} \frac{\mathrm{d}\overline{f}^{(0)}(\overline{y}^+)}{\mathrm{d}\overline{y}^+} = 0, \tag{32}$$

$$\varepsilon^1: \lim_{\overline{y}^+ \longrightarrow \pm\infty} \frac{\mathrm{d}\overline{f}^{(1)}(\overline{y}^+)}{\mathrm{d}\overline{y}^+} = \lim_{y^+ \longrightarrow y^{\pm}_{\text{Stoke}}} \frac{\mathrm{d}f^{(0)}(y^+)}{\mathrm{d}y^+}, \tag{33}$$

$$\varepsilon^2: \lim_{\overline{y}^+ \longrightarrow \pm\infty} \frac{\mathrm{d}\overline{f}^{(2)}(\overline{y}^+)}{\mathrm{d}\overline{y}^+} = \overline{y}^+ \lim_{y^+ \longrightarrow y^{\pm}_{\text{Stoke}}} \frac{d^2 f^{(0)}(y^+)}{\mathrm{d}y^+} + \lim_{y^+ \longrightarrow y^{\pm}_{\text{Stoke}}} \frac{\mathrm{d}f^{(1)}(y^+)}{\mathrm{d}y^+}. \tag{34}$$

Next, we determine the zeroth-order matching solutions for the couple Stokes–Brinkman equations.

3.4. The Zeroth-Order Solution. In this section, we couple the zeroth-order solutions of the governing equations (3), (4) by using the matching conditions provided in Section 3.3. Before using the matching conditions, we differentiate the zeroth-order and first-order inner solutions (17) and (18) with respect to $\overline{y}^+$ and taking the limit $\overline{y}^+ \longrightarrow +\infty$ on both sides, we obtain

$$\lim_{\overline{y}^+ \longrightarrow +\infty} \frac{\mathrm{d}\overline{U}^{+(0)}}{\mathrm{d}\overline{y}^+} = m_1, \tag{35}$$

$$\lim_{\overline{y}^+ \longrightarrow +\infty} \frac{\mathrm{d}\overline{U}^{+(1)}}{\mathrm{d}\overline{y}^+} = m_3, \tag{36}$$

respectively. According to the matching condition (32), we have $m_1 = 0$. Then, from (17), we obtain

$$\overline{U}^{+(0)} = m_2. \tag{37}$$

Next, we provide the matching process of the outer solutions in domains ω_2 and ω_1. Differentiating the zeroth-order outer solutions (11) and (13) for the outer regions ω_2 and ω_1, respectively, with respect to y^+, and taking the limit $y^+ \longrightarrow y^{\pm}_{\text{Stoke}}$ on both sides, we obtain

$$\lim_{y^+ \longrightarrow y^+_{\text{Stoke}}} \frac{dU^{+(0)}}{dy^+} = w_1\sqrt{\frac{\ell_2}{2\ell_1}}e^{\sqrt{\ell_2/2\ell_1}y^+_{\text{Stoke}}} + w_1\sqrt{\frac{\ell_2}{2\ell_1}}e^{-\sqrt{\ell_2/2\ell_1}y^+_{\text{Stoke}}} - \sqrt{\frac{\ell_2}{2\ell_1}}\left(-\frac{\ell_3}{\ell_2} + \frac{1}{\ell_2}\frac{dP^+}{dx^+} - \frac{h^2\varepsilon^l}{\ell_2 k_{11}}a_0\right) e^{-\sqrt{\ell_2/2\ell_1}y^+_{\text{Stoke}}} + \frac{h^2\varepsilon^l}{\ell_2 k_{11}}a_1, \tag{38}$$

$$\lim_{y^+ \longrightarrow y^+_{\text{Stoke}}} \frac{dU^{+(0)}}{dy^+} = \left(\frac{1}{2} - \frac{\ell_3}{2}\right)y^+_{\text{Stoke}} + w_3, \tag{39}$$

respectively. Substituting (36) and (38) into (33), we obtain

$$m_3 = w_1\sqrt{\frac{\ell_2}{2\ell_1}}e^{\sqrt{\ell_2/2\ell_1}y^+_{\text{Stoke}}} + w_1\sqrt{\frac{\ell_2}{2\ell_1}}e^{-\sqrt{\ell_2/2\ell_1}y^+_{\text{Stoke}}} - \sqrt{\frac{\ell_2}{2\ell_1}}\left(-\frac{\ell_3}{\ell_2} + \frac{1}{\ell_2}\frac{dP^+}{dx^+} - \frac{h^2\varepsilon^l}{\ell_2 k_{11}}a_0\right)e^{-\sqrt{\ell_2/2\ell_1}y^+_{\text{Stoke}}} + \frac{h^2\varepsilon^l}{\ell_2 k_{11}}a_1, \tag{40}$$

in region ω_2. Similarly, substituting (36) and (39) into (33), we have

$$m_3 = \left(\frac{1}{2} - \frac{\ell_3}{2}\right)y^+_{\text{Stoke}} + w_3, \tag{41}$$

in region ω_1. Since (40) is equal to (41), we then have

$$w_3 = -\left(\frac{1}{2} - \frac{\ell_3}{2}\right)y^+_{\text{Stoke}} + w_1\left(\sqrt{\frac{\ell_2}{2\ell_1}}e^{\sqrt{\ell_2/2\ell_1}y^+_{\text{Stoke}}} + \sqrt{\frac{\ell_2}{2\ell_1}}e^{-\sqrt{\ell_2/2\ell_1}y^+_{\text{Stoke}}}\right) - \sqrt{\frac{\ell_2}{2\ell_1}}\left(-\frac{\ell_3}{\ell_2} + \frac{1}{\ell_2}\frac{dP^+}{dx^+} - \frac{h^2\varepsilon^l}{\ell_2 k_{11}}a_0\right)e^{-\sqrt{\ell_2/2\ell_1}y^+_{\text{Stoke}}} + \frac{h^2\varepsilon^l}{\ell_2 k_{11}}a_1. \tag{42}$$

Define

$$z_1 = \sqrt{\frac{\ell_2}{2\ell_1}}, z_2 = \frac{1}{2} - \frac{\ell_3}{2}, z_3 = \frac{1}{2\ell_1}\frac{dP^+}{dx^+} - \frac{\ell_3}{2\ell_1}, z_4 = \frac{\ell_3}{\ell_2} + \frac{1}{\ell_2}\frac{dP^+}{dx^+} - \frac{h^2\varepsilon^l}{\ell_2 k_{11}}a_0 \text{ and } z_5 = \frac{h^2\varepsilon^l}{\ell_2 k_{11}}a_1, \tag{43}$$

which are known constants. Applying (43) to (42) and (11), this yields

$$w_3 = -z_2 y^+_{\text{Stoke}} + w_1\left(z_1 e^{z_1 y^+_{\text{Stoke}}} + z_1 e^{-z_1 y^+_{\text{Stoke}}}\right) - z_1 z_4 e^{-z_1 y^+_{\text{Stoke}}} + z_5, \tag{44}$$

$$\left[U^{+(0)}\right]^{(p)} = w_1 e^{z_1 y^+} - w_1 e^{-z_1 y^+} + z_4 e^{-z_1 y^+} + z_5 y^+ - z_4; 0 < y^+ < y_{\text{Stoke}}, \tag{45}$$

respectively, where $[U^{+(0)}]^{(p)}$ means the zeroth-order solution in the porous-medium domain ω_2. Substituting (43) and (44) into (13), we have

$$\left[U^{+(0)}\right]^{(f)} = \frac{z_2 y^{+2}}{2} + D_0 - \frac{z_2}{2} + \left[-z_2 y^+_{\text{Stoke}} + w_1\left(z_1 e^{z_1 y^+_{\text{Stoke}}} + z_1 e^{-z_1 y^+_{\text{Stoke}}}\right) - z_1 z_4 e^{-z_1 y^+_{\text{Stoke}}} + z_5\right] \tag{46}$$

$$(y^+ - 1); y_{\text{Stoke}} < y^+ < 1,$$

where $[U^{+(0)}]^{(f)}$ means the zeroth-order solution in the free-fluid domain ω_1. Now, we obtain $[U^{+(0)}]^{(p)}$ and $[U^{+(0)}]^{(f)}$ in terms of w_1.

To illustrate our results, the solution (45) is plotted in Figure 4, where the angles between the cilia and the horizontal plane considered in this work are 40°, 50°, 60°, 70°, 80°, and 90°, respectively. In this research, we assume that the cilia have the highest velocity at $\theta = 90°$ and stop beating at $\theta = 40°$. The values of the variables used in (45) are presented in Tables 1 and 2. The values in Table 1 are used for all angles θ and the values of the variables in Table 2 are different for each angle θ, which are obtained from [8, 28], where they have obtained the data from a biological experiment [29]. We concentrate on only one viscosity because we intend to find the solutions that are close to the real problem and the solutions do not change with the different viscosities. The results for the different angles are interesting because we determine the PCL velocities due to the movement of cilia, which means the angle changes. The Earth gravity, solid velocity, and permeability variables in (5) are fixed according to our designed problem. Pressure can be modified but for this problem the most effect on the velocity of the PCL fluid is the solid phases, rather than pressure gradient. The variables x and y in (5) are independent variables, which give the position of the fluid velocity on the domain.

Figure 4 shows the velocity of the PCL fluid with different angles θ in domain ω_2. The highest velocity occurred at $\theta = 90°$ as expected. This is because, in this study, we assume that the maximum velocity of cilia occurs at $\theta = 90°$. Notice that the velocities decrease when the angles between the cilia and the horizontal plane decrease.

In the next section, we compare our solution with an experimental data where the velocity of the solid phases in our solution is set to be zero.

4. Comparison with an Experimental Study

In this section, we compare the mass flow rate Φ of our result with the study of Beavers and Joseph [22], where

$$\Phi = \frac{M_f - M_p}{M_p}, \tag{47}$$

where M_f is the mass flow rate in the free-fluid region and M_p is the mass flow rate in the porous medium. In their study, BJ carried out the experiment to measure the flow rate of a long porous block and a small uniform gap immediately

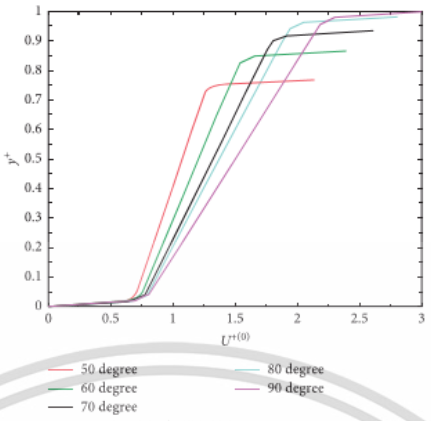

Figure 4: The asymptotic solution $U^{+(0)}$, equation (45).

Table 1: Values of the variables applied to the solution (45) to plot Figure 4.

Variable	Value	Unit	Variable	Value	Unit
a_0	0	[1]	U_0	1	$[\mu m/s]$
h	7.5	$[\mu m]$	K_0	1	$[\mu m^2]$
ρ	992.2×10^{-15}	$[g/\mu m^3]$	dP^*/dx^*	1	[1]
μ	3×10^{-6}	$[g/\mu m \cdot s]$	w_1	0	[1]
g	9.81×10^6	$[\mu m/s^2]$			

Table 2: Values of the variables used to plot Figure 4 for each angle θ.

Variable	50°	60°	70°	80°	90°
y_{Stoke}	0.7672	0.8638	0.9353	0.9818	1.0000
K^+	0.0012	0.0015	0.0016	0.0017	0.0018
ε	0.6717	0.7099	0.7331	0.7439	0.7487
a_1	1.2	1.4	1.6	1.8	2

above the block, while in this study, we analytically find the mass flow rate of the fluid flow in the PCL in human lung by using the asymptotic expansion method. The porous medium in the experimental study is stationary porous blocks, while the porous medium in this study is the ciliary layer, which is a motion medium. Therefore, we compare our solution with the experimental data at only one porosity and the solid velocity is set to be zero. Since Beavers and Joseph provide the data, the mass flow rate, only on the free-fluid domain, as the result, only the solution on the free-fluid domain is compared.

By applying the zeroth-order solutions (45), (46) provided in Section 3.4 to (47), the mass flow rate obtained from both equations is

$$\Phi = \frac{1/2\left(1/2 - \sigma^2 K_0 \rho g^* g_0/2\mu U_0\right)\sigma^2 K_0 + D_0 - 1/4\left(1 - \sigma^2 K_0 \rho g^* g_0/\mu U_0\right) + \left[\begin{array}{c} -\left(1/2 - \sigma^2 K_0 \rho g^* g_0/2\mu U_0\right) y^*_{\text{Stoke}} + w_1\left(\sigma\sqrt{1/2K^+}\, e^{\sigma\sqrt{1/2K^+}\, y^*_{\text{Stoke}}} + \sigma\sqrt{1/2K^+}\, e^{-\sigma\sqrt{1/2K^+}\, y^*_{\text{Stoke}}}\right) \\ +\sigma\sqrt{1/2K^+}\left(\left(\rho g^* g_0 K_0 K^+/\mu U_0\right) + \left(h^2/\sigma^2 K_0\right)\right) e^{-\sigma\sqrt{1/2K^+}\, y^*_{\text{Stoke}}} \end{array}\right]\left(\sigma\sqrt{K_0} - 1\right)}{w_1 e^{\sigma^2\sqrt{\varepsilon K_0/2K^+}} - w_1 e^{-\sigma^2\sqrt{\varepsilon K_0/2K^+}} - \left(\left(\rho g^* g_0 K_0 K^+/\mu U_0\right) + \left(h^2/\sigma^2 K_0\right)\right) e^{-\sigma^2\sqrt{\varepsilon K_0/2K^+}} + \left(\rho g^* g_0 K_0 K^+/\mu U_0\right) + \left(h^2/\sigma^2 K_0\right)} - 1, \tag{48}$$

where $\sigma = y^+/\sqrt{K_0}$ and $y_{\text{Stoke}} \le y^+ \le 1$. To compare the result with the experimental data, we use the same values of the variables as in the experiment. The dynamic viscosity and the density of water are $8.9 \times 10^{(-4)}$ [Pa · s] and 997[kg/m^3], respectively [27]. The gravity g^+g_0 is 9.8[m/s^2]. The length of the free-fluid domain ranges from 3.37046×10^{-4} to 1, where y_{Stoke} is assumed to be 3.37046×10^{-4}. The porosity is 0.78 and the characteristic permeability K_0 is 7.1×10^{-9}. The values of other variables used in (48) are $K^+ = k_{11}/K_0$, $k_{11} = 0.4$, $w_1 = -2.5$, $U_0 = 1$, $D_0 = 1$ and $h = 7.5$, and Φ is normalized by 10^4.

Figure 5 shows the comparison of the mass flow rate in this study (solid line) through the free-fluid domains as a function of σ, with the mass flow rate in the experimental study of Beavers and Joseph [22]. As can be seen from Figure 5, the solution of our study (solid line) is in a good agreement with the experimental data of Beavers and Joseph [22].

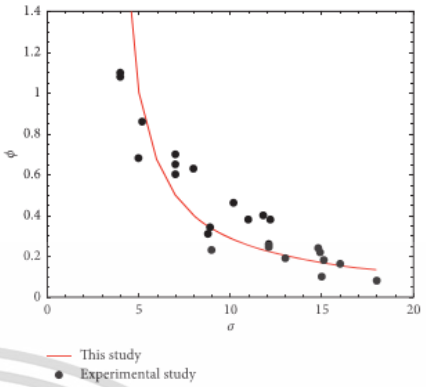

Figure 5: The mass flow rate in this study and the experimental data [22].

5. Boundary Conditions at the Free-Fluid/Porous-Medium Interface

In this section we find the boundary condition at the free-fluid/porous-medium interface by using the two solutions in the two domains ω_1 and ω_2. Based on solutions (45) and (46), we can now obtain the boundary condition at the free-fluid/porous-medium interface, which is

$$\begin{aligned}\left[U^{+(0)}\right]^{(f)} &= \frac{z_2 y^{+2}}{2} + D_0 - \frac{z_2}{2} + \left[-z_2 y^+_{\text{Stoke}} - z_1 z_4 e^{-z_1 y^+_{\text{Stoke}}} + z_5\right](y^+ - 1) \\ &+ \left[\frac{1}{\left(e^{z_1 y^+} - e^{-z_1 y^+}\right)}\left\{\left[U^{+(0)}\right]^{(p)} - z_4\left(e^{-z_1 y^+} - 1\right) - z_5 y^+\right\}\right]\left(z_1 e^{z_1 y^+_{\text{Stoke}}} + z_1 e^{-z_1 y^+_{\text{Stoke}}}\right) \\ &\cdot (y^+ - 1).\end{aligned} \tag{49}$$

Next, we provide another boundary condition at the free-fluid/porous-medium interface.

Differentiating the zeroth-order solutions (45) and (46) with respect to y^+ both sides, we have

$$\frac{d\left[U^{+(0)}\right]^{(P)}}{dy^+} = w_1 z_1 e^{z_1 y^+} + w_1 z_1 e^{-z_1 y^+} - z_1 z_4 e^{-z_1 y^+} + z_5, \tag{50}$$

$$\frac{d\left[U^{+(0)}\right]^{(f)}}{dy^+} = z_2 y^+ - z_2 y^+_{\text{Stoke}} + w_1\left(z_1 e^{z_1 y^+_{\text{Stoke}}} + z_1 e^{-z_1 y^+_{\text{Stoke}}}\right) - z_1 z_4 e^{-z_1 y^+_{\text{Stoke}}} + z_5, \tag{51}$$

respectively. Therefore we obtain another boundary condition at the free-fluid/porous-medium interface, which is

$$\begin{aligned}\frac{d\left[U^{+(0)}\right]^{(f)}}{dy^+} &= z_2\left(y^+ - y^+_{\text{Stoke}}\right) \\ &+ \frac{\left(e^{z_1 y^+_{\text{Stoke}}} + e^{-z_1 y^+_{\text{Stoke}}}\right)}{\left(e^{z_1 y^+} + e^{-z_1 y^+}\right)}\left[\frac{d\left[U^{+(0)}\right]^{(P)}}{dy^+} + z_1 z_4 e^{-z_1 y^+} - z_5\right] - z_1 z_4 e^{-z_1 y^+_{\text{Stoke}}} + z_5.\end{aligned} \tag{52}$$

Thus, we obtain two boundary conditions at the free-fluid/porous-medium interface, which are proper for the fluid flow in the PCL due to the movement of cilia.

6. Summary and Conclusions

The movement of the cilia in the PCL layer plays an important role in the clearance of mucus and in preventing foreign materials from entering the lower respiratory tract. Determining the velocity of the PCL fluid flow in motile cilia is necessary for a better understanding of the clearance mechanism. The velocity of PCL fluid can be determined using an ordinary differential equation (ODE), which requires boundary conditions. This research quantifies the boundary conditions at the interface between the porous-medium and free-fluid regions using Stokes–Brinkman equations. To achieve our aim:

(i) We apply the Stokes equation to the free-fluid domain and the Brinkman equation to the porous-medium region.

(ii) We also assumed two boundary conditions: The first boundary condition is no-slip boundary condition, applied at the bottom of the porous-medium domain; the second boundary condition is that the velocity of the PCL fluid is bounded when y tends to a constant, applied at the top of the free-fluid region.

(iii) The velocity of the PCL fluid due to the movement of cilia is obtained by using the matched asymptotic expansion.

(iv) The results are illustrated in Figure 4 with different angles, $\theta = 40^\circ, 50^\circ, 60^\circ, 70^\circ, 80^\circ, 90^\circ$, that the cilia make with the horizontal plane. The variables employed to plot the graph of the solutions are shown in Tables 1 and 2.

(v) We find that the velocity of the PCL fluid reaches its maximum value when $\theta = 90^\circ$ and decreases when θ decreases, which satisfies our assumption that the highest velocity of cilia occurs when the cilia are perpendicular to the horizontal plane and the cilia velocities decrease with decreasing angle θ.

(vi) We also found that the solution in this study is consistent with the experimental data studied by Beavers and Joseph, which is shown in Figure 5.

As mentioned above, not only are there two domains, porous domain and free-fluid domain, but also there is the interface between the free-fluid domain and porous medium. The boundary conditions at the interface between the porous-medium and the free-fluid regions are determined from the zeroth-order solutions provided in Section 3.4.

(i) The first boundary condition is the relationship between the two zeroth-ordered solutions in the two domains while the second boundary condition is the derivative of those two solutions.

(ii) It should be noted that, in this study, the solid phases in the porous domain are self-propelled motion and we provide proper boundary conditions for the problem. On the contrary, in previous studies, they are stationary. Although they are moved, available literature has not provided appropriate boundary conditions for the fluid flow in PCL.

(iii) The limitation of this study is that the asymptotic expansion method applied in this study is good for a linear equation, but it is not easy to find the solutions for nonlinear equations.

(iv) The disadvantage of this study is that we calculate the zeroth-order approximation solution, where the other orders are cut off.

(v) In future work, the more realistic solution such as every angle is considered in one calculation rather than one angle. Applications of the boundary conditions to some other problems are, for example, flows in rice field [30–34].

Nomenclature

a_0: A constant (6)
a_1: A constant (6)
$B(y^+)$: A function of y^+ (3)
D_0: A constant (8)
$\mathrm{d}P/\mathrm{d}x$: The pressure gradient $[\mathrm{d}P/\mathrm{d}x] = M/L^2T^2$ (1)
g: The gravity $[g] = L/T^2$ (1)
g_0: Characteristic gravity $[g_0] = L/T^2$ (5)
h: The characteristic length $[h] = L$ (5)
K_0: Characteristic permeability $[K_0] = L^2$ (5)
K^+: Dimensionless permeability $[K^+] = 1$ (5)
k_{11}^{-1}: The inverse of the permeability tensor $[k_{11}^{-1}] = 1/L^2$ (1)
k_{11}: A permeability tensor $[k_{11}] = L^2$ (1)
ℓ_1: A constant (3)
ℓ_2: A constant (3)
ℓ_3: A constant (3)
m_1: A constant (17)
m_2: A constant (17)
m_3: A constant (18)
m_4: A constant (18)
M_f: The mass flow rate in the free-fluid region $[M_f] = M/T$ (3.35)
M_p: The mass flow rate in the porous medium $[M_p] = M/T$ (3.35)
P: Pressure $[P] = M/LT^2$ (1)
U_0: A volumetric average velocity in a porous medium $[U_0] = L/T$ (5)
U^+: Dimensionless average velocity (5)
$\overline{U}^+$: Dimensionless velocity in the inner region (15)
$U^{+(0)}$: Dimensionless zeroth-order solution of the outer region (10)
$U^{+(1)}$: Dimensionless first-order solution of the outer region (10)
v^l: The velocity of the liquid phase $[v^l] = L/T$ (1)
v^s: The velocity of the solid phases $[v^s] = L/T$ (1)
w_1: A constant (11)
w_3: A constant (13)
w_5: A constant (12)
w_7: A constant (14)
y^+: Dimensionless y (5)
$\overline{y}^+$: Dimensionless y in inner region (15)
y_{Stoke}: The height of the porous-medium domain $[y_{\mathrm{Stoke}}] = L$ in Figure 2.
y_{Stoke}^+: y_{Stoke} in free-fluid region $[y_{\mathrm{Stoke}}^+] = L$ (22)
y_{Stoke}^-: y_{Stroke} in porous-medium region $[y_{\mathrm{Stoke}}^-] = L$ (22)
z_1: A constant (43)
z_2: A constant (43)
z_3: a constant (43)
z_4: A function depending on ε^l and k_{11} (43)
z_5: A function depending on ε^l and k_{11} (43)
ω: Periciliary layer (PCL) $[\omega] = L^2$ Figure 2.
ω_1: Free-fluid domain $[\omega_1] = L^2$ Figure 2.
ω_2: Porous medium $[\omega_2] = L^2$ Figure 2.
ε^l: A porosity $[\varepsilon^l] = 1$ (1)
ρ: The fluid density $[\rho] = M/L^3$ (1)
μ: A dynamic viscosity $[\mu] = M/\mathrm{LT}$ (1)
Φ: The mass flow rate in the total domain $[\Phi] = 1$ (48).

Data Availability

The data used to support the findings of this study are obtained from the previous study [22].

Conflicts of Interest

All authors declare that they have no conflicts of interest.

Acknowledgments

This research was funded by King Mongkut's Institute of Technology Ladkrabang, Bangkok 10520, Thailand.

Supplementary Materials

Supplementary data are available upon request. (*Supplementary Materials*)

References

[1] A. E. Tilley, M. S. Walters, R. Shaykhiev, and R. G. Crystal, "Cilia dysfunction in lung disease," *Annual Review of Physiology*, vol. 77, no. 1, pp. 379–406, 2015.

[2] B. Button, L.-H. Cai, C. Ehre et al., "A periciliary brush promotes the lung health by separating the mucus layer from airway epithelia," *Science*, vol. 337, no. 6097, pp. 937–941, 2012.

[3] P. F. Zhu, X. Li, A. Li, Y. Liu, D. D. Chen, and Y. Q. Xu, "Simulation study on the mass transport in PCL based on the ciliated dynamic system of the respiratory tract," *Hindawi Computational and Mathematical Methods in Medicine*, vol. 2019, Article ID 6036248, 2019.

[4] M. M. Shahmardan, M. H. Sedaghat, M. Norouzi, and M. Nazari, "Immersed boundary-lattice Boltzmann method for simulation of muco-ciliary transport: effect of mucus depth at various amounts of cilia beat frequency," *IOP Conference Series: Materials Science and Engineering*, vol. 100, p. 012065, 2015.

[5] S. Chateau, U. D'Ortona, S. Poncet, and J. Favier, "Transport and mixing induced by beating cilia in human airways," *Frontiers in Physiology*, vol. 9, p. 161, 2018.

[6] K. Wuttanachamsri, "Free interfaces at the tips of the cilia in the one-dimensional periciliary layer," *Mathematics*, vol. 8, no. 11, p. 1961, 2020.

[7] K. Wuttanachamsri and L. Schreyer, "Effects of cilia movement on fluid velocity: I model of fluid flow due to a moving solid in a porous media framework," *Transport in Porous Media*, vol. 136, no. 2, pp. 699–714, 2021.

[8] K. Wuttanachamsri and L. Schreyer, "Effects of cilia movement on fluid velocity: II numerical solutions over a fixed domain," *Transport in Porous Media*, vol. 134, no. 2, pp. 471–489, 2020.

[9] M. Chandesris and D. Jamet, "Boundary conditions at a planar fluid-porous interface for a Poiseuille flow," *International Journal of Heat and Mass Transfer*, vol. 49, no. 13-14, pp. 2137–2150, 2006.

[10] F. J. Valdés-Parada and D. Lasseux, "A novel one-domain approach for modeling flow in a fluid-porous system including inertia and slip effects," *Physics of Fluids*, vol. 33, no. 2, Article ID 022106, 2021.

[11] S. Poopra and K. Wuttanachamsri, "The velocity of PCL fluid in human lungs with beaver and Joseph boundary condition by using asymptotic expansion method," *Mathematics*, vol. 7, no. 6, p. 567, 2019.

[12] T. Carraro, C. Goll, A. Marciniak-Czochra, and A. Mikelić, "Pressure jump interface law for the Stokes-Darcy coupling: confirmation by direct numerical simulations," *Journal of Fluid Mechanics*, vol. 732, pp. 510–536, 2013.

[13] S. B. Naqvi and A. Bottaro, "Interfacial conditions between a free-fluid region and a porous medium," *International Journal of Multiphase Flow*, vol. 141, 2021.

[14] M. Ehrhardt, "An introduction to fluid-porous interface coupling," in *Book: Progress in Computational Physics. Vol 2: 2 Coupled Fluid Flow in Energy, Biology and Enviromental Research*, pp. 3–12, Bentham Books, 2012.

[15] Z. Abbas, M. Y. Rafiq, A. S. Alshomrani, and M. Z. Ullah, "Analysis of entropy generation on peristaltic phenomena of MHD slip flow of viscous fluid in a diverging tube," *Case Studies in Thermal Engineering*, vol. 23, 2021.

[16] R. E. Ado-Elkhair, K. S. Mekheimer, and A. M. A. Moawad, "Cilia walls influence on peristatically induced motion of magneto-fluid through porous medium at moderate Reynolds number: numerical study," *Journal of the Egyptian Mathematical Society*, vol. 25, pp. 238–251, 2017.

[17] A. Z. Zaher, A. M. A. Moawad, K. S. Mekheimer, and M. M. Bhatti, "Residual time of sinusoidal metachronal ciliary flow of non-Newtonian fluid through ciliated walls: fertilization and implantation," *Biomechanics and Modeling in Mechanobiology*, vol. 20, no. 2, pp. 609–630, 2021.

[18] G. Du and L. Zuo, "Local and parallel finite element method for the mixed Navier-Stokes/Darcy model with Beavers-Joseph interface conditions," *Acta Mathematica Scientia*, vol. 37, no. 5, pp. 1331–1347, 2017.

[19] J. A. Ochoa–Tapia and S. Whitaker, "Momentum transfer at the boundary between a porous medium and a homogeneous fluid – II," *International Journal of Heat and Mass Transfer*, vol. 38, no. 14, pp. 2635–2646, 1995.

[20] B. Goyeau, D. Lhuillier, D. Gobin, and M. G. Velarde, "Momentum transport at a fluid-porous interface," *International Journal of Heat and Mass Transfer*, vol. 46, no. 21, pp. 4071–4081, 2003.

[21] S. Whitaker, "Flow in porous media I: a theoretical derivation of Darcy's law," *Transport in Porous Media*, vol. 1, no. 1, pp. 3–25, 1986.

[22] G. S. Beavers and D. D. Joseph, "Boundary conditions at a naturally permeable wall," *Journal of Fluid Mechanics*, vol. 30, no. 1, pp. 197–207, 1967.

[23] M. Sahraoui and M. Kaviany, "Slip and No-slip velocity boundary conditions at interface of porous, plain media," *International Journal of Heat and Mass Transfer*, vol. 35, no. 4, pp. 927–943, 1992.

[24] J. H. Cushman, L. Bennethum, and B. Hu, "A primer on upscaling tools for porous media," *Advances in Water Resources*, vol. 25, no. 8, pp. 1043–1067, 2002.

[25] S. M. Vanaki, D. Holmes, P. G. Jayathilake, and R. Brown, "Three-dimensional numerical analysis of periciliary liquid layer: ciliary abnormalities in respiratory diseases," *Applied Sciences*, vol. 9, no. 19, p. 4033, 2019.

[26] N. Liron and F. A. Meyer, "Fluid transport in a thick layer above an active ciliated surface," *Biophysical Journal*, vol. 30, no. 3, pp. 463–472, 1980.

[27] J. Kevorkian and J. D. Cole, "Introduction to perturbation methods," *Applied Mathematical Sciences*, vol. 34, 1981.

[28] K. Chamsri and L. S. Bennethum, "Permeability of fluid flow through a periodic array of cylinders," *Applied Mathematical Modelling*, vol. 39, no. 1, pp. 244–254, 2015.

[29] P. R. Sears, K. Thomson, M. R. Knowles, and C. W. Davis, "Human airway ciliary dynamics," *American Journal of Physiology - Lung Cellular and Molecular Physiology*, vol. 3, pp. 170–183, 2012.

[30] H. Matsui, S. H. Randell, S. W. Peretti, C. W. Davis, and R. C. Boucher, "Coordinated clearance of periciliary liquid

and mucus from airway surfaces," *Journal of Clinical Investigation*, vol. 102, no. 6, pp. 1125–1131, 1998.

[31] M. Mierzwiczak, A. Fraska, and J. K. Grabski, "Determination of the slip constant in the beavers-joseph experiment for laminar fluid flow through porous media using a meshless method," *Mathematical Problems in Engineering*, vol. 2019, pp. 1–12, Article ID 1494215, 2019.

[32] G. Z. Voyiadjis and C. R. Song, *The Coupled Theory of Mixtures in Geomechanics with Applications" eBook*, Springer, New York, 2006.

[33] K. Wuttanachamsri, "Formulation of a well-posed Stokes-brinkman problem with a permeability tensor," *Journal of Mathematics*, vol. 1, no. Issue 1, pp. 1–7, 2015.

[34] M. Griebel and M. Klitz, "Homogenization and numerical simulation of flow in geometries with textile microstructures," *Multiscale Modeling and Simulation*, vol. 8, no. 4, pp. 1439–1460, 2010.

Author Biography

Name Miss Sudaporn Poopra

Date of Birth 21 June 1984

Address 24/1 Maidad Sub-direct, Bangrachan District,
Singburi Province, 16130, Thailand

E-mail ordinary_555@hotmail.com

Education

- 2006. Bachelor of Science in Mathematics. Srinakharinwirot University
- 2010. Master of Science in Applied Mathematics. King Mongkut's Institute of Technology Ladkrabang
- 2022. Doctor of Philosophy in Applied Mathematics. King Mongkut's Institute of Technology Ladkrabang

Scholarship

Thepsatri Rajabhat University, Thailand